University of Alberta
Department of Civil &
Environmental Engineering

Structural Engineering Report No. 263

BEHAVIOUR OF COLLARED CONCRETE COLUMNS UNDER CONCENTRIC OR ECCENTRIC LOADS

by

James R. Chapman

and

Robert G. Driver

January 2006

Behaviour of Collared Concrete Columns Under Concentric or Eccentric Loads

by

James R. Chapman

and

Robert G. Driver

Structural Engineering Report 263

Department of Civil and Environmental Engineering
University of Alberta
Edmonton, Alberta, Canada

January 2006

ACKNOWLEDGEMENTS

The research presented in this report was funded primarily by the Natural Sciences and Engineering Research Council of Canada. The first author is also thankful to the University of Alberta, Halsall Engineering Consultants of Toronto, Ontario and Cohos Evamy of Edmonton, Alberta for providing personal financial support.

The research contributions of Munawar Hussain are greatly appreciated. The authors would also like to thank Michael Jelicic for his dedication to establishing a partnership between Halsall Engineering Consultants and the University of Alberta. John Dutton of Lafarge Concrete and Paul Zubick of Waiward Steel Fabricators Ltd. provided valuable assistance in acquiring quality construction materials and components for the fabrication of test specimens.

Special thanks are due to the technical staff of the I.F. Morrison Structural Engineering Laboratory at the University of Alberta, Larry Burden and Richard Helfrich; their assistance during the experimental part of this research program was invaluable.

ABSTRACT

One strategy for the rehabilitation of deficient reinforced concrete structures is to target the improvement of specific local vulnerabilities in the columns related to inadequate axial strength or poor ductility. Fourteen full-scale columns were tested to evaluate the performance of a rehabilitation technique for square or rectangular reinforced concrete columns using a system of discrete external steel collars. Collared columns, tested under either concentric or eccentric axial loading, showed significant improvements in both strength and ductility compared with conventionally reinforced columns. Parameters investigated include: collar spacing, collar flexural stiffness, active confining pressure, and load eccentricity.

An analytical model is presented for predicting the capacity of concentrically loaded columns with external steel collars. The model utilizes a generalized plastic analysis of the steel collars that, unlike existing confinement models, accounts for their high axial and flexural stiffness. Good agreement was achieved between predicted and experimental column behaviour.

TABLE OF CONTENTS

LIST OF TABLES

LIST OF FIGURES

NOTATION

A_{collar} = collar cross-sectional area

A_g = column gross cross-sectional area

A_s = total area of longitudinal reinforcing steel

c = distance to column neutral axis

C = coefficient of elastic bending

D_f = dynamic amplification factor

e = load eccentricity

E_c = secant modulus of concrete (= f_{cc}/ε_{cc})

E_c' = secant modulus of concrete at peak stress (= $f_{cc}'/\varepsilon_{cc}'$)

E_{co} = initial concrete elastic modulus

E_{collar} = collar secant modulus (= $\sigma_{collar}/\varepsilon_{lat}$)

E_s = elastic modulus of collar steel

F = axial force in collar section

F_n = axial force in collar section during analysis stage n

$F_{n\ total}$ = total accumulated axial force in collar section

f_{cc} = confined concrete stress

f_{cc}' = peak confined concrete stress

f_{co}' = peak unconfined concrete stress

f_y = yield strength

F_y = collar section axial yield force

f_u = ultimate strength

h = width of column

I_{collar} = collar section moment of inertia

K = total confinement efficiency factor

K_{dist} = confinement distribution factor

K_{eff} = confinement effectiveness factor

M = bending moment in collar section

M_{cpeak} = column bending moment at peak load

M_n = bending moment at collar plastic hinge location during analysis stage n

$M_{n\ total}$ = total accumulated bending moment at collar plastic hinge location

M_o = theoretical column moment capacity

M_{oc} = theoretical column concrete-only moment capacity

M_p = collar section plastic moment

M_y = collar section yield moment

n = analysis stage number

N = ratio of column axial strength enhancement (for collar spacing ratio s_1'/ s_2')

P = column axial load

P_{cmax} = peak column concrete-only axial load

P_{max} = peak column axial load

P_o = theoretical column axial capacity

P_{oc} = theoretical column concrete-only axial capacity

P_{occ} = theoretical column core concrete-only capacity

P_s = axial load in vertical reinforcing bars

s = collar spacing

s' = collar clear spacing

s_1'/ s_2' = ratio of larger to smaller collar clear spacing

t = collar thickness (in contact with concrete surface)

α_1 = $0.85 - 0.0015 f_{co}' \geq 0.67$ (CSA standard A23.3-04)

Δ_{axial} = collar lateral deflection due to axial force

Δ_{bend} = collar lateral deflection due to bending

Δ_c = net concrete lateral deflection

Δ_{co} = concrete outward lateral deflection

Δ_{ci} = concrete inward lateral deflection

Δ_{collar} = collar lateral deflection

Δ_n = collar lateral deflection during analysis stage n

$\Delta_{n\ total}$ = total accumulated collar lateral deflection at end of analysis stage n

ε_{cc} = confined concrete axial strain

ε_{cc}' = confined concrete axial strain at peak stress

ε_{lat} = column lateral strain

$\varepsilon_{lat\ n}$ = column lateral strain at the end of analysis stage n

ε_{pmax} = column axial strain at peak load

ε_{rate} = axial strain rate during loading

ε_y = yield strain

ε_u = ultimate strain (at peak stress)

ν_c = concrete secant Poisson's ratio

ν_{co} = initial concrete Poisson's ratio

σ_{active} = active confining pressure

σ_{collar} = uniform pressure applied to collar

σ_h = uniform lateral pressure

σ_{max} = maximum collar pressure

$\sigma_{passive}$ = passive confining pressure

σ_n = collar pressure change during analysis stage n

σ_{total} = total confining pressure at collar level

σ_{total}' = total equivalent uniformly applied confining pressure

1. INTRODUCTION

1.1 Foreword

Rehabilitation of existing reinforced concrete columns may be required for a number of reasons, the most common of which are the need for strengthening due to, for example, changes of occupancy or the need to improve the performance of a structure during an earthquake. In the latter case, the low probability of a major seismic event and the potentially high cost of structural upgrades make rehabilitation difficult to justify economically. Therefore, the most practical solutions for rehabilitation are often those that mitigate the risk of structural collapse through rehabilitation of selected critical components. In the case of reinforced concrete columns, schemes designed to improve the ductility and robustness of plastic hinge regions can significantly improve structural performance in an earthquake. If required, this approach can be supplemented with other rehabilitation schemes.

1.2 Problem Definition

Significant advancements in our understanding of structural behaviour and the geologic science of earthquakes have occurred over the past 30 years. Older design codes (pre-1970s) relied mainly on the provision of strength to resist seismic loads without giving due consideration to proper detailing to enhance ductility and energy dissipation at potential locations of plastic hinges (Hussain and Driver 2005b). The lack of stringent design criteria in older reinforced concrete structures has made them particularly susceptible to failure under seismic loading conditions. Often a strong-beam weak-column failure mode results due to poor detailing of column reinforcement and participation of the slab which strengthens the beam. Column detailing deficiencies found in older reinforced concrete structures typically include: widely spaced transverse ties giving poor confinement, ties with 90 degree hooks allowing anchorage failure, and lap splices located just above the slab level that weaken plastic hinging regions. Confinement is required to delay the softening of concrete under ultimate load conditions and allow a ductile response of the column. Failure of a primary structural member, and particularly a column, can be catastrophic and can lead to partial or complete structural

collapse. As a result, many older buildings in regions of moderate or high seismic risk require rehabilitation.

In addition to seismic risk, there are also functional reasons that buildings may require rehabilitation such as a change in use and occupancy or a planned structural addition that requires strengthening of the existing building. Due to the capacity benefits from confinement of the column concrete, many of the attributes that are beneficial for seismic rehabilitation are also beneficial for static strengthening. An effective and economical solution is needed to rehabilitate deficient reinforced concrete columns that is suitable for both static strengthening and seismic upgrading applications.

Providing confinement to columns through externally applied reinforcing elements (jackets, straps, collars, wraps, etc.) has been identified by many researchers as a suitable rehabilitation method for deficient reinforced concrete columns. The external confining elements are passive in action; they react against the lateral dilation of the column under compressive strain providing additional confining pressure, which delays the softening of the concrete and effectively increases its strength. Since these systems rely mainly on the engagement of the external confining elements, any strain gradient on the column cross-section influences the confinement pressure developed by the system. Column strain gradients are common in building structures due to construction tolerances and imbalanced floor loading, and can become severe during a seismic event. Thus, studying the influence of strain gradient on the confinement mechanism is vital to the understanding of this type of column rehabilitation technique.

1.3 External Collar Confinement System

Numerous research programs have focused on external confinement of reinforced concrete columns using a variety of elements including: thin steel jackets, fibre reinforced polymer wraps, and reinforced concrete jackets. Due to their low flexural stiffness, these confining elements tend to be more appropriate for circular column applications that demand only axial stiffness from the confining element. The current research program investigates a confinement system for square or rectangular columns that utilizes steel collars with substantial flexural stiffness.

The proposed external steel collar confinement system has the advantage of a less invasive installation method as compared to most other common confinement schemes. The collars are simply bolted onto the exterior of the column; the clamping action of the collar secures its position. Other external confinement systems can require chipping of the concrete, creating airborne particulate matter and noise pollution, or may require the use of mixed adhesives or on-site welding that affect air quality. Concrete jackets, in addition to potential drilling into the existing structure for anchorage, require the construction of custom formwork that can be costly. Furthermore, disruption of the building function during the rehabilitation process can result in a significant increase in the total project cost. The simplified bolt-on collar installation of the proposed system makes it ideal for sensitive building environments such as hospitals, libraries, and heritage buildings.

Earlier research initiatives at the University of Alberta have focused on the behaviour of columns with steel collars fabricated from standard hollow structural sections (HSS). The HSS collars had either a bolted or welded corner configuration, as shown in Figure 1.1a and 1.1b, respectively. Testing of HSS collars was completed under concentric axial load (Hussain and Driver 2005a) and combined axial and lateral cyclic loading (Hussain and Driver 2003). Although successful in enhancing column performance, to improve economics, a modified version of the collar concept was developed with input from the steel fabrication industry that uses solid section collars cut from flat steel plate (Figure 1.1c). Investigations into the performance of the solid collar system are currently being performed; this report outlines the results of the first such investigation.

a) Bolted HSS Collar b) Welded HSS Collar c) Solid Collar

Figure 1.1: External Confinement Collars

1.4 Objectives and Scope of Research Program

This investigation is part of a larger ongoing research program at the University of Alberta on the rehabilitation of reinforced concrete buildings. A primary objective of the larger research program is to develop a system of steel collars that would allow the successful integration of a steel plate shear wall (SPSW) into an existing reinforced concrete frame building as a means of seismic rehabilitation. The function of the collars is multi-fold: they alleviate the ductility incompatibility between the SPSW and the existing deficient concrete frame through confinement, they improve strength by inhibiting concrete spalling, they provide shear reinforcement, and they provide an attachment point to secure the steel infill panel to the surrounding frame, as shown in Figure 1.2. The SPSW places significant ductility demand on the adjacent columns to anchor the tension field that develops in the thin steel infill panel. Column locations away from the SPSW may also require increased ductility at potential plastic hinging locations to ensure their axial load capacity during the inelastic excursions required to mobilize the energy dissipation of the SPSW.

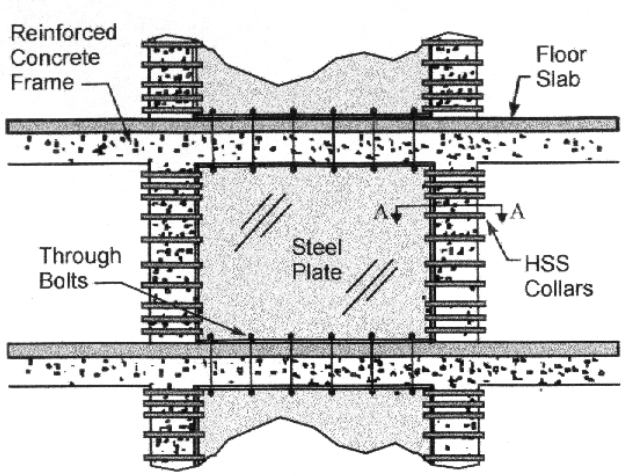

Figure 1.2: Use of External Steel Collars for Integration of a SPSW
(Hussain and Driver 2005b)

Before the composite system of collars and a SPSW is tested, it was considered important to conduct a comprehensive investigation of the fundamental behaviour of the collared columns themselves. In doing so, it was discovered that the system of steel collars may also be useful when used alone (without a SPSW) to meet less extensive

rehabilitation objectives. Earlier investigations have indicated that the use of external steel collars can significantly improve the strength and ductility of concrete columns (Hussain and Driver 2005a). The objective of the current investigation is to expand the experimental data pool and improve our understanding of the rehabilitation of concrete columns using external steel collars. In particular, the behaviour of columns rehabilitated using the solid steel collars is of interest.

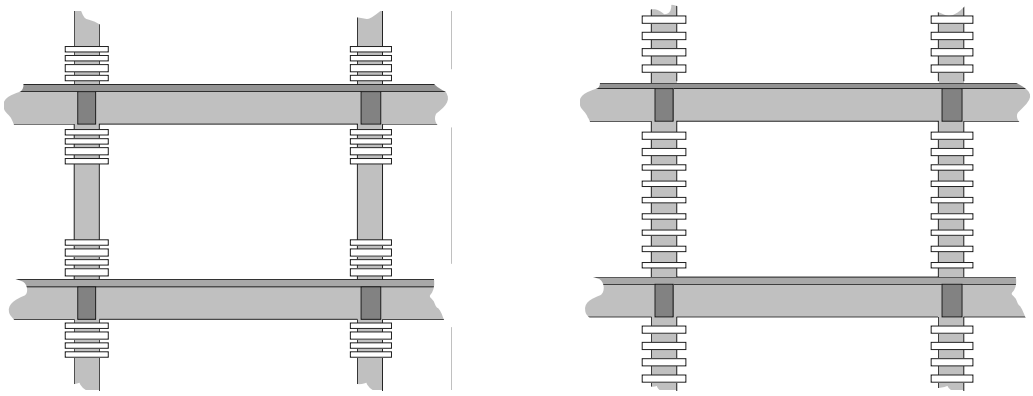

a) Collars in Plastic Hinge Regions b) Collars on Full Column Height

Figure 1.3: Rehabilitation Schemes Using External Steel Collars

The proposed rehabilitation scheme uses a system of steel collars installed at critical column locations within a building structure where the demand on the column exceeds the original design capacity or available ductility. Significant ductility demand can be placed on columns at the base of a structure and at slab levels due to inter-storey drift during a seismic event; the use of steel collars would target these potential plastic hinging regions, as depicted in Figure 1.3a. Alternatively, increased axial demand may result from a structural addition or change of building occupancy, requiring columns to be rehabilitated, in which case steel collars would be used along the full height of critical columns, as shown in Figure 1.3b.

The scope of this research program includes:

1) an evaluation of the performance of the newly-developed solid collar configuration through a total of 14 full-scale column tests;

2) an evaluation of the key experimental variables: collar flexural stiffness, collar spacing, pretensioning of collar bolted connections, and initial load eccentricity.

3) an evaluation of the influence that strain gradient in the column cross-section has on the collar confinement mechanism;

4) the development of a simple analytical tool for predicting the peak load capacity of collared columns;

5) and the identification of requirements for improvement of the proposed external collar system.

1.5 Format and Organization of Report

This report has been organized into six chapters. References used throughout the report are listed in pages following the last chapter. The notation used is consistent throughout the report and is listed in the prefatory pages.

Chapter 2 presents a review of selected recent literature relating to concrete confinement. Topics include: seismic performance and rehabilitation of reinforced concrete structures, column confinement systems, and the influence of flexural strain gradients on the performance of column confinement systems.

Chapter 3 includes the details of the current experimental program. The fabrication of specimens, properties of materials, testing set-up, instrumentation, and loading protocol are discussed.

Chapter 4 presents the results of the current experimental program. The general behaviour of concentrically and eccentrically loaded specimens is discussed. Conclusions are developed based on the influence of specific testing parameters.

Chapter 5 presents a simple analytical model for predicting the axial load versus strain history of concrete columns confined with external steel collars. The model is applied to the concentrically loaded specimens from the current research program and is validated using the results of another experimental program by Hussain and Driver (2005a).

Chapter 6 includes a summary of the main conclusions drawn from the experimental program. Recommendations are made for the successful use and implementation of the proposed rehabilitation system. Finally, suggestions are made regarding the future direction of research involving confinement of concrete columns using steel collars.

2. REVIEW OF SELECTED LITERATURE

2.1 Introduction

This chapter focuses on research pertaining to the enhancement of strength and ductility of existing reinforced concrete columns through the provision of a confinement mechanism. The information presented is not intended as a complete summary of this area of study, as the body of research is vast. Instead, a selection of recent literature is presented that supports the findings of the current project and aids in the understanding of the intended use of the proposed confinement system. Specific areas of focus include an overview of seismic rehabilitation research, a review of different column confinement systems, and research on the effects of flexural strain gradients on concrete confinement. A more complete review of concrete confinement research, including a review of various analytical models for confinement, can be found in the report by Hussain and Driver (2005b).

2.2 Seismic Performance and Rehabilitation of Concrete Structures

In recent years there has been increasing concern about the safety of reinforced concrete structures that have structural elements that were not designed based on current seismic design provisions. The performance of columns designed for gravity loads only, which generally have reinforcement detailing that would be expected to perform poorly in an earthquake, are a main concern. A series of three investigations completed at the State University of New York are reviewed in the following; the performance and rehabilitation of gravity load designed (GLD) structures subjected to seismic forces was the focus of the study.

Bracci et al. (1995a) studied the seismic resistance of a three-storey GLD reinforced concrete frame structure. Their investigation included analytical modelling and testing of a 1/3 scale building frame (one bay deep × three bays long) using a shake table to simulate seismic loading. The structure was designed in accordance with the non-seismic portion of the ACI 318-89 design code. The resulting structure had specific internal reinforcing details that are considered deficient from a seismic design standpoint. Reinforcement deficiencies included: inadequate lap splices and transverse

reinforcing designed for shear only located in potential column plastic hinging zones (just above floor slab levels), discontinuous bottom reinforcement in the beams, and low levels of transverse confinement steel in beam-to-column connections.

The scale model was tested under three levels of intensity representing minor, moderate, and major seismic events. The study found that although not explicitly designed for seismic resistance, the model structure had adequate strength and ductility to resist minor earthquake forces. However, when subjected to stronger ground motions the structure approached its lateral strength capacity and greatly exceeded recommended drift limitations. GLD structures, similar to the one studied, are typically dominated by weak column-strong beam behaviour. Based on analytical modelling, Bracci et al. (1995a) found that under ultimate load conditions the structure would have failed in an undesirable column side-sway/soft-storey collapse mechanism. Furthermore, due to inadequate ductility of the columns, premature failure of the structure may have occurred during severe dynamic motion.

In a companion study by Aycardi et al. (1994), the seismic performance of 1/3 scale GLD structural components were studied including typical interior and exterior columns and slab–beam–column connections. By incorporating the results of the companion study, Bracci et al. (1995a) found that the overall strength and behaviour of their GLD model structure could be predicted accurately using plastic limit analysis or pushover analysis using inelastic analysis software. Stiffness reductions for specific structural elements are also suggested that allow accurate prediction of the structural behaviour in a damaged state. The authors emphasize the importance of accurately predicting the behaviour of a structure (in the undamaged or damaged condition) before the rehabilitation is undertaken to allow identification of the most critical structural components and also to avoid unnecessary rehabilitation costs. Furthermore, the authors stress the importance of an accurate analysis of the post-rehabilitated structure to ensure that the desired structural response will result from the modifications made.

In a later study, Bracci et al. (1995b) investigated several different techniques to rehabilitate the failed 1/3 scale GLD model structure from their first investigation. The rehabilitation objective involved reconfiguring the distribution of strength within the structure to change the mode of failure from a column side-sway mechanism to a more

desirable beam hinging behaviour. The options explored included: partially prestressed concrete jacketing, masonry jacketing, and partial masonry infill walls. Each option was analyzed through inelastic modelling using component stiffness and hysteretic behaviour that was representative of the structure's damaged state. Modelling showed that all proposed rehabilitation methods improved the performance of the damaged structure to varying degrees. The authors recognized that the selection of a specific rehabilitation technique would likely depend on functional and economic factors. However, due to the availability of potential retrofit materials at the appropriate scale, the 1/3-scale model structure was eventually rehabilitated using the partially prestressed concrete jacket option, which was applied to interior columns. Testing of the retrofitted structure showed that the overall structural behaviour was improved compared with the original structure. It was found that the ductility of columns was not improved by the rehabilitation technique, but the margin of safety against structural collapse was increased due to a reduction in ductility demand on the columns.

2.3 Review of Column Confinement Systems

Demand for structural rehabilitation has stimulated the development of many different systems for external confinement. The defining characteristics of these systems are the geometric and material composition (steel, fibre reinforced polymers, concrete, etc.) of the confining elements themselves. The selection of a specific rehabilitation system depends not only on structural performance but also on certain practical and economical factors such as disruption of building operations and capital investment required for the rehabilitation. However, most systems are functionally similar in that they provide increased levels of confinement to the concrete, thereby improving the structural behaviour. Various confinement systems are reviewed in the following sections to characterize the differences and similarities between the proposed steel collar system and other confinement systems.

2.3.1 Internal Steel Ties

Internal steel ties are used in most existing reinforced concrete columns to provide shear reinforcement, core confinement, and lateral support for the longitudinal bars in varying degrees. Reinforcing ties are mainly used in new construction, but can be utilized as part

of an external column rehabilitation technique, as discussed in Section 2.3.5. This section focuses on the performance of columns designed with internal steel reinforcing only (i.e., without external confinement). The development of many current external confinement models, including the model presented in Chapter 5, is based on earlier research on internal confinement with steel reinforcing ties. An approach similar to the one presented by Mander et al. (1988a) is utilized in the current investigation, and is accordingly reviewed here. A study on the effect of flexural stiffness of internal reinforcing ties was also selected for review because of the parallels with the current research program which investigates the same parameter.

Khaloo and Bozorgzadeh (2001) studied the influence of the flexural stiffness of reinforcing ties on the performance of four medium-strength (60 MPa) and four high-strength (90 MPa) concrete columns. In cross-section, the columns were semi-circular with a 76 mm radius on two sides separated by a 76 mm straight length on the other two (similar to an ellipse) so that the ties provided confinement on two sides largely in flexure. Each of the concrete strengths was tested with two different internal tie spacings, giving lateral reinforcing volumetric ratios of 0.87% or 1.73%. Columns were constructed with no concrete cover and nominal longitudinal reinforcing intended only to secure the position of the transverse ties. By comparing the results of the study to an earlier experimental program (Khaloo et al. 1999), which used similar column specimens except with larger reinforcing ties, the authors evaluated the influence of the reinforcing tie flexural stiffness. The results showed that columns confined with ties having lower flexural stiffness (1/2 moment of inertia of larger ties) had lower strength and ductility than columns with ties having higher flexural stiffness. Medium-strength and high-strength concrete columns had peak strengths as much as 15% and 39% lower, respectively, compared to columns with stiffer ties. The study also found that when the tie spacing was cut in half, the peak column strength increased by 20% and columns exhibited improved post-peak behaviour.

Mander et al. (1988a) developed a unified model for predicting the stress versus strain curve of confined concrete in rectangular or circular columns with any general arrangement of internal steel reinforcing ties. The model has appropriate allowances for static or dynamic loading, applied either monotonically or cyclically. A single equation, originally proposed by Popovics (1973), is used to define the stress versus strain

relationship. The compressive strength of confined concrete, f_{cc}', is based on an ultimate strength surface for multiaxial compressive stresses proposed by William and Warnke (1975). Using an equation proposed by Richart et al. (1928), the increase in strain at ultimate stress is assumed to be five times the strength gain when each quantity is normalized by the respective values associated with unconfined concrete. The influence of various confining steel arrangements are accounted for by using a confinement effectiveness coefficient, which is taken as the ratio of the effectively confined concrete area at the critical section midway between the ties to the total area of concrete in the core. The area of effectively confined concrete is determined by assuming that a parabolic shaped (45 degree initial tangent) concrete arching action occurs vertically between tie levels and horizontally between the positions of longitudinal reinforcing bars. The model uses an energy balance method to predict the ultimate concrete compressive strain corresponding to the first fracture of a transverse reinforcing tie; the strain energy (equal to the area under the stress versus strain curve) in the transverse reinforcing ties is equated to the strain energy stored in the concrete as a result of confinement.

In a companion paper, Mander et al. (1988b) reported the results of an experimental program which was used to validate the confined concrete model developed by the same authors (Mander et al. 1988a). Thirty-one large scale columns of circular, square or rectangular cross-section were tested under monotonic concentric axial loading at either quasi-static or high strain rates. The proposed model was found to give accurate predictions of the concrete stress versus strain behaviour and strength enhancement achieved due to confinement. The proposed energy balance method also had good accuracy in predicting the ultimate concrete strain, showing the usefulness of the approach for calculating ductility enhancement achieved due to the concrete confinement.

2.3.2 Steel Collars

As mentioned previously, the current investigation is part of a larger ongoing research program on externally confined concrete columns being performed at the University of Alberta. Earlier investigations examined the performance of columns rehabilitated with external HSS collars under concentric axial load (Hussain and Driver 2005a) and under axial load combined with lateral cyclic load (Hussain and Driver 2003). The next

generation of the external collar system, presented in this report, was developed based on the experience gained from earlier investigations which are reviewed below. Some specific results from the testing programs by Hussain and Driver (2005a, 2003) are shown in Table 2.1 and Figure 2.1. The same treatment of experimental results is not given to all literature reviewed; specific results are reported in this section because of the direct relation to the current project and the use of these data in later chapters.

In order to gain a fundamental understanding of the behaviour of columns confined externally using collars with high axial and flexural stiffness, Hussain and Driver (2005a) performed tests on concentrically loaded columns rehabilitated with HSS collars. Parameters investigated include: collar stiffness, spacing, and corner connection (bolted or welded), and active confining pressure. Eleven columns (300×300×1500 mm) were tested consisting of two conventionally reinforced control columns and nine externally collared columns. All specimens had the same longitudinal reinforcing, but collared columns did not have internal reinforcing ties so that the effects of external confinement could be studied separately. Conventionally reinforced columns were designed based on either gravity load or seismic design provisions of CSA Standard A23.3, giving different spacing of internal reinforcing ties. The gravity load designed column failed in a brittle manner because of the relatively wide spacing of ties, while the seismically designed column had a more ductile response due to the closely spaced ties. Externally collared columns had improved performance compared to conventionally reinforced columns. The area of the confined core concrete was effectively increased by the use of external collars because concrete spalling was completely prevented beneath collars and inhibited in the spaces between the collars.

The collar system developed by Hussain and Driver (2005a) works by providing passive confinement developed through restraint of the lateral dilation of a concrete column under high load levels. Variation of collar parameters allowed the confinement mechanism to be examined. Collars were either welded or bolted to the column to provide an assessment of the limits of fixity at the collar corner connection. Welded collars required grouting to secure the position of the collar. Columns with welded collars reached load levels significantly higher than columns with bolted collars. However, due to the sudden fracture of the welded connection, columns with welded collars failed at a lower strain level than equivalent columns with bolted collar connections. The

performance of welded collars was expected to improve with the use of complete penetration welds. Increased collar spacing was found to reduce the performance of the collar system due to the associated decreased in level of core confinement. Columns with collars having higher axial and flexural stiffnesses had improved strength and ductility characteristics. However, large increases in stiffness provided comparatively small improvements in column performance. Pretensioning of connection bolts allowed an active confining pressure to be applied to some columns. The active pressure was found to improve column behaviour up to the peak load, but expedited softening occurred in the post-peak region due to rapid spalling of concrete between the collars of those specimens. A summary of the specific numerical results from the experimental program described above are shown in Table 2.1.

Table 2.1: Summary of Experimental Results from Hussain and Driver (2005a)

Specimen	Confinement Type	Spacing c/c (mm)	Collar Corner Connection	f_{co}' (MPa)	Peak Load (kN)	Axial Strain at Peak
C00A	ϕ10 rebar ties	267	–	34.4	3475	0.0035
C00B	ϕ15 rebar ties	70	–	35.0	3419/ 3342 *	0.0034/ 0.0305 *
C01	HSS 51×51×6.35	122	bolted	37.9	4874	0.0300
C02	HSS 76×51×6.35	122	bolted	38.7	5283	0.0356
C03	HSS 76×51×6.35 **	122	bolted	37.8	6093	0.0350
C04	HSS 76×51×6.35	170	bolted	37.8	4135	0.0064
C05	HSS 76×51×6.35	95	bolted	36.4	6600 §	0.0450 §
C06	HSS 51×51×6.35	122	welded	34.8	6409	0.0359
C07	HSS 76×51×6.35	122	welded	47.0	8882	0.0259
C08	HSS 102×51×6.35	122	welded	52.8	9802	0.0318
C09	HSS 76×51×6.35	170	welded	36.3	5123	0.0267

* Values presented for first / second peak reached by this column

** Active confining pressure applied through bolt pretensioning

§ Lower bound result – capacity of testing equipment reached

The performance of externally collared concrete columns under extreme lateral cyclic loading was also investigated by Hussain and Driver (2003). Columns were tested under constant axial load and fully reversed lateral cyclic loading, with multiple cycles being applied at each increasing level of lateral displacement. Nine columns (300×300×2100 mm) were tested including one control column with conventional internal reinforcing satisfying the seismic design provisions of CSA Standard A23.3 and eight externally collared columns with varying test parameters. The effects of collar spacing, collar stiffness, axial load index, and shear-span were studied. Collars used in this test program were fabricated from HSS sections and had welded corner connections. In order to study the effects of external collars separately, no internal reinforcing ties were used in the test region.

The results of the experimental program showed that all collared columns had excellent behaviour under severe cyclic loading with stable hysteresis curves indicating significant energy dissipation. Collared columns were also found to be more resistant to degradation under severe cyclic loading than conventionally reinforced columns. Enhancement in ductility and strength of columns was shown to be dependant on the level of confinement, which is a function of the collar stiffness and spacing, confirming the results of tests by the authors on concentrically loaded columns. Specimens with higher axial load levels generally had an increased rate of strength degradation at large displacements, decreased stiffness retention, and lower energy dissipation. However, columns with an axial load level representative of service loads had slightly improved ductility over columns without axial load for short shear spans, which was attributed to quicker mobilization of confinement from the external collars and the improvement of shear capacity under axial compression. The rate of strength degradation was found to be higher in columns with a short shear-span compared to columns with a long shear-span. Moreover, columns with a longer shear-span had improved stiffness retention, energy dissipation, and ductility.

All the collared columns showed very good behaviour under severe cyclic loading. As an example of the column behaviour achieved in testing, the hysteresis curve for a typical specimen with a long shear span and no axial load (CL1) from the experimental program is given in Figure 2.1. A total of 45 load cycles were applied to this specimen and no strength degradation was observed. The final cycle was applied using the full stroke

available from the testing apparatus, allowing the column to reach a displacement ductility level (ratio of maximum displacement to yield displacement) of 12.

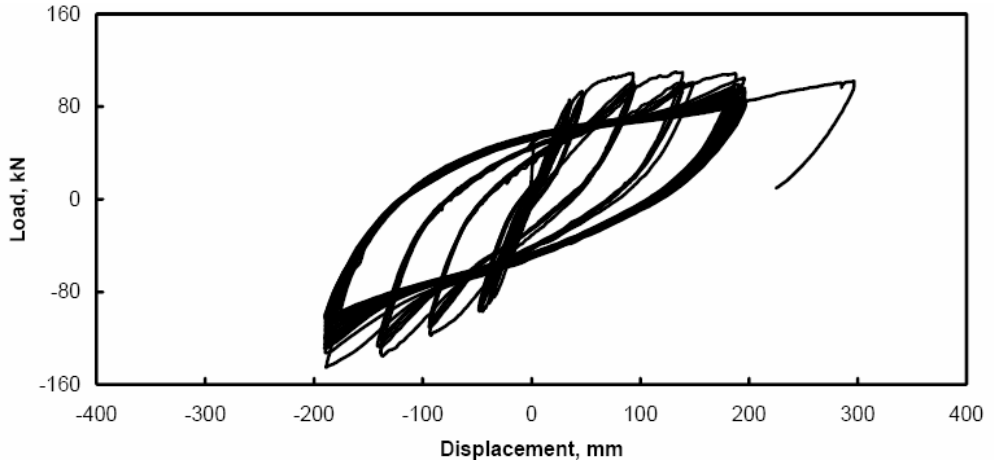

Figure 2.1: Typical Hysteresis Curve from Hussain and Driver (2003)

In summary, the desired enhancement in strength and ductility was achieved through confinement of concrete columns using external HSS collars. The presence of the collars made the columns very resistant to degradation under concentric axial loading and also under combined axial and lateral cyclic loading. It was therefore concluded that the use of external HSS collars would be an effective means of rehabilitating columns in seismically deficient reinforced concrete buildings.

2.3.3 Thin Steel Jacketing

The use of steel jackets can increase the shear strength of columns significantly, but due to their low flexural stiffness steel jackets typically have poor confinement efficiency for square and rectangular columns, which limits the effectiveness of the system for increasing deformability of those columns. Xiao and Wu (2003) investigated an improved steel jacketing technique for rehabilitation of rectangular concrete columns. The system utilizes steel elements to stiffen a thin steel jacket (3.2 mm thick) in potential plastic hinging zones at the ends of the column, where increased confinement is required. Five columns (254×254×1016 mm) were tested under constant axial load ($0.3A_g f_{co}'$) combined with fully reversed lateral cyclic loading. In order to simulate a rehabilitation scenario, all specimens were designed with internal reinforcing typical of pre-1970s

construction, including transverse reinforcement with 90 degree hooks. Test specimens included: one as-built column (no rehabilitation applied), one column with a full-height thin steel jacket, and three columns with thin steel jackets stiffened with different steel elements (thick plate, angle, or square HSS) welded to the exterior of the jacket.

The results of the experimental program showed that the stiffened steel jacket system could significantly improve the strength and ductility of seismically deficient concrete columns. The as-built column failed in a brittle manner, characterized by severe degradation in load carrying capacity upon failure. The specimen rehabilitated with an unstiffened steel jacket had improved column performance but was unable to achieve a ductile response. Failure of that specimen occurred due to bulging of the steel jacket followed by rupture of the corner welds. Specimens with stiffened steel jackets had significantly increased ductility and stable hysteric behaviour, with ultimate drift ratios (maximum displacement divided by column length) exceeding 8%.

Xiao and Wu (2003) also developed a simple technique to proportion the steel jacket stiffeners, which is based on an equivalent confinement pressure derived from the seismic provisions of ACI 318-99. The model uses a beam analogy to describe the limit state where the stiffener element forms plastic hinges, similar to the procedure used in the analytical model presented in Chapter 5 of this report. Hussain and Driver (2005c) discussed the simplifying assumptions made in the formulation of the procedure proposed by Xiao and Wu (2003) for proportioning the steel jacket stiffeners, which have similarities to external steel collars. The first assumption was that the steel stiffeners should be designed to develop a confining pressure equivalent to the seismic design provision in ACI 318-99 for conventionally reinforced columns. This method leads to conservatism because the ACI 318-99 code provision accounts for the ineffectiveness of conventional ties due to their low flexural rigidity. Consequently, the target confining pressure is higher than required because the steel stiffeners have an improved confinement mechanism compared with conventional ties. The second assumption was that the confining pressure is uniformly distributed beneath the confining element. This assumption allows considerable simplification, but must be accounted for in the model because the pressure distribution is non-uniform. The third assumption was that the stiffener could be designed based on AISC beam-column design equations, which have integrated conservatism, and apply to many different cross-sectional shapes. The model

could have more accurately designed the stiffeners based on a closed form solution for the exact shape of the confining elements. The fourth assumption was that the axial force in the confining elements could be neglected, which leads to a non-conservative design. Axial force and axial stiffness of confining elements has been shown in the current investigation and others (e.g., Hussain and Driver 2001) to be a highly influential component of the confinement mechanism, even where there is also significant flexural stiffness. Finally, the discussion paper includes comments on the practicality of the proposed stiffened steel jacket system. The proposed procedure combines two proven rehabilitation systems, steel jackets and steel collars. The resulting “double system” has redundancy, but may be uneconomical compared with other systems. Moreover, the stiffened steel jacket system requires significant amounts of welding, which further reduces its economic viability.

2.3.4 Fibre Reinforced Polymer Jacketing

Mirmiran et al. (1998) performed an experimental investigation on over 100 specimens to study the effects of cross-section shape, column slenderness, and interface bond on the confinement effectiveness of fibre reinforced polymer (FRP) jackets for external confinement of concrete columns. The use of FRP jackets was shown to provide significant increases in column strength and ductility compared with unconfined concrete specimens.

Investigating the shape effect, Mirmiran et al. (1998) demonstrated that FRP jackets are less effective in confining square column sections compared with similar circular sections. Circular cross-sections have a uniform confining pressure that is a function of the hoop strength of the jacket, while the confining pressure for square cross-sections varies from a maximum at the corners of the column to a minimum at the centre of the column face. This variation in confining pressure is a result of the low flexural rigidity of the FRP jacket in the span between the corners of the column. A modified confinement ratio based on corner radius and column width was presented that accounts for reduced confinement effectiveness in square columns. It was also shown that variation of the FRP jacket thickness had little effect on the confinement efficiency of square columns because the flexural rigidity of the jacket remained low regardless of the number of FRP layers used.

By examining concentrically loaded specimens with length-to-width ratios between two and five, Mirmiran et al. (1998) examined the effect of column slenderness on confinement behaviour. Minor load eccentricities developed in longer specimens causing a slight strain gradient on the column cross-section. The strain gradient may have resulted from second order bending but could also have been attributed to non-uniform distribution of confining pressure, stress concentrations, or localized flaws in the concrete and FRP jacket. Column slenderness had very little effect on the behaviour of the tested specimens. The authors concluded that the load eccentricities and associated strength reduction were within the ACI 318-95 code provisions for the design of tied columns, which recommends a 20% reduction in ultimate strength capacity to allow for accidental load eccentricity.

Mirmiran et al. (1998) also studied the effect of adhesive and mechanical bond at the interface between the FRP jacket and column concrete. Testing of bonded and unbonded concrete jackets showed that adhesion between the jacket and concrete had no significant influence on the behaviour of columns. However, when shear connection ribs were included in the jacket, it was shown that mechanical bond can considerably increase the load carrying capacity of FRP jacketed columns. The shear connection ribs were found to provide a more effective distribution of confinement pressure in the column.

Saadatmanesh et al. (1994) performed an analytical investigation into the use of FRP as a discrete confinement system for rectangular or circular concrete columns. The system proposes the use of FRP straps applied in concentric rings or a continuous spiral around the column. The analytical model developed by Saadatmanesh et al. (1994) indicated that significant increases in concrete compressive strength and strain at failure could be expected from columns confined with FRP straps compared with unconfined concrete columns. The analytical model uses the same stress versus strain relation for confined concrete as presented by Mander et al. (1988a), reviewed in Section 2.3.1. The model accounts for unconfined concrete regions by assuming a parabolic arching action between FRP straps, and applying a confinement efficiency factor based on the clear space between straps. By using an energy balance approach the strain in the FRP strap is traced until it ruptures, at which point column failure is assumed to occur. The proposed model is applied to columns with circular cross-sections, which displayed

significant increases in both strength and ductility. The authors report similar results when the model is applied to rectangular column cross-sections, which is contrary to the experimental results of Mirmiran et al. (1998). The model fails to address critical differences in the behaviour of circular and rectangular confined columns that result from the low flexural stiffness of the FRP straps.

2.3.5 Reinforced Concrete Jacketing

Rodriguez and Park (1994) studied the seismic behaviour of reinforced concrete columns repaired and/or strengthened by full-height reinforced concrete jackets. The original columns had internal reinforcing typical of pre-1970s construction, now considered inadequate for seismic design, including low levels of transverse reinforcement and plain (undeformed) reinforcing bars. Four specimens (305×305×3600 mm) that represented the column portion between the mid-heights of successive building storeys, including the beam-to-column connection, were tested. Two specimens were strengthened before testing, and the remaining two were tested and then repaired using the same concrete jacketing technique. The jacket consisted of a 100 mm thickness of additional reinforced concrete and one of two different arrangements of added longitudinal and transverse reinforcement: one where longitudinal bars were bundled in the corners of the concrete jacket (with square transverse hoops) and another where longitudinal bars were distributed around the jacket (with octagonal and square transverse hoops). Columns were subjected to fully-reversed lateral cyclic loading under constant axial load. Testing showed that the as-built columns had low ductility and significant strength degradation during testing. Jacketed columns had a ductile response with up to three times the strength and stiffness of the as-built columns. The tests also indicated that the initial damage had no significant effect on the overall performance of the repaired columns and that the two arrangements of added reinforcing provided similar results. The authors indicated that although the rehabilitation technique was effective, it was also labour intensive. In order to ensure proper bond of the jacket, the surface of the existing concrete requires roughening in the case of undamaged columns, and requires extensive cleaning to ensure that all compromised concrete is removed in the case of repaired columns. Furthermore, the scheme requires drilling into the beam and slab to allow passage of added reinforcement in the column jacket.

The rehabilitation of some non-ductile reinforced concrete frame buildings requires the addition of infill panels or bracing to enhance the lateral strength of the structure. These infill panels require anchorage to the existing structure which can significantly increase the demand on the existing columns by introducing bending and tensile forces that the columns were not originally designed to resist. This problem can be amplified if the columns have poorly detailed lap splices, which are often located in the region of increased column demand just above the floor slab level. The columns may therefore become weak links in the system, limiting the performance of the rehabilitated structure. To address this, Valluvan et al. (1993) investigated strengthening of columns with poorly confined lap splices using either welding of the lapped bars or increased confinement of the splice region. Several different confinement methods were investigated including: external confinement using steel strap and angle elements (grouted or ungrouted), confining the splice region externally using ties (fully grouted, partially grouted, or ungrouted), and placing additional internal ties by chipping away the cover concrete. A total of 12 columns (305×305×1830 mm) were tested under reversed cyclic axial load representing the frame-wall action of a concrete moment frame rehabilitated using an infill panel.

The results of testing by Valluvan et al. (1993) showed that providing continuity in the splice region by welding the longitudinal bars allowed the column to reach yielding in tension. However, due the eccentricity between the spliced bars an outward thrust was generated that requires additional confinement. External confinement using a system of steel straps welded to vertical corner angles provided increased splice strength; failure of these columns occurred outside of the splice region. The authors indicated difficulty in matching the steel elements to the existing concrete surface and concluded that the grouting was required to ensure effective confinement of the splice. External confinement using reinforcing ties was found to be effective in increasing the strength and ductility of the splice region, provided that the ties were adequately grouted to the column. Partially grouting the ties with bands of concrete gave similar performance to fully grouting the ties using a concrete jacket. The addition of internal reinforcing ties was not found to be an adequate method for rehabilitation of the column. Removal of the concrete cover to place additional ties may have caused microcracking of the core concrete, reducing the column strength more than the benefit achieved from the additional ties.

2.4 Effect of Strain Gradient on Confinement Design

Purely concentric axial loading is uncommon in a real building structure. Column out-of-straightness, construction tolerances, and uneven floor loading are examples of occurrences that will produce eccentrically applied axial loads in building columns. Moreover, severe flexural strain gradients can be induced during a seismic event due to inter-storey drift or the anchorage of forces from infill panels or bracing. The resulting strain gradient influences the confinement mechanism by producing a non-uniform confining pressure. The influence of strain gradient on the effectiveness of the external steel collar confinement system is one of the main focuses of the current research program. This subject has been studied by other researchers investigating column behaviour using various confinement systems; two such investigations are reviewed below.

Saatciouglu et al. (1995) performed a combined experimental and analytical investigation on conventionally reinforced concrete columns under eccentric axial load. They tested 12 large scale columns (210×210×1640 mm) under two different load eccentricities, e, that gave e/h ratios of 0.28 and 0.36, where h is the width of the column cross-section. Other parameters investigated were the arrangement and spacing of transverse tie reinforcement and the volumetric ratio of longitudinal reinforcement. All columns tested exhibited a ductile response, with similar behaviour up to the peak load. Specimens with lower volumetric reinforcement ratios and/or larger spacing of transverse ties had an increased rate of strength decay beyond the peak load. The difference between the two load eccentricities was not great enough to have any appreciable effect on the performance of the columns.

Saaticiouglu et al. (1995) could not derive conclusions about the influence of strain gradient on the efficiency of the confinement method because their test program did not include any concentrically loaded specimens. Alternatively, the authors make use of the test data for an analytical study to assess the validity of using an existing confined concrete model (Saaticiouglu and Razvi 1992), developed based on concentric loading, for prediction of the behaviour of eccentrically loaded columns with a strain gradient. The authors appreciated that the distribution of strain on the cross-section was significantly different from the condition under which the model was developed. Consequently, the

lateral confinement pressure predictions based on concentric loading are not representative of those generated under eccentric loading. However, they found that the confinement pressure calculated from the existing model based on the strain at the extreme compression fibres could be applied over the entire compression region without causing any appreciable error between the model predicted and experimental column response. The concrete near the neutral axis has proportionally lower strain and less participation in the response of the column, thus overestimation of the confinement pressure in that region had little effect on the predicted flexural response of the column. Moment–curvature relationships developed using the analytical model showed good agreement with the experimental results. The results indicated that a confined concrete model developed based on concentric loading can be used for columns with a strain gradient.

Parvin and Wang (2001) studied the behaviour of FRP jacketed square concrete stub columns subjected to eccentric loading. The effect of strain gradient was examined experimentally by testing at three different levels of load eccentricity giving e/h values of 0, 0.07, and 0.14. The effect of jacket stiffness was also investigated by using either 1-ply or 2-ply unidirectional carbon FRP jackets. Nine small scale specimens (108×108×305 mm) with no internal reinforcing were tested under monotonically increasing quasi-static loading. The results showed that the FRP jacket greatly enhanced the strength and ductility of all specimens compared with the unconfined control columns. However, the strain gradient was found to reduce the efficiency of the FRP confinement mechanism in the eccentrically loaded columns. Eccentrically loaded specimens had 6% to 20% lower axial strength enhancement, and 247% to 511% lower axial ductility enhancement than equivalent concentrically loaded columns, when comparing to unconfined columns. The stiffness of the FRP jacket was also found to have a significant effect on the strength and ductility of the tested columns. Specimens with a 2-ply FRP jacket had 33% to 46% higher strength enhancement, and 191% to 425% higher axial ductility enhancement than columns with 1-ply FRP, when comparing to unconfined columns. A finite element model was generated using non-linear finite element analysis software, which gave good agreement with experimental results.

All specimens in the study by Parvin and Wang (2001) failed due to crushing of the concrete when the FRP jackets ruptured, triggering a loss of confinement pressure. The

FRP jackets ruptured due to stress concentrations in the corners of the column specimens. In a rehabilitation scenario, a square column would require chipping of the concrete to ensure that a minimum corner radius was achieved to prevent premature rupture of the jacket. Furthermore, the FRP may be sensitive to sharp irregularities requiring additional surface preparation. These problems reduce the practicality of implementing FRP jacket rehabilitation on square columns. However, because of the extremely high tensile strength of FRPs the use of this system for structural rehabilitation of circular columns, which transmit only hoop stresses into the jacket, is an ideal application.

2.5 Summary and Conclusions

A selection of recent literature on seismic rehabilitation and concrete confinement was presented. Particular emphasis was given to the rehabilitation of seismically deficient concrete columns through the provision of a confinement mechanism. Seismic deficiencies can result from inadequate detailing of internal reinforcement (based on earlier design codes) or increased demand on the column, possibly due to the addition of structural bracing or walls. A number of different column confinement systems were reviewed including: conventional internal reinforcing ties, external steel collars, steel jacketing, reinforced concrete jacketing, and FRP jacketing. The influence of the flexural stiffness of confining elements was shown to be a reoccurring challenge in both the development of confined concrete material models and confinement systems. Unlike the confinement of circular columns, which is mainly dependent on hoop stresses, the confinement of rectangular columns requires that the confining elements have flexural rigidity to achieve optimal efficiency. Strain gradients on the cross-section of building columns commonly occur due to construction tolerances and uneven floor loading, and can be severe during seismic events. These strain gradients reduce the efficiency of the confinement mechanism and must be accounted for in the design of rehabilitation systems that rely on concrete confinement. The research reviewed demonstrates that by increasing the level of confinement in regions of high ductility demand, significant enhancements in both strength and ductility of concrete columns can be achieved.

3. EXPERIMENTAL PROGRAM

3.1 Introduction

The experimental program investigates the performance of a two-piece solid steel collar system, with a combination of bolted and continuous corners, for providing enhancements in strength and ductility of concrete columns through confinement. Earlier investigations have examined the performance of collared columns under concentric axial load, and a combination of cyclic lateral and axial loading. Due to construction tolerances and possible imbalances in floor loading the idealized condition of purely concentric loading is rarely encountered in practice. Furthermore, because the external collar system relies primarily on the passive pressure developed when concrete dilates under axial strain, the presence of a strain gradient across the column cross-section influences the magnitude of confining pressure that the collar provides. Thus, the performance of collared columns under eccentric loading is investigated in this experimental program.

3.2 Description of Test Specimens

3.2.1 Specimen Preparation

All preparation of specimens and testing was performed in the I.F. Morrison Structural Engineering Laboratory at the University of Alberta. A total of 14 columns, 300 mm $\times$ 300 mm in cross-section and 1500 mm in length, were cast vertically from a single batch of ready-mix concrete. The concrete was consolidated using an internal vibrator. The formwork used during casting is shown in Figure 3.1. Twenty-five 150 mm × 300 mm and six 100 mm × 200 mm concrete cylinders were cast simultaneously with the column specimens according to the procedures of ASTM standard C192M. The columns and cylinders were both initially moist cured for seven days, then cured at ambient laboratory conditions for a minimum of 21 days.

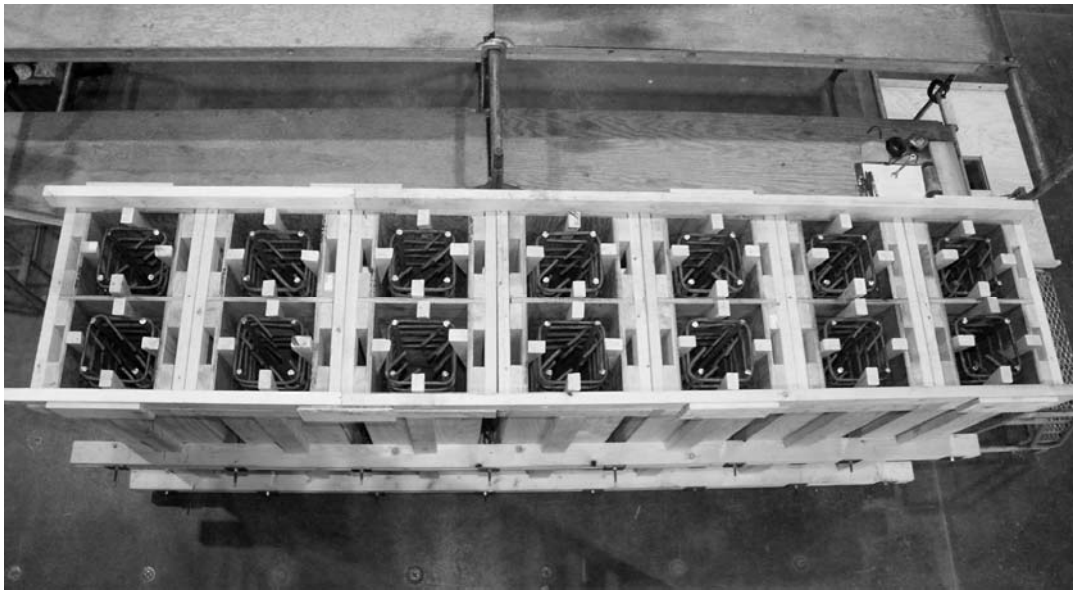

Figure 3.1: Column Formwork and Internal Reinforcing Cages before Casting

3.2.2 Internal Reinforcement Details

In order to facilitate direct comparisons to the specimens of Hussain and Driver (2005a), the arrangement of internal reinforcement used previously was maintained in this experimental program. Each column had four 20M longitudinal reinforcing bars positioned near the corners of the column cross-section, resulting in a longitudinal reinforcement ratio of 1.33%.

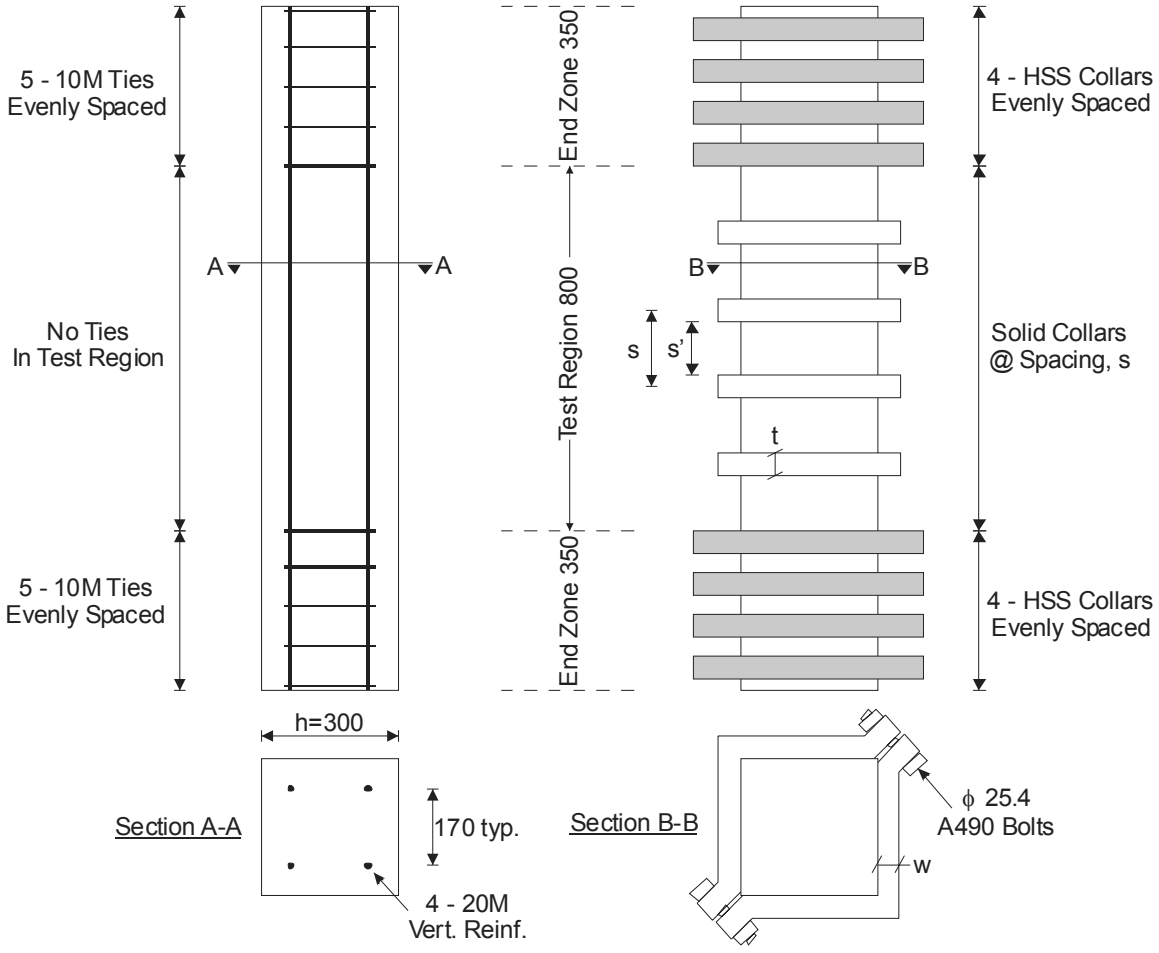

a) Internal Reinforcing (except CE04) b) External Reinforcing

Figure 3.2: Steel Reinforcing Details

The arrangement of transverse steel ties in the columns was divided into three regions: top and bottom end zones each 350 mm in length, and a central test region 800 mm in length. The end zones were reinforced using closely spaced 10M ties with 135 degree hooks (in a addition to stiff external HSS collars described in Section 3.2.3) to prevent failure of the column from occurring outside of the test region. With the exception of specimen CE04, no internal reinforcing ties were placed in the test region so that the influence of the external confinement collars could be examined separately. Internal ties were placed in the test region of specimen CE04 so that the column could be preloaded, without buckling the longitudinal bars, in order to investigate whether the effectiveness of the collars is affected by any lateral expansion due to the presence of service loads prior to collar installation. The internal ties were strategically placed at the same elevation as external collars, which would dominate the effect of the internal tie once installed. The geometric details of the internal reinforcing are shown in Figure 3.2a.

The control specimens of Hussain and Driver (2005a), C00A and C00B, were also used in conjunction with this test program and are therefore described here for convenience. These specimens had the same cross-section and longitudinal reinforcement used for columns in this test program, but had no external collars and differed in the design of the internal transverse reinforcing used in the test region of the column. Both specimens C00A and C00B were designed based on the criteria outlined by CSA standard A23.3-94. However, specimen C00A was designed for gravity loads only, whereas specimen C00B was designed for seismic loading. The resulting internal tie configuration for the columns was 10M bars spaced at 267 mm and 15M bars spaced at 70 mm for the gravity load only and seismic designs, respectively. All reinforcing ties had 135 hooked ends.

3.2.3 External Collar Details

The collars were cut from either 50.8 mm or 40.0 mm (nominal) thick steel plate using a numerically controlled cutting table with four oxy-acetylene torches so that four collars could be cut simultaneously. A nested cutting pattern was established that maximized the plate usage while still allowing the collar shape to be cut accurately. The cutting process is shown in Figure 3.3. Other processes, such plasma-arc cutting, were investigated but it was found that the plate thicknesses used made achieving vertical

cuts extremely difficult. The collars were fabricated by Waiward Steel Fabricators Limited of Edmonton, Alberta.

It should be noted that the steel supplier substituted metric sized plate, 40 mm thick, for the 1.5 in. (approx. 38 mm) thick imperial sized plate that was requested for some collars in this testing program. This discrepancy in the plate sizing causes a slight variation in the collar axial stiffness (between 50 × 38 and 40 × 50 collar sections), a test parameter that was originally intended to be a constant. The difference in axial stiffness between the two collar sections is less than 4%, and is considered negligible hereafter.

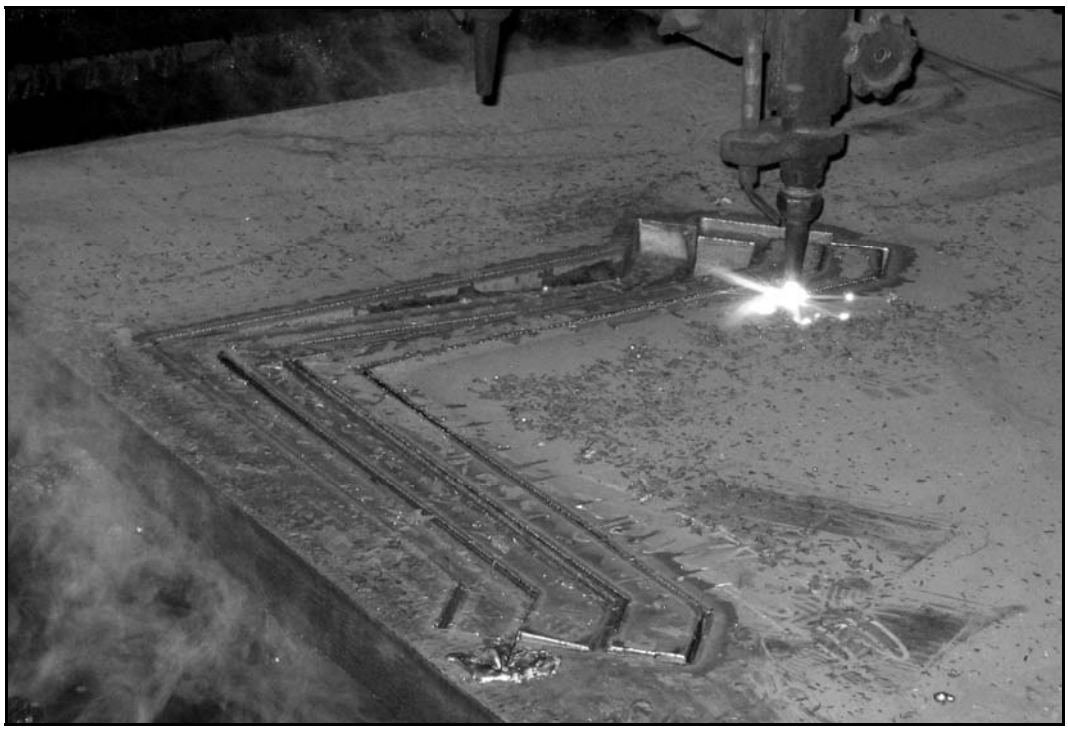

Figure 3.3: Collar Cutting Process

The steel collars are attached to the exterior of the column using bolted corner connections, as shown in Figures 3.2b. The two-piece design makes this collar configuration sensitive to fabrication tolerances. There are two main geometric sensitivities that must be controlled during fabrication to achieve full contact between the collar and concrete surfaces. First, the angle between the collar legs must match the angle of the column corner. Second, the plane of the inside face of the collar must be

close to vertical (assuming the column face is vertical). The collar leg is truncated at the bolted connection just before the corner of the column, leaving a gap between adjacent collar legs that accounts for any fabrication inaccuracy in the collar length and permits the collars to be clamped effectively to the columns during installation. However, any difference in the angle of the contact plane between the collar and column will leave gaps. If the gaps are small enough, dilation of the concrete will fill the space and engage the collar. In cases where a good fit between the collar and column cannot be achieved, grouting or shimming may be required to ensure good performance of the system.

Collars were fabricated in three batches. It was found that tolerances that eliminate the need for shimming or grouting could be achieved using this manufacturing process. However, in one batch of collars the angle between the collar legs was not cut as specified (90 degrees). Furthermore, the inside faces of these collars were not quite vertical. This provided an opportunity to test a possible solution to this problem and shimmed collars were included in the testing program for this batch. As indicated by the fabricator, the source of the problem may have been the plate temperature during the cutting process and/or a misalignment of the cutting heads. The plate stock was stored outside, and because the fabrication was performed during winter months, the steel reached very low temperatures. The temperature differential across the plate may have caused the cutting plane to become skewed. The fabricator corrected the problem in subsequent batches by warming the plate to room temperature and checking the table set-up before initiating the cutting process. However, despite the good collar tolerances readily achievable by this process, the tolerances of the concrete columns themselves can prevent the two surfaces from mating properly. Thus, the fit of collars needs to be assessed on a case-by-case basis. During the installation of collars in the current investigation, any gaps that exceeded 1 mm were filled using thin steel shims, as shown in Figure 3.4c. Shims were used on columns CE02, CE04, CE05, CE12, and CE13. The shims are believed to have had no significant effect on the collar behaviour, so hereinafter no distinction is made between shimmed and non-shimmed collars.

Two sizes of collar cross-sections were used (vertical $\times$ horizontal): 50 mm $\times$ 38 mm ($I = 229\times10^3$ mm^4, taken about the vertical centroidal axis of the collar leg) and 40 mm $\times$ 50 mm ($I = 417\times10^3$ mm^4). The latter section was chosen to examine the influence of increasing the collar flexural stiffness on the performance of the system,

while maintaining a similar cross-sectional area. The collars were evenly spaced with four, six, or eight collars in the test region. Figure 3.2b shows a schematic diagram of the collar spacing for a typical column specimen. Specific details of the collar sizes and spacing for each test specimen are also listed in Table 3.1. In addition to the collars in the test region, four evenly spaced HSS $102 \times 51 \times 6.4$ collars (painted yellow) were used in the end zones of each specimen to prevent failure from occurring outside of the test region.

The two sections of each collar were bolted together at opposite corners of the column using standard 25.4 mm diameter ASTM A490 structural grade bolts. This grade was selected to ensure that rupture of the bolts would not occur during the tests. However, based on measurements of the bolt forces taken during the tests, ASTM A325 bolts would also have had adequate strength. The end of each collar leg was cut with a 45 degree extension, in which an oversized bolt hole was drilled to allow for fabrication tolerances. The positions of the bolted corners were staggered at each collar level to distribute the influence of the bolted corner along the length of the column. The system allows an active confining pressure to be applied to the column by pretensioning the bolts during installation. Pretensioning of bolts was performed using readings from an annular load cell placed around the shank of one bolt; the remaining bolts were pretensioned using the turn of nut method to achieve similar values of preload. The bolts on the majority of specimens were pretensioned to about 25 kN, which was found to be just adequate to ensure that slippage of the collars would not occur, while minimizing the active confining pressure. In order to examine the potential benefits of active confining pressure, the collars of specimen CE05 and CE13 were pretensioned to approximately 150 kN. This value was chosen as the point where significant crushing began to occur locally in the column corners under the bolts. At the time of testing, the bolt load cell showed that the pretensioned bolts had relaxed to 144 kN and 135 kN for specimens CE05 and CE13, respectively, corresponding to about 35% of the ultimate tensile strength of the bolt based on nominal capacity. Details of bolt pretensioning for each specimen are listed in Table 3.1.

Table 3.1: Details of Column Specimens

	Loading Condition		External Collars				
Specimen	**Initial Load Eccentricity (mm)**	**End Condition**	**# Collars**	**Size t x w (mm)**	**c/c Spacing (mm)**	**Clear Spacing (mm)**	**Avg. Bolt P/T (kN)**
C00A*	0	fixed	0	n/a	n/a	n/a	n/a
C00B*	0	fixed	0	n/a	n/a	n/a	n/a
CE01	0	fixed	6	50 × 38	122	72	25
CE02	0	fixed	8	50 × 38	95	45	25
CE03	0	fixed	4	50 × 38	170	120	25
CE04**	0	fixed	6	50 × 38	122	72	25
CE05	0	fixed	6	50 × 38	122	72	144
CE06	0	fixed	6	40 × 50	122	82	25
CE07	30	pinned	6	50 × 38	122	72	25
CE08	60	pinned	6	50 × 38	122	72	25
CE09	10	pinned	6	50 × 38	122	72	25
CE10	0	pinned	6	50 × 38	122	72	25
CE11	30	pinned	8	50 × 38	95	45	25
CE12	30	pinned	4	50 × 38	170	120	25
CE13	30	pinned	6	50 × 38	122	72	135
CE14	30	pinned	6	40 × 50	122	82	25

* Non-collared column tested by Hussain and Driver (2005a)
** Column pre-loaded to 1400 kN before collar installation

a) Undeformed Collar

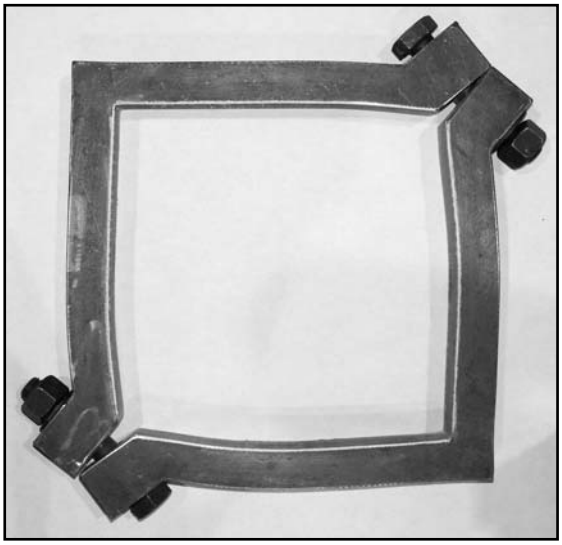

b) Deformed Collar

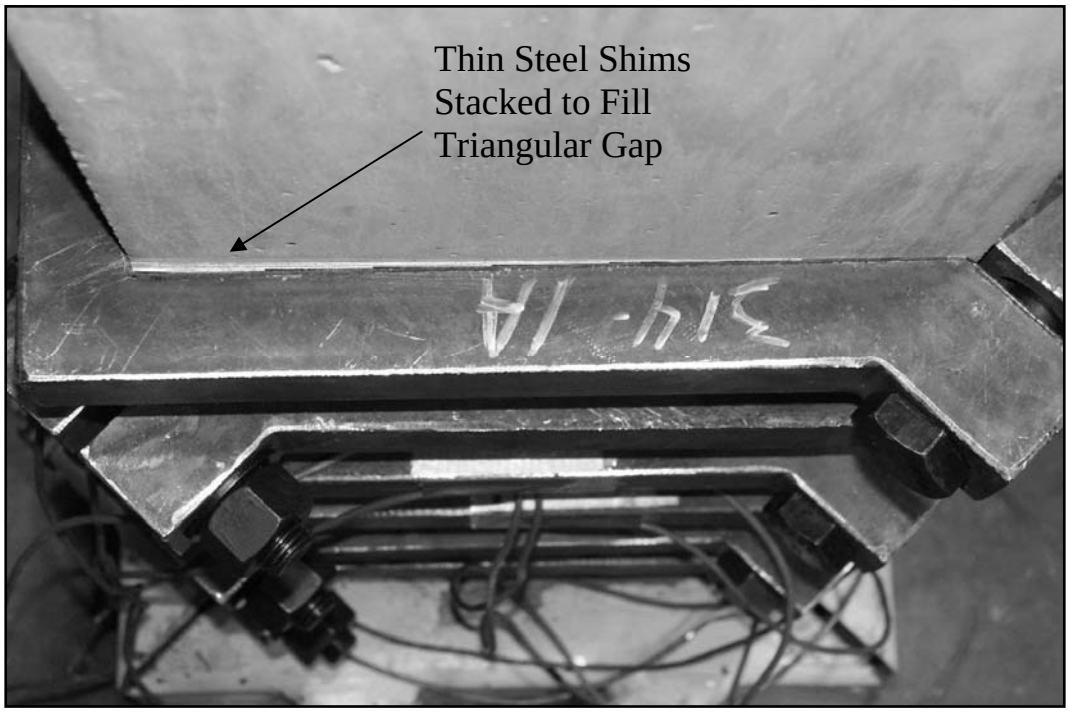

c) Collar Shimming

Figure 3.4: External Collar Configuration

3.3 Parametric Groupings

Details of the test parameters for each specimen have been summarized in Table 3.1. However, it is convenient to view the organization of the test program according to the parametric groupings, as shown in Figure 3.5. Only parameters that vary from those in the control group or, in cases stemming from specimen CE07, those in the preceding level are listed with individual specimens. Specimens C00A (gravity load design) and C00B (seismic load design) tested by Hussain and Driver (2005a) are shown as part of the control group, although they were not tested in this phase of the research.

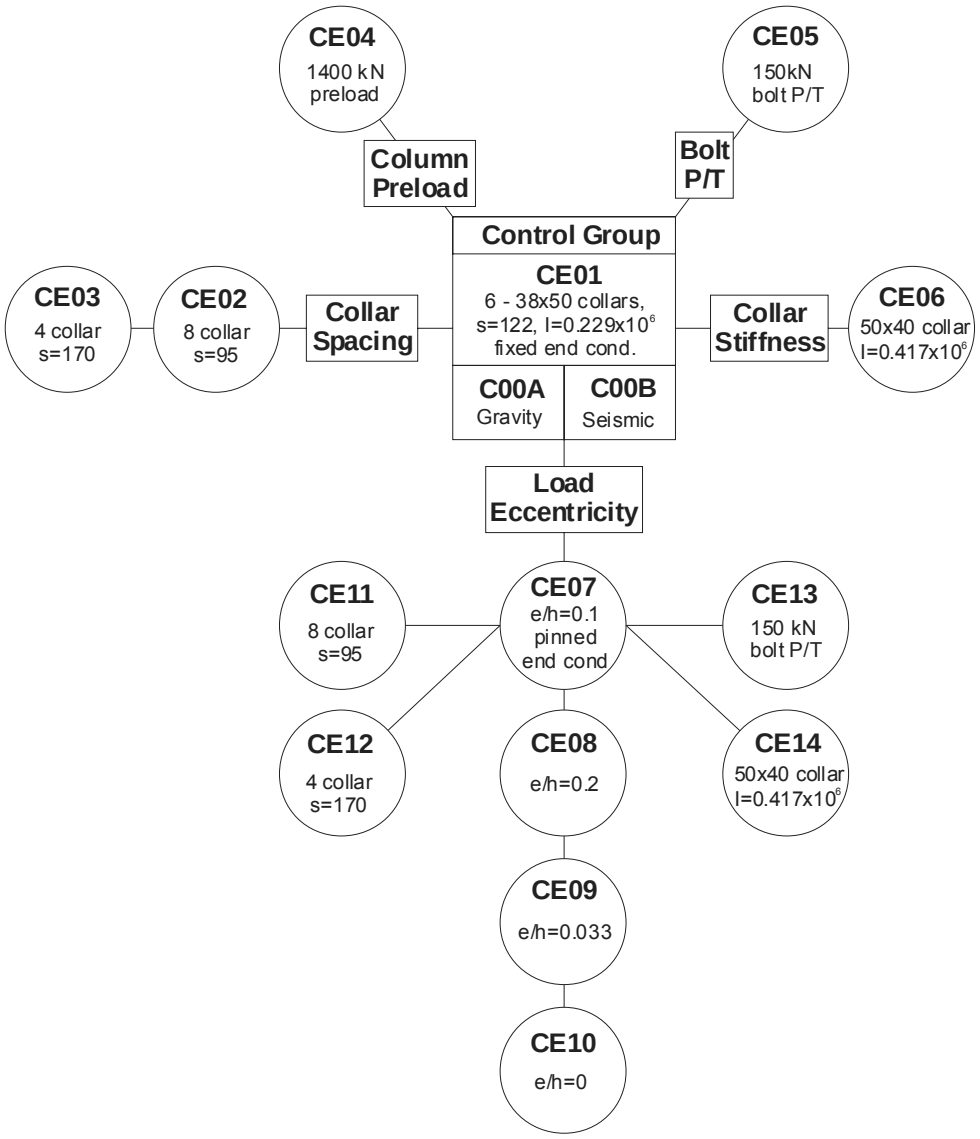

Figure 3.5: Test Matrix According to Parametric Groupings

3.4 Material Properties

3.4.1 Concrete

A single 3 m^3 batch of concrete supplied by Lafarge Concrete Limited of Edmonton, Alberta was used for casting all collared columns and cylinders. The mix design for the concrete, as reported by the supplier, was as follows: 265 kg/m^3 type 10 cement, 900 kg/m^3 sand, 410 kg/m^3 crushed rock (14 to 20 mm), 610 kg/m^3 crushed rock (5 to 14 mm), 158 kg/m^3 water, 2% air (by volume), and 1380 mL/m^3 water reducing agent. All materials used in the concrete mix were sourced locally. Some additional water was added at the time of pouring to achieve the desired slump of 100 mm, based on a standard cone test.

The mechanical properties of the concrete used for the column specimens were determined by testing cylinders according to the procedures outlined in ASTM standards C39 and C469. All cylinders were capped using a sulphur-based compound according to ASTM standard C617. Typically, two to three 150 mm $\times$ 300 mm cylinders were tested each week throughout the test program to monitor the strength gain of the concrete (column tests took place at concrete ages between 30 days and 111 days.) The concrete strength reached a plateau of 31.7 MPa (mean value from all 18 tests after 28 days) at an age of approximately 21 days, as shown in Figure 3.6, and this strength is considered to apply to all collared specimens. Three 100 mm $\times$ 200 mm cylinders were tested to determine the Poisson's ratio for concrete. ASTM standard E177 states that tests of duplicate cylinders should not differ by more than 5% from the average value achieved. Since the Poisson values from the tests exceeded the ASTM standard limit for precision by a considerable margin, a specific value for Poisson's ratio could not be determined. Consequently, a typical value of 0.17 (recorded during one of the three cylinder tests for Poisson's ratio) was assumed for use in the analytical model described in Chapter 5. The mean values and associated standard deviations of the concrete properties from this experimental program are reported in Table 3.2. Concrete properties for specimens C00A and C00B, as reported by Hussain and Driver (2005b), are also included in Table 3.2 for convenience.

Table 3.2: Concrete Material Properties

	Current Research	Hussain & Driver (2005b)	
Property	**CE01 to CE14 Mean (Std. Dev.)**	**C00A Mean (Std. Dev.)**	**C00B Mean (Std. Dev.)**
Compressive Strength (MPa)	31.7 (0.8)	34.4 (3.21)	35.0 (4.23)
Secant Modulus* (MPa)	22 300 (917)	22 900	23 200
Strain at Peak Stress (με)	2550 (215)	2600	2600

* At 40% of compressive strength

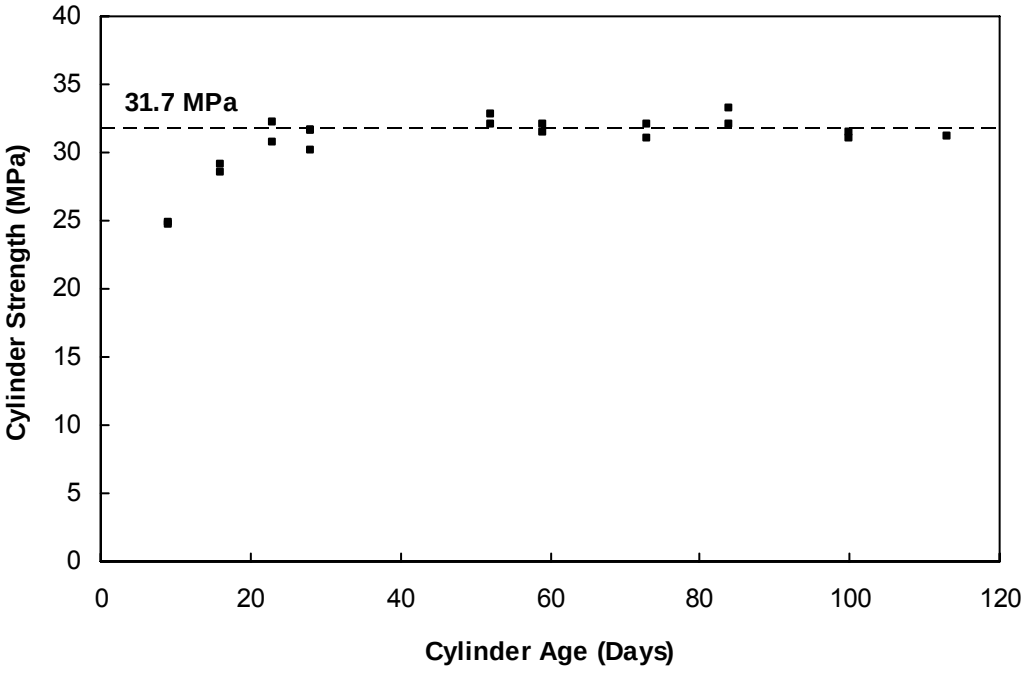

Figure 3.6: Concrete Cylinder Strength History

3.4.2 Internal Reinforcement

Reinforcing bars conformed to CSA Standard G30.18 grade 400 and were tested as per ASTM standard A370. Three coupons were tested in tension for the 20M longitudinal reinforcing bars, the results of which were averaged, and the material properties are reported in Table 3.3. The yield stress of the reinforcing bars was determined using the 0.2% offset method when a well defined yield plateau was not exhibited by the material.

3.4.3 External Collars

The steel used to fabricate the external collars conformed to CSA standard G40.21. Collars cut from 50 mm plate were grade 300W steel, and collars cut from 40 mm plate were grade 350WT steel. The material properties of the collar steel were determined using ASTM standard A370 testing methods. Three different heats of steel were used to fabricate the three batches of collars; two coupons were tested from each heat. Steel from collar batch #1 was used to fabricate collars for column specimens CE01, CE03, CE07, CE08, CE09, CE10, and CE12, steel from batch #2 was used to fabricate collars for specimens CE02, CE04, CE05, CE10, and CE13, and steel from batch #3 was used to fabricate collars for specimens CE06 and CE14. The capacity of the MTS 1000 universal testing machine used for testing the coupons required that the coupons cut from the 50 mm thick steel plate be undersized to ensure that the ultimate tensile strength could be reached. The coupon throat widths were 30 mm and 40 mm for the 50 mm and 40 mm thick plate specimens, respectively. In order to avoid introduction of residual stresses and changes to the material properties from the introduction of heat, the coupons were water-jet cut then mechanically milled to shape. All steel coupons exhibited a well-defined yield plateau. The average values of the material properties for each steel heat are reported in Table 3.3. Accurate strain values for batch #2 are not available beyond the onset of strain hardening due to slippage of the coupons in the hydraulic grips of the testing machine.

3.4.4 Collar Bolts

The bolts used for collar attachment conformed to ASTM grade A490 and were supplied in two batches. The ultimate strength of the bolts was determined using tensile testing; two bolts from each batch were tested. Bolts from batch #1 were used for column specimens CE01, CE03, CE07, CE08, CE09, CE10 and CE12 and bolts from batch #2 were used in specimens CE02, CE04, CE05, CE06, CE11, CE13, and CE14. The average values of material properties for each batch of bolts are reported in Table 3.3.

Table 3.3: Steel Material Properties

Batch No.	f_y* (MPa)	f_u* (MPa)	E_s (MPa)	ε_y** ($\mu\varepsilon$)	ε_u** ($\mu\varepsilon$)
20M Longitudinal Reinforcing Bars					
1	445	767	205 000	2470	111 000
External Collars					
1 (50 mm)	309	470	200 000	1760	163 000
2 (50 mm)	272	456	209 000	1430	n/a
3 (40 mm)	351	441	202 000	1910	166 000
25.4 mm Collar Bolts					
1	1170	1210	357 000	5430	9760
2	1230	1260	333 000	5840	8960

* Static values
** 50 mm gauge length

3.5 Test Set-up

All column specimens were tested in an MTS 6000 universal testing machine with a compressive capacity of 6500 kN. The columns were tested vertically under either concentric or eccentric axial loading as indicated in Table 3.1. A schematic diagram of the column set-up is shown in Figure 3.7. Each specimen was plumbed and then grouted with plaster at the top and bottom to ensure uniform bearing. In the case of concentric loading, the specimen was centred and the heads of the testing machine were locked to prevent rotation, creating a fixed-end condition. In the case of eccentric loading, specialized end fixtures (shown in Figure 3.8c) were used that allow rotation at the top and bottom of the column, creating a pinned-end condition. The position of the end fixtures was adjusted to ensure that the initial load eccentricity was equal at the top and bottom of the column. Typical test set-ups for concentric loading and eccentric loading are shown in Figures 3.8a and 3.8b, respectively.

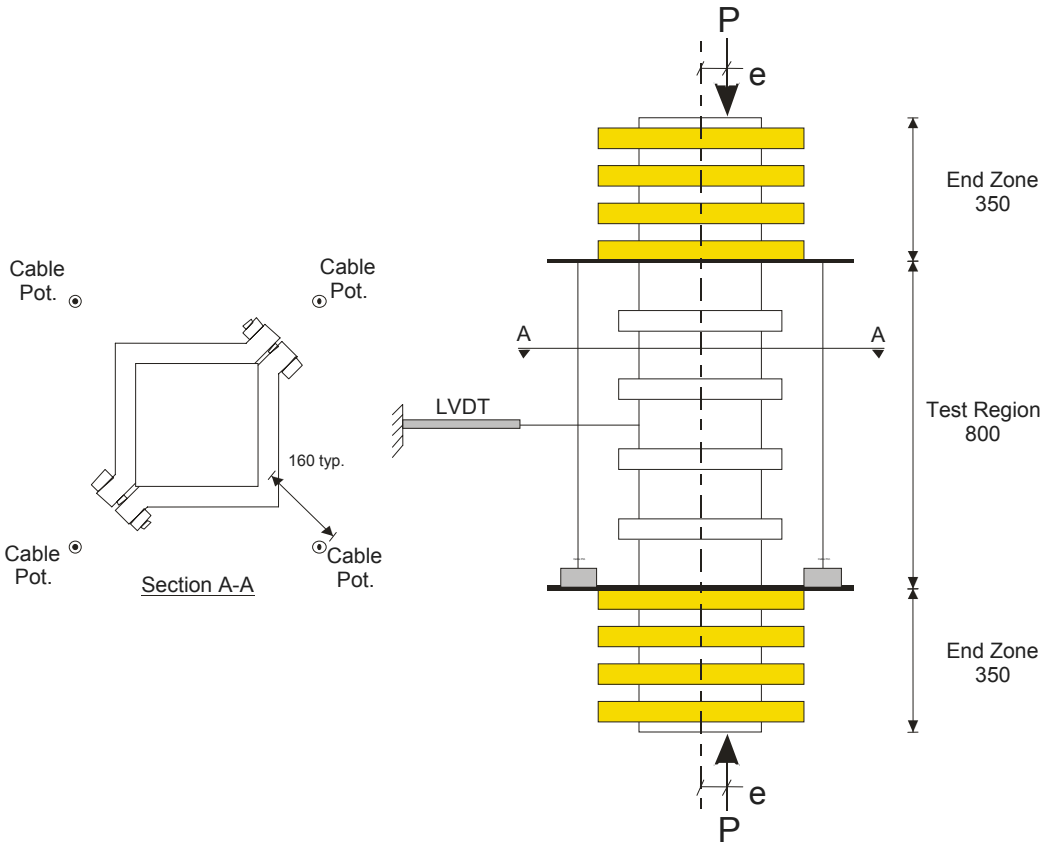

Figure 3.7: Typical Column Testing Set-up

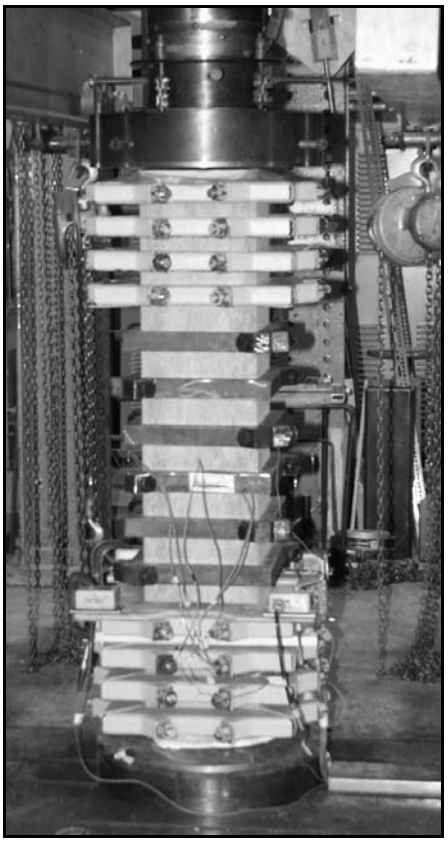

a) Concentric Specimen CE01

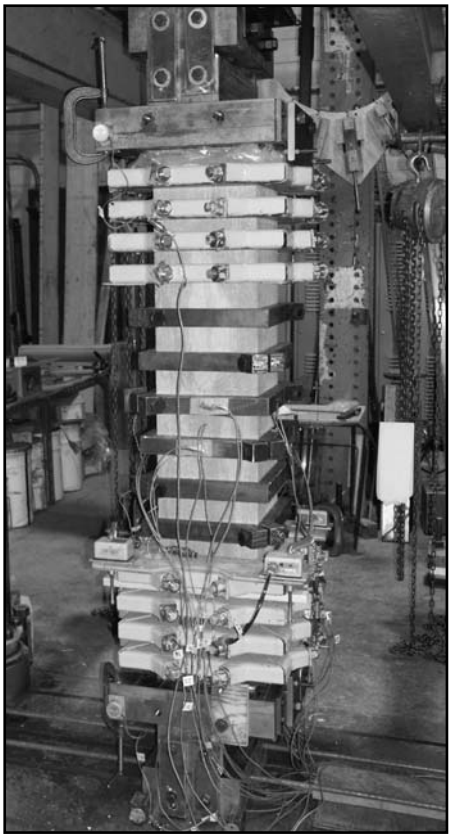

b) Eccentric Specimen CE07

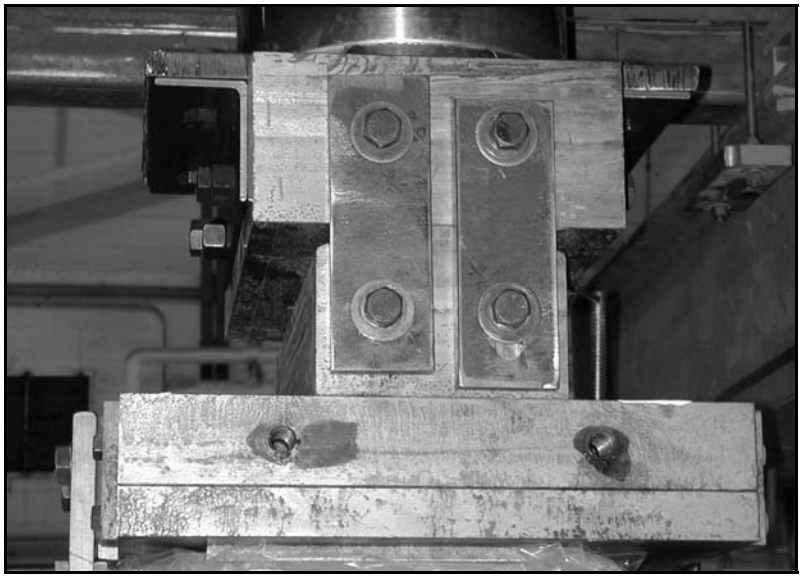

c) Upper Eccentric Loading End Fixture (vertical plates loose during test)

Figure 3.8: Column Set-up Details

3.6 Instrumentation

3.6.1 Column Instrumentation

Column loads were measured using the internal load cell of the MTS 6000 universal testing machine. The axial deformation of the column was monitored using cable potentiometers placed at each corner of the column. Axial deformation was also measured using bondable electrical resistance strain gauges affixed at the mid-height of the longitudinal reinforcing bars. Concentrically loaded columns were instrumented with one strain gauge mounted on each longitudinal bar, while eccentrically loaded specimens had two strain gauges on each bar to allow measurement of the strain gradient across the bar perpendicular to the axis of column bending. In the case of eccentric loading, the column end rotation was monitored using a rotation meter attached to each end fixture. The lateral displacement of the column at mid-height was measured using a linear variable displacement transducer (LVDT). All data were collected using a FLUKE data acquisition system.

3.6.2 Collar Instrumentation

The deformation of the external steel collars was monitored using bondable electrical resistance strain gauges attached at the mid-point of all four collar legs on the central two collars. Collars on specimens CE01 and CE03 were monitored on two legs only, with the position of the strain gauges being staggered between the upper and lower central collars. The strain gauges were oriented to measure longitudinal strain in the collar. In order to measure the strain gradient across the collar section, two strain gauges were placed at each location along the length of the collar. The first gauge was placed on the top of the collar 10 mm from the column face and the second gauge was placed on the outside of the collar. The force in the collar bolts was also monitored at one position during testing using an annular load cell placed on the bolt shank between the bolt head and the collar.

3.7 Loading Protocol

Columns were loaded monotonically until failure or until the capacity of the testing machine was reached. The latter case occurred for specimen CE02 only, which was heavily reinforced with closely spaced external collars. Specimen CE02 was then loaded cyclically to show the robustness of the external collar system and display the lack of collar slippage under load reversals. The load was cycled a total of nine times up to the capacity of the testing machine (6500 kN). The column failure criterion was deemed to be a drop in capacity to 85% of the peak load. Some columns were loaded beyond the failure criterion to emphasize the ductility level that can be achieved with the proposed collar system.

Load was applied in a quasi-static manner using stroke control of the loading head. The loading rate was limited to ensure the column strain rate was acceptably low in order to avoid dynamic amplification of the column response. The average compressive strain rate for all columns up to the peak load was 2.6 $\mu\varepsilon$/s and over the total load history was 4.7 $\mu\varepsilon$/s. The strain rate of eccentrically loaded columns was taken as the strain rate at the compressive face. Mander et al. (1988a) reported an exponential relationship between strain rate, ε_{rate}, and dynamic magnification, D_f, of concrete strength, f_{co}', which was derived based on a regression analysis of the experimental results of Watstein (1953):

$$D_f = \frac{1+\left[\dfrac{\varepsilon_{rate}}{0.035(f_{co}')^2}\right]^{\frac{1}{6}}}{1+\left[\dfrac{0.00001}{0.035(f_{co}')^2}\right]^{\frac{1}{6}}} \qquad [3.1]$$

Based on Equation 3.1, a loading rate of 2.6 $\mu\varepsilon$/s results in a dynamic magnification of approximately 1.3 %, which is within the expected experimental variability and has therefore been neglected.

Specimen CE13 was fully unloaded during the ascending portion of load history in order to make an adjustment to the lower end fixture. The adjustment was required to ensure

the fixture could rotate freely. Upon reloading the column, the load level peaked close to the level that was achieved during the original loading cycle. The column may have achieved a slightly higher peak load had the initial loading cycle, and associated damage, been avoided. However, the effect of this occurrence is considered to be relatively small.

To simulate an existing building column in a rehabilitation scenario, specimen CE04 was preloaded to 1400 kN before the collars were installed in the test region. The purpose was to determine whether the dilation of the concrete under the preload would be small enough so as not to lessen the confining efficiency of the collars at the ultimate load, thereby validating the loading procedure used for the other columns. The collar installation process took approximately one hour (this column required collar shimming). During collar installation, the column experienced some creep displacement and associated load loss (due to stroke controlled loading). The stroke position was adjusted intermittently to maintain the 1400 kN load level. After the collars were installed, the specimen was loaded to failure in the usual manner. Specimen CE04 conservatively represents a column in a realistic rehabilitation scenario because the 1400 kN preload slightly exceeds the factored design capacity of the uncollared column.

3.8 Conclusion

As part of an ongoing research investigation at the University of Alberta, 14 concrete columns were tested to examine the performance of an external confinement system using solid steel collars. The material properties of all steel and concrete elements were measured using standardized testing methods. In order to facilitate direct comparison between different collar types, the specimen geometries and test set-up for this program were similar to initial investigations performed by Hussain and Driver (2005a), who used HSS collars as confining elements. Both concentric and eccentric loading was investigated so that the influence of strain gradient on the performance of the collar system could be evaluated. The results of the testing program are given in Chapter 4.

4. EXPERIMENTAL RESULTS AND DISCUSSION

4.1 Introduction

Fourteen concrete columns were tested to evaluate the performance of the proposed external collar system. The details of the testing protocol are discussed in Chapter 3 of this report. The results of the experimental program, including a discussion of the observed specimen behaviour and the effects of various test parameters, are presented below. As a basis for comparison, the behaviour of two non-collared columns (C00A and C00B) tested by Hussain and Driver (2005a) are also presented and discussed.

4.2 Overall Column Behaviour

4.2.1 Concentrically Loaded Columns

4.2.1.1 General Behaviour and Mode of Failure

All columns tested in this experimental program exhibited a ductile mode of failure. Columns behaved in a controlled manner, were initially axially stiff, had a long plateau before peaking, and a gradual post-peak load decline. In most specimens failure occurred due to crushing of the concrete between collars. Specimen CE03, with the widest collar spacing, failed due to a combination of crushing and buckling of the longitudinal reinforcement between the collars. Significant increases in strength were achieved by all specimens compared with both of the non-collared columns, but results varied widely with varying test parameters. The ductilities greatly exceeded that of the non-collared column designed for gravity loads (C00A) and were comparable to that of the seismically designed non-collared column (C00B). The effect of individual test parameters on column performance is discussed in detail in Section 4.5.

At the peak load, the columns typically exhibited shallow, evenly distributed spalling between collars, resulting in only a small reduction in column cross-sectional area at these locations. The column maintained its full integrity at the collar locations. The

physical damage to the columns at peak load was generally minor, as shown in Figure 4.1a.

At the designated failure load (85% of the peak load in the descending branch), the columns were significantly damaged, with deeper spalling between the collars. Most columns developed elevated damage in localized areas that caused the test region to deform asymmetrically; this phenomenon can readily be seen in photographs due to the inclined angle of the collars (e.g., second collar in Figure 4.1b). The angle of the collars should not be mistaken for slippage of the collars themselves; careful examination of the column surface after testing revealed that the collar had not slipped. Furthermore, no spalling had occurred beneath the collars, even at the end of the test. The appearance of a typical column at the failure load is shown in Figure 4.1b. The appearance of all concentrically loaded specimens at the end of testing (with the collars removed) is shown in Figure 4.2. It should be noted that some columns were loaded well beyond the designated failure criterion, and therefore have damage that is not representative of the column at the failure load.

Columns C00A and C00B are control columns with internal reinforcing designed based on gravity load and seismic load design criteria, respectively. The behaviour of these non-collared columns is used as a basis for comparison to evaluate the performance benefits achieved using external collars. Column C00A failed in a brittle manner at a relatively low level of strain typical of very nominally confined concrete, while column C00B failed in a ductile manner with an elongated descending branch. Specimen C00B had two distinct load peaks. The first peak occurred when the concrete cover was still in place carrying a portion of the vertical load and the concrete in the core was behaving as unconfined. The subsequent drop in load is due to cover spalling, after which the strength of the core concrete began to increase due to the development of confinement up to the second peak (Hussain and Driver 2005a).

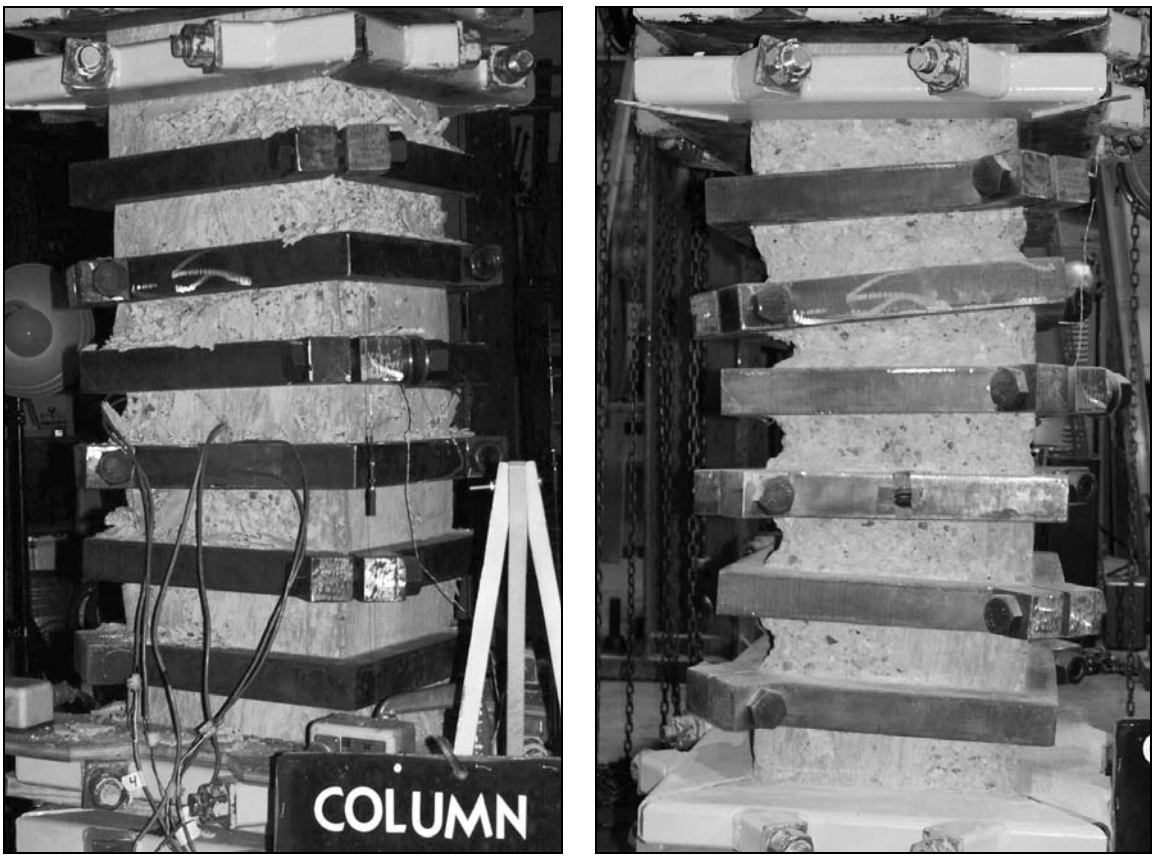

a) Column at Peak Load

b) Column at Failure Load

Figure 4.1: Specimen CE01 During Testing

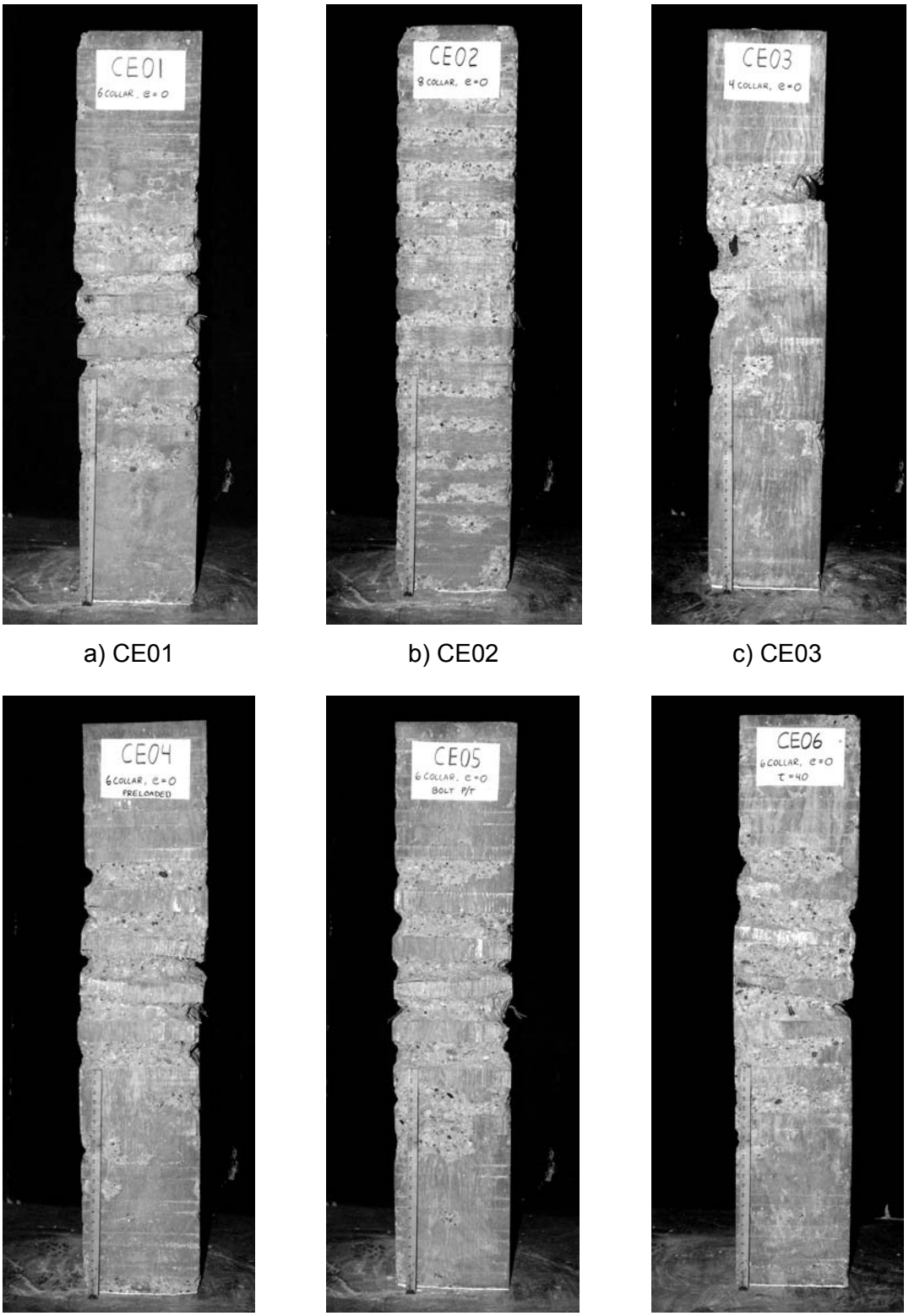

a) CE01 b) CE02 c) CE03

d) CE04 e) CE05 f) CE06

Figure 4.2: Concentrically Loaded Columns After Collar Removal
(scale in photographs is 585 mm long)

4.2.1.2 Axial Load versus Strain Response

The behaviour of tested columns is summarized by reporting the axial load level and compressive strain at milestones reached throughout the load history, including the peak load, designated failure load, and at the end of test. The column response summary is listed in Table 4.1. Strain values reported are calculated using the average strain in the test region recorded by four cable potentiometers positioned at the corners of the column. Specimen CE02 could not be failed with the testing equipment used; therefore, values presented for the peak load and strain of CE02 are lower bound results.

Table 4.1: Concentrically Loaded Column Response Summary

	Peak		Failure		End of Test	
Specimen	**Load (kN)**	**Strain**	**Load (kN)**	**Strain**	**Load (kN)**	**Strain**
C00A*	3475	0.0035	2954	0.0041	1200	0.0070
C00B*	3419 / 3342**	0.0034 / 0.0305**	2906	0.0555	1080	0.0800
CE01	5200	0.0344	4493	0.0650	4493	0.0650
CE02	6500 §	0.0203 §	–	–	6500 §§	0.0257 §§
CE03	3905	0.0104	3319	0.0220	2268	0.0439
CE04	5607	0.0275	4766	0.0748	4657	0.0774
CE05	5950	0.0189	5058	0.0424	4635	0.0555
CE06	5516	0.0219	4689	0.0328	4403	0.0401

* Results from Hussain and Driver (2005a)
** Both peaks presented
§ Lower bound value
§§ After nine cycles

The axial load versus strain responses of all concentrically loaded columns tested are plotted in Figure 4.3. The load versus strain curve for specimen CE02 is truncated at the peak capacity of the testing machine (6500 kN). The load for this specimen was cycled a total of nine times up to the capacity of the testing machine to display the robustness of

the column behaviour. The load cycles for specimen CE02 are plotted separately in Figure 4.4 to ensure the clarity of the other curves in Figure 4.3.

A direct comparison between specimens C00A and C00B and those tested in this program using Figure 4.3 is not completely accurate due to small differences in material properties of the concrete and reinforcing steel used. Despite this, specimens C00A and C00B are included in the figure for the purpose of reporting their individual load versus strain responses. Direct comparisons can be made among specimens CE01 through CE06 using Figure 4.3 as they were cast from the same batch of concrete that had reached its strength plateau by the time testing began and used reinforcing bars from the same heat.

In order to facilitate direct comparison between C00A, C00B, and columns tested in this experimental program, confined concrete material curves (normalized confined concrete stress versus axial strain) were generated for all concentrically loaded specimens and are shown in Figure 4.5. Based on fully composite action between the concrete and reinforcing steel, the confined concrete stress, f_{cc}, is calculated as follows:

$$f_{cc} = \frac{P - P_s}{A_g - A_s} \qquad [4.1]$$

where P is the total axial force on the column section, P_s is the force in the longitudinal reinforcing bars, A_g is the gross column cross-sectional area, and A_s is the area of longitudinal reinforcing steel in the column cross-section. The force in the reinforcing bars, P_s, is calculated from strain data collected from electrical resistance strain gauges mounted on the bars. The confined concrete stress is normalized by the unconfined *in situ* concrete strength, f_{co}', which is taken as 0.85 times the mean cylinder strength, f_c', achieved during material testing. Although the column specimens in the current experimental program were not exposed to sustained loads representative of *in situ* building columns, the commonly-used value of 0.85 was still utilized as a conversion factor to account for differences in the loading condition and *in situ* mechanical properties between the cylinder tests and the column specimens.

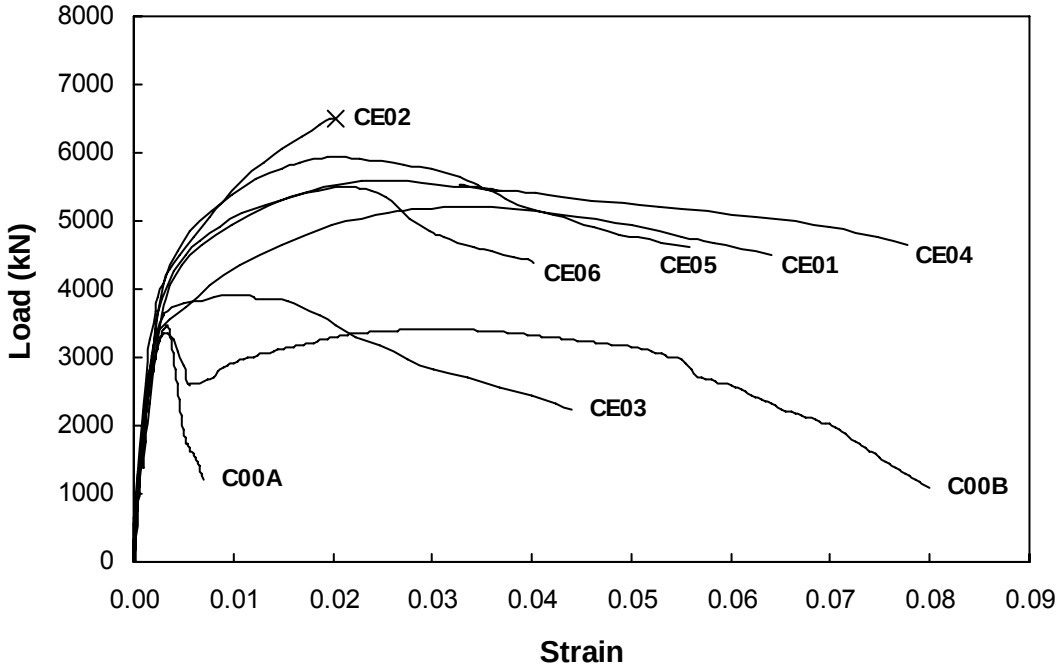

Figure 4.3: Axial Load versus Axial Strain for Concentrically Loaded Specimens

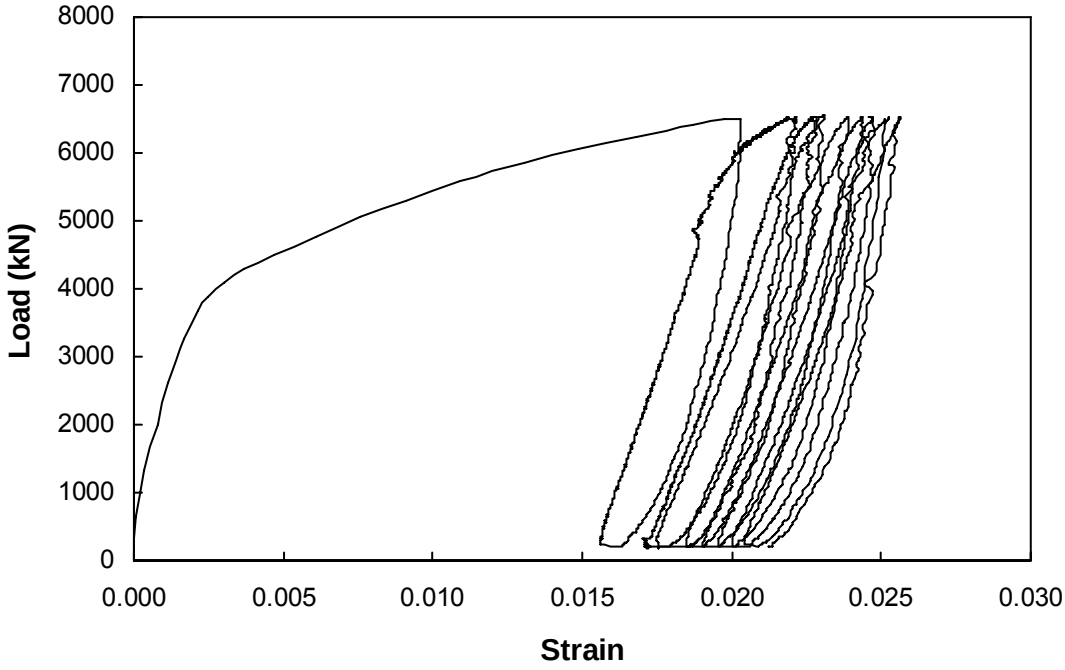

Figure 4.4: Specimen CE02 Axial Load versus Strain

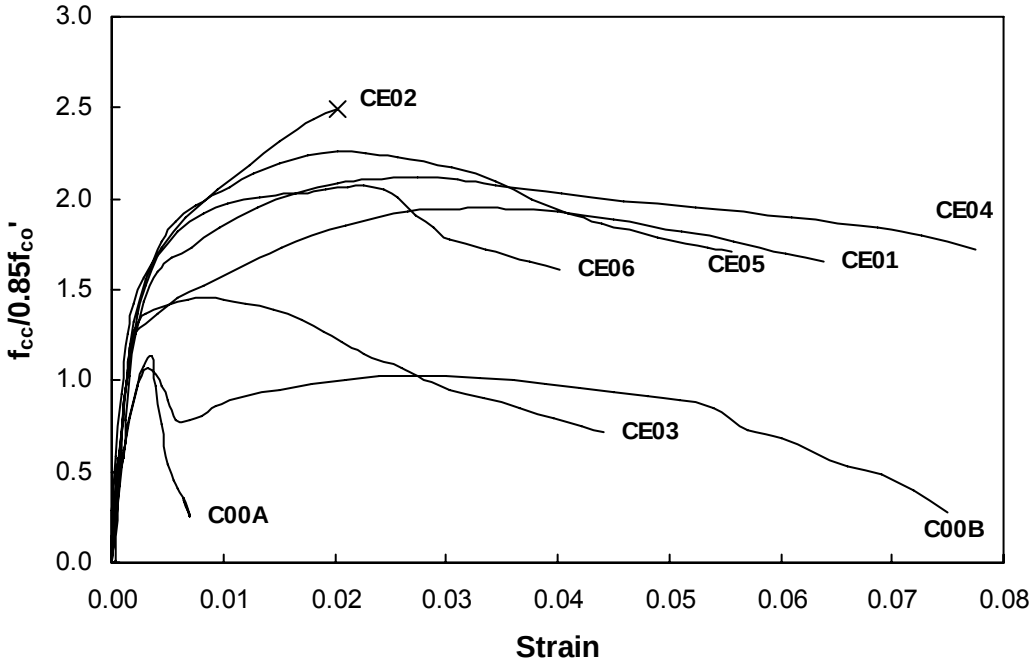

Figure 4.5: Normalized Confined Concrete Material Response

Examination of Figures 4.3 and 4.5 shows that all externally collared columns achieved much higher load and normalized concrete stress levels than the conventionally reinforced columns without collars. Most collared columns exhibited excellent ductility, reaching their peak loads at levels of strain approximately five (CE03, with four collars) to seventeen (CE01, with six collars) times that which would be expected for unconfined normal strength concrete. Furthermore, most collared columns exhibited excellent toughness with high post peak load levels being sustained over significant levels of strain before the failure criterion was met. Specimen CE03 had a less ductile response with an earlier load peak and a somewhat accelerated post-peak loss of capacity. The relatively poor performance of CE03 is a result of the wide collar spacing used on that specimen. A comparison among specimens and discussion of the effect of the various test parameters is reported in Section 4.5.

4.2.2 Eccentrically Loaded Columns

4.2.2.1 General Behaviour and Mode of Failure

Due to the different support conditions used, the failure modes of concentrically and eccentrically loaded specimens were significantly different. Unlike the concentrically loaded specimens, rotation was allowed to occur freely at the ends of the eccentrically loaded specimens.

All eccentrically loaded specimens had a ductile response and failed in single curvature bending, as shown in Figure 4.6. Similar to the concentrically loaded specimens, the concrete between the collars on the compression face of the column spalled during loading. The tension face typically developed a single tension crack between each pair of adjacent collars in the test region that progressively widened during loading.

Visible damage to the eccentrically loaded specimens was typically delayed until close to the peak load. Spalling on the compression face usually started just before the peak load was reached. Spalling extended from the compression face around the sides of the column to approximately the middle of the column. Measurements of the crack depth at the column surfaces were made on some columns during testing and were used to estimate the position of the neutral axis and thereby confirm the linear strain distribution assumed during calculations.

The appearance of the columns after testing, with the collars removed, is shown in Figures 4.7 (frontal view showing compression face) and 4.8 (side view showing column curvature). The damage to the test region is generally well distributed and spalling at the collar locations was completely prevented.

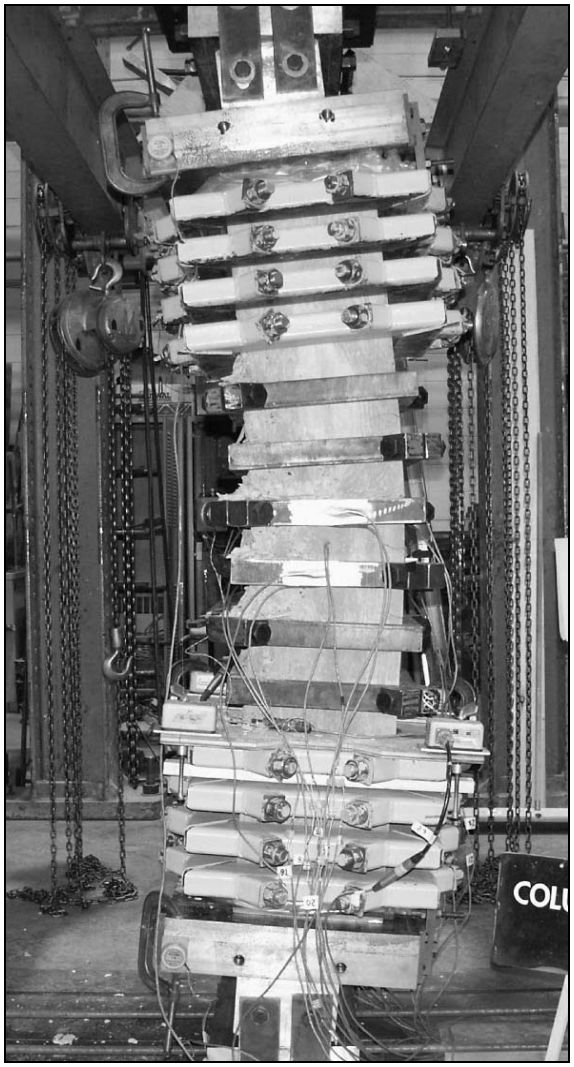

Figure 4.6: Specimen CE07 at Failure Load

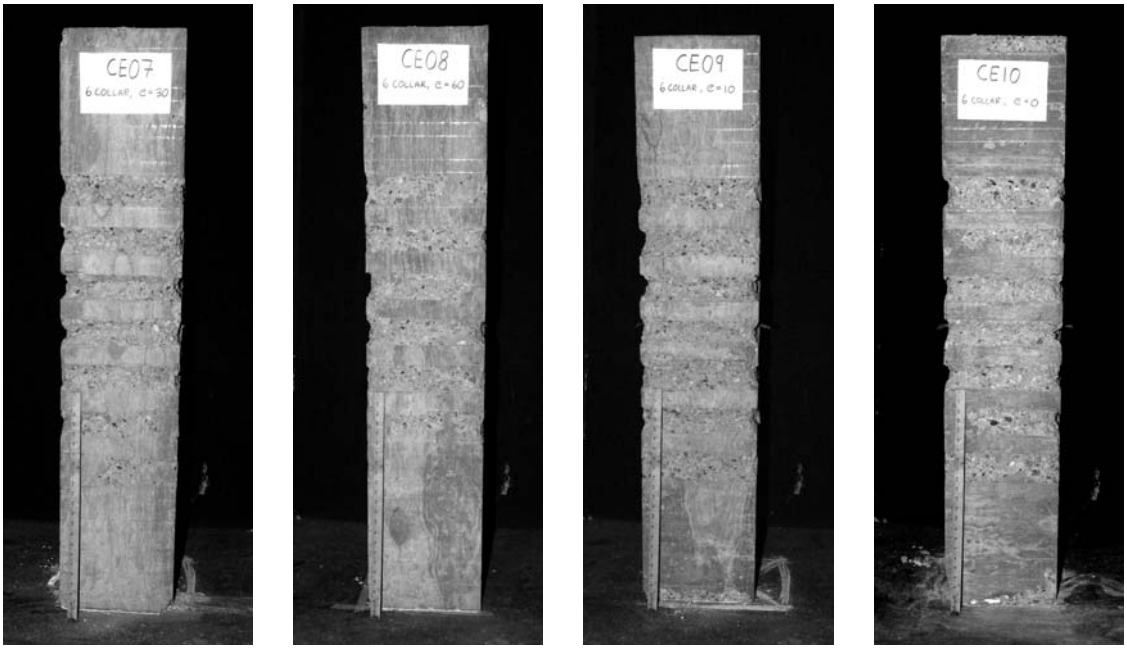

a) CE07 b) CE08 c) CE09 d) CE10

e) CE11 f) CE12 g) CE13 h) CE14

Figure 4.7: Frontal (Compression Face) View of Eccentrically Loaded Specimens After Testing (scale in photographs is 585 mm long)

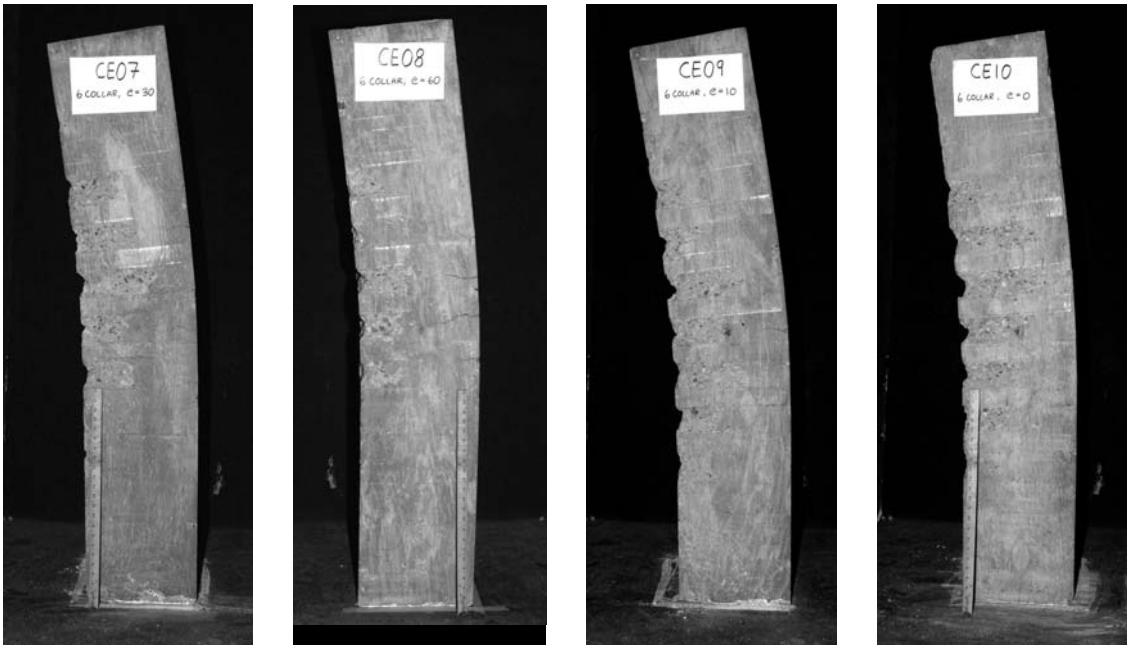

a) CE07 b) CE08 c) CE09 d) CE10

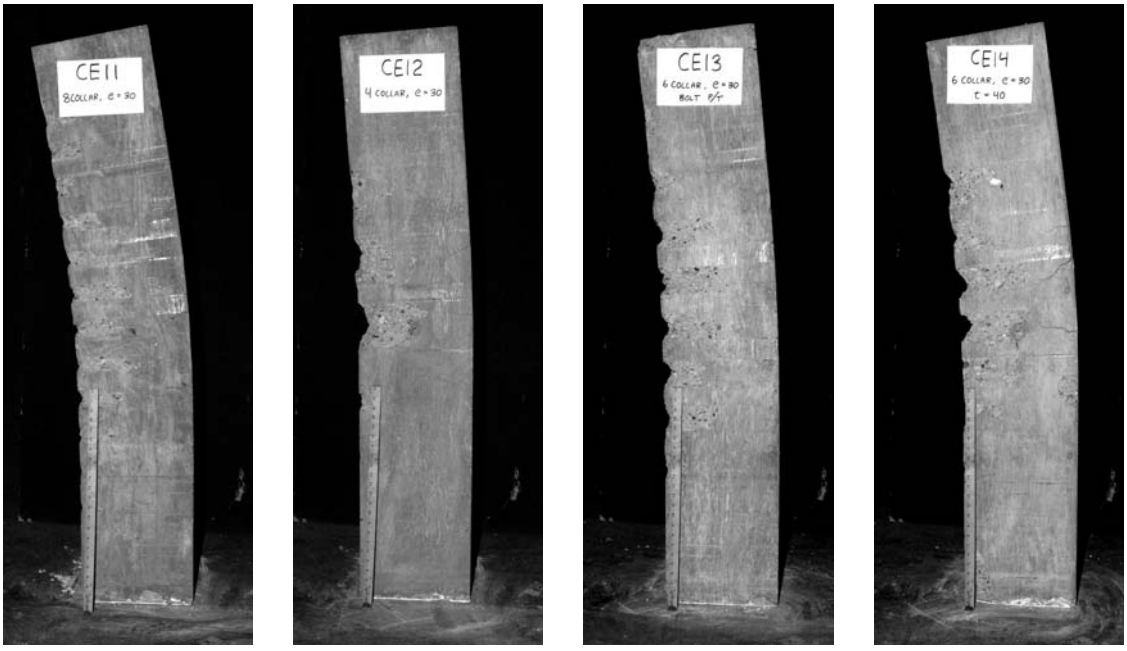

e) CE11 f) CE12 g) CE13 h) CE14

Figure 4.8: Side View of Eccentrically Loaded Specimens After Testing
(scale in photographs is 585 mm long)

4.2.2.2 Axial Load versus Moment Interaction

The behaviour of the eccentrically loaded column specimens is described using the interaction between axial load and moment throughout the column load history, as shown in Figure 4.9. Table 4.2 lists concurrent axial load and moment values at milestones throughout the load history including: the peak load, designated failure load (85% of peak load in the descending branch), and end of test. The strain gradient and position of the neutral axis from the compression face (assuming a linear strain distribution) are reported in Table 4.3. Values of moment and strain gradient are variable along the height of the column due to second order effects. The moments are reported for the mid-height of the column (location of maximum moment). The strain information at the peak load is reported as both the average value over the length of the test region and the value at the mid-height of the column, as indicated in Table 4.3. Average strain values were measured using cable potentiometers on each side of the column, and strain values at the column mid-height were measured using electrical resistance strain gauges bonded to the internal reinforcing bars. Because the strain gauges ceased to function at very large strains, only the average strain values are presented for the failure load and at the end of the test.

Second order effects due to lateral deflection of the column caused a considerable increase in total eccentricity from the initial load eccentricity introduced by offsetting the position of the column from the axis of the testing machine. The maximum effective load eccentricity was a combination of the initial eccentricity, lateral deflection at mid-height of the column, and lateral translation of the loading point as the end support bracket rotated. It will be shown subsequently that the initial eccentricity had a significant effect on the early response of the column, but second order effects tended to dominate the overall response of the column.

The peak load of concentrically loaded specimen CE01 (nominally identical to CE07 through CE10) is indicated in Figure 4.9 to provide a visual comparison of the effect of eccentric loading and end restraint. Figure 4.9 also includes the axial load versus moment interaction curve based on CSA standard A23.3-04, referred to hereafter as the design interaction envelope. The upper limit of the A23.3-04 interaction envelope ($0.8P_o$ or $0.85P_o$, where P_o is the concentrically loaded column capacity) used to account for

accidental column load eccentricities is not included in figures of this report because load eccentricity was a controlled parameter during testing. The design interaction envelope is calculated using a rectangular stress block, measured material strength properties, a maximum concrete strain of 0.0035, and resistance factors taken as unity. The design interaction envelope represents the expected performance of a non-collared column of the same size and with the same longitudinal reinforcing as the specimens tested, and with transverse ties meeting the requirements of the standard. Points inside the design interaction envelope represent safe combinations of axial load and moment, while points outside this curve represent combinations causing failure of the column as specified by the design standard. The failure of all tested specimens occurs well outside the CSA A23.3-04 interaction envelope, showing the substantial increase in capacity achieved using the external collar system under conditions of combined axial load and moment.

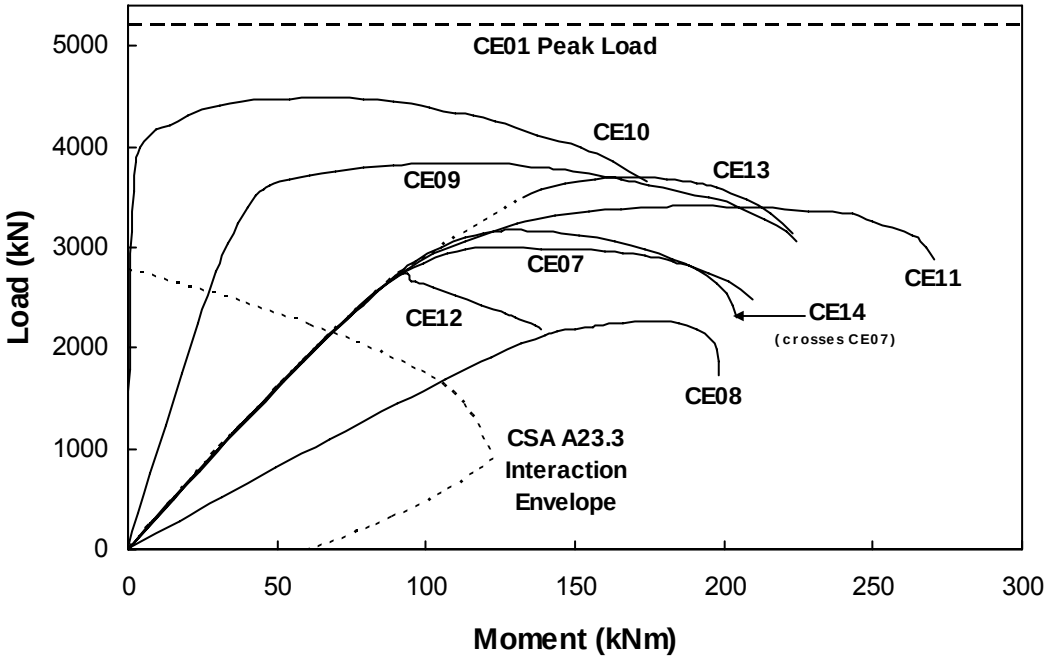

Figure 4.9: Axial Load versus Moment Interaction for Eccentrically Loaded Columns

The initial loading cycle for specimen CE13 was removed from Figure 4.9. Had this cycle with unintentional rotational restraint not occurred, it is expected that specimen CE13 would have initially followed the behaviour of the group of specimens with the same initial load eccentricity (CE07, CE11, CE12, and CE14). As seen in Figure 4.9, all specimens with an initial eccentricity of 30 mm follow the same load versus moment path

and begin to diverge from each other at a common point. The expected interaction curve for specimen CE13 (with pretensioned collar bolts) is shown in the figure as a dashed line until it intersects the actual curve. It is possible that column damage occurring during the initial cycle may have reduced the peak load in the second load excursion. Conclusions about column strength enhancement arising from collar bolt pretensioning are therefore considered to be conservative. However, since the capacity of specimen CE13 was significantly higher than that of CE07 (identical except with snug tight bolts), it is believed that the effect of the initial cycle on the overall behaviour of specimen CE13 is relatively small. The complete axial load versus moment response for specimen CE13, including the initial loading cycle, is shown in Figure 4.10.

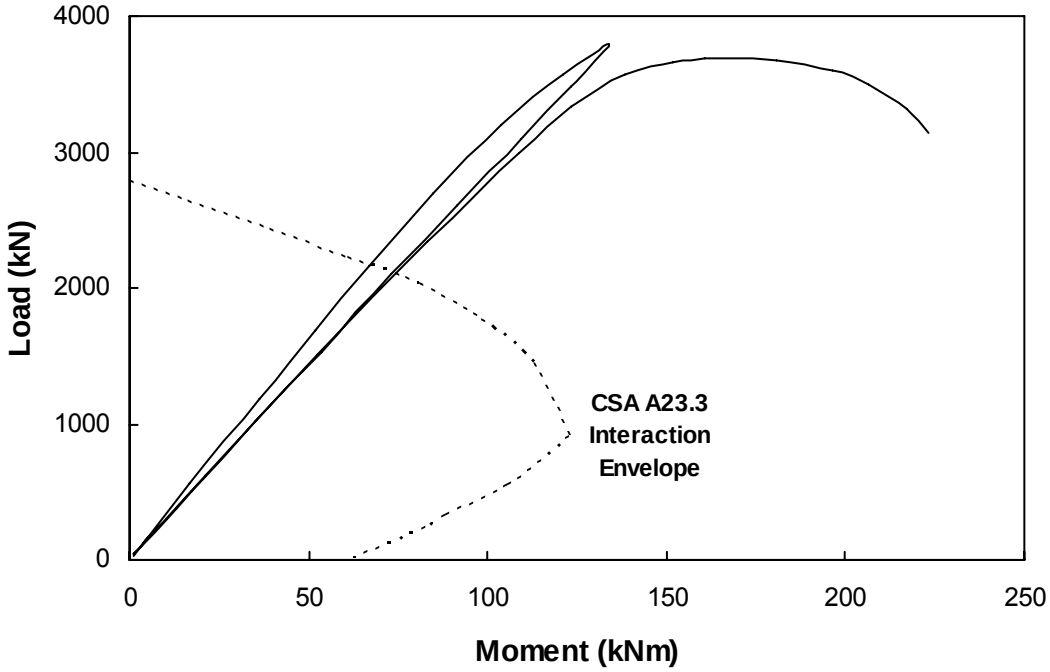

Figure 4.10: Specimen CE13 Axial Load versus Moment Interaction

Inspection of Figure 4.9 shows that the accumulation of moment is highly dependent on the initial eccentricity of the column load. The load versus moment curves have two distinct regions. The initial part of the curve is close to linear and its slope is dependent on the initial load eccentricity. The second region of the curve commences close to the peak load, where rapid accumulation of moment initiates arising from increasing second order eccentricity at the critical cross-section. This leads eventually to failure of the column primarily in bending.

Table 4.2: Eccentrically Loaded Column Response Summary

	Peak		Failure		End of Test	
Specimen	**Load (kN)**	**Moment (kNm)**	**Load (kN)**	**Moment (kNm)**	**Load (kN)**	**Moment (kNm)**
CE07	2997	124	2547	207	2484	209
CE08	2276	177	1935	198	1735	198
CE09	3861	113	3282	215	3049	224
CE10	4490	66	3817	165	3649	174
CE11	3415	193	2903	269	2876	271
CE12	2744	94	2332	128	2191	139
CE13	3695	166	3141	223	3061	225
CE14	3171	127	2695	195	2304	204

Table 4.3: Summary of Average Strain Values Over Test Region

	Peak*			Failure		End of Test	
Specimen	**Strain on Comp. Face**	**Neutral Axis** (mm)**	**Strain Gradient (με/mm)**	**Neutral Axis** (mm)**	**Strain Gradient (με/mm)**	**Neutral Axis** (mm)**	**Strain Gradient (με/mm)**
CE07	0.0100 (0.0138)	251 (246)	40 (56)	211	191	213	201
CE08	0.0126 (0.0154)	200 (200)	63 (77)	172	161	163	208
CE09	0.0197 (0.0276)	274 (290)	72 (95)	229	205	222	237
CE10	0.0202 (0.0248)	321 (314)	63 (79)	256	182	251	203
CE11	0.0217 (0.0267)	233 (226)	93 (119)	202	233	201	237
CE12	0.0048 (0.00729)	300 (270)	16 (27)	222	92	215	121
CE13	0.0132 (0.0137)	254 (253)	52 (54)	216	153	213	163
CE14	0.00904 (0.0104)	266 (254)	34 (41)	211	160	197	223

* Values presented in brackets are measured at the mid-height of the column
** Distance to neutral axis measured from compression face

4.3 Column Load versus Bolt Force Response

Measurement of the force in the collar connection bolts was a convenient way to evaluate when and how the collars began reacting to the behaviour of the column. Monitoring the bolt force also revealed the consistency of the confining pressure; a decrease in the bolt force would expose degradation in the confining pressure. A graph of column load versus bolt force for all concentrically loaded specimens is shown in Figure 4.11 and a similar graph for eccentrically loaded specimens is shown in Figure 4.12. The curve shown for specimen CE04 does not begin until a column axial load of 1400 kN (the point when collars were affixed to that column). The annular load cell used to measure bolt force during testing was also used to measure the bolt pretension applied during attachment of the collars. A bolt pretension of approximately 25 kN was used for most specimens (the variability can be seen in the figures), representing a snug tight condition of the collar intended to secure the collar without slippage. Higher bolt pretensioning of approximately 150 kN (specimens CE05 and CE13) was used to evaluate the influence of active confining pressure on the performance of the collar system.

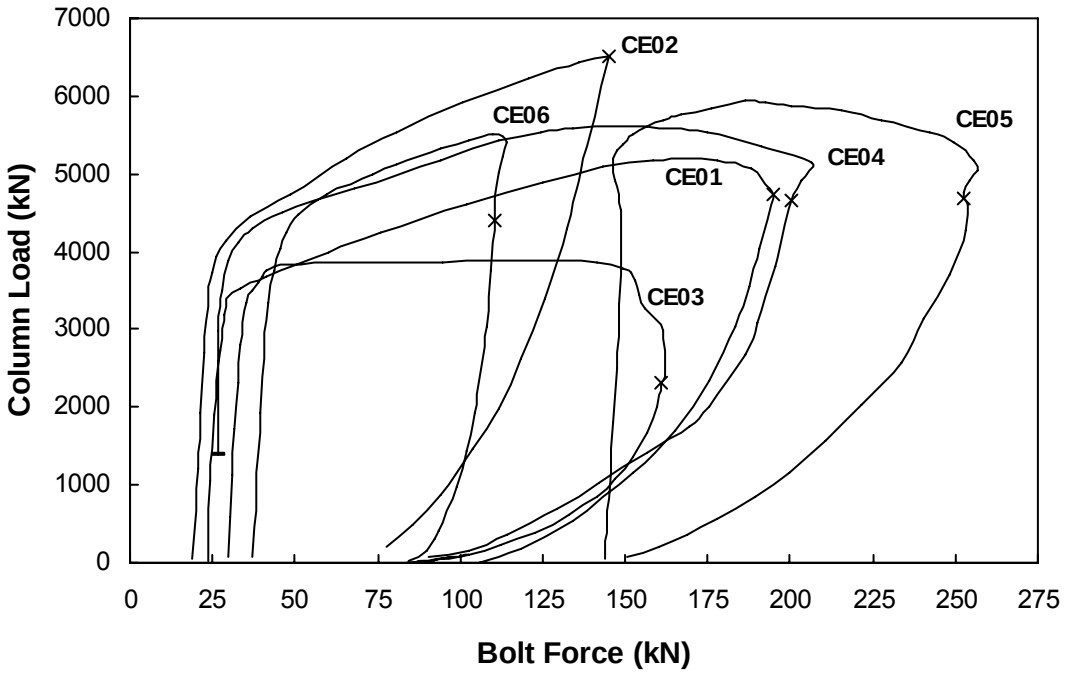

Figure 4.11: Column Load versus Bolt Force for Concentrically Loaded Columns

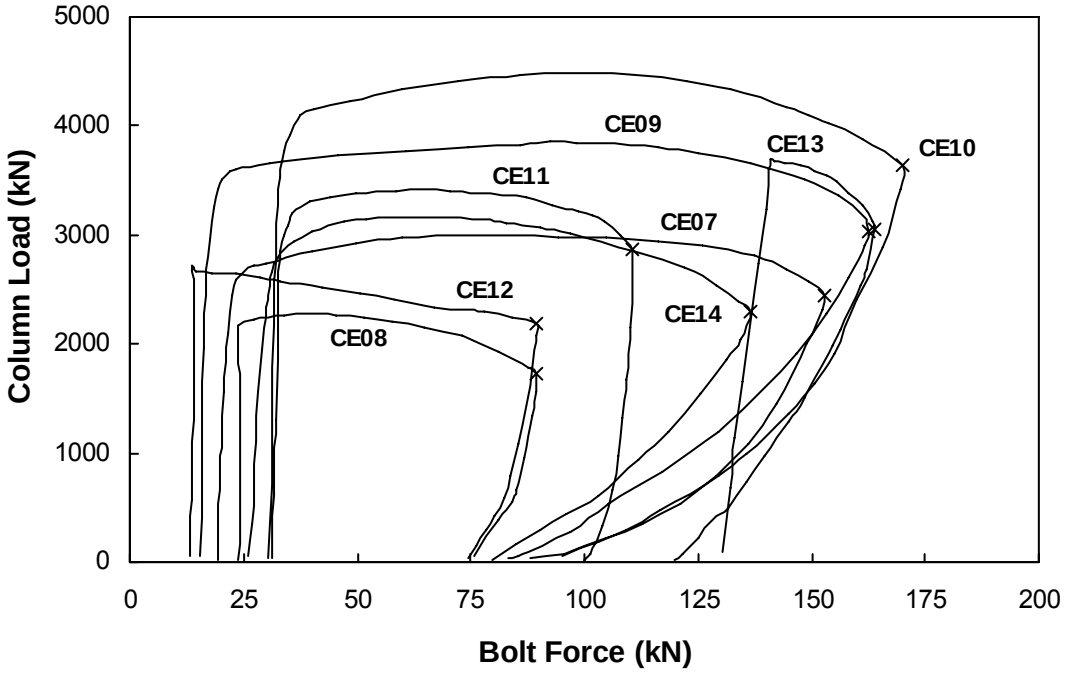

Figure 4.12: Column Load versus Bolt Force for Eccentrically Loaded Columns

The collar bolt force did not begin to increase until well into the load history of the column, as revealed by the nearly vertical initial curves in Figures 4.11 and 4.12. This behaviour implies that the lateral expansion of the column in this load range is very small. The bolt force began rising at approximately the same time as the onset of concrete spalling when the demand on the remaining integral concrete increased. This observation supports the predicted behaviour of the collars which were not expected to be engaged until the column began to dilate significantly.

In Figures 4.11 and 4.12, the point of intentional column unloading at the end of the test is indicated with an '×'. In most cases there is no reduction of bolt force before the column is unloaded, suggesting that the confining pressure from the collar is sustained throughout the load history. In specimens CE04, CE05, and CE06 the bolt load dropped by 5 to 10 kN before column unloading; this slight relaxation of bolt force is considered negligible and occurred well after the peak load of the column was reached. The relaxation of the bolt force during unloading of the column corresponds to the rebounding of the column dilation when load is removed.

The maximum bolt tensile force reached was 260 kN (specimen CE05 with pretensioned bolts), which is equal to approximately 66% of the nominal ultimate tensile strength of the grade A490 bolts used. Grade A325 bolts could also be used as an alternative during implementation of the collar system; the maximum bolt force reached during testing is approximately 83% of the nominal ultimate tensile strength of grade A325 bolts of the same diameter. Observations of the bolts themselves after testing showed that most bolts had deformed plastically in combined tension and bending as adjacent legs of the collar deflected outward. Bolt selection during collar design should also consider the possibility of force amplification due to prying action at the bolted connection; fracture of the bolt would result in a sudden loss of confinement pressure and expedite failure of the column.

4.4 Behaviour of External Collars

Using pairs of electrical resistance strain gauges located at the centre of the column face, the axial strain and strain gradient in selected external collars were monitored during testing. At the failure load many collars had large plastic deformations and a curved appearance between the corners of the column, as shown in Figure 4.13. Other collars had a less pronounced deflected shape.

Figure 4.13: Deformed Shape of Collar During Loading

The behaviour of the collars was evaluated using forces derived from inelastic analysis of the collar cross-section through the strain data collected. The inelastic analysis is based on an exact solution developed by Terro and Hamoush (1996) for analysis of rectangular cross-sections subjected to combined axial and bending forces. A linear distribution of strain and elastic-perfectly plastic behaviour are assumed for the analysis.

The position of the bolted corner is staggered at each collar level, but no correlation was found between the position of the bolt and the collar strains at the centre of the column face. Therefore, the collar strain readings are taken as the average from collars on individual faces of the column (column faces are denoted as North, South, East, or West). Due to symmetry of the loading, the sample size for the strain readings of concentrically loaded columns is further increased by using an average of the strain levels on all four faces of the column.

Due to the large strain database collected from the collars during testing, an axial force versus moment interaction curve format is chosen for presentation. These curves are reported at two points in the load history: the peak column load and the column failure load. The collar axial force versus moment interaction curves for concentrically loaded specimens is given in Figure 4.14 and those for eccentrically loaded specimens in Figures 4.15 and 4.16.

The North face of eccentrically loaded specimens is the compression face of the column, and the most representative location for describing collar behaviour. Collar strain levels on the East, West and South faces of eccentrically loaded columns were comparatively lower than the North face and are reported in Figure 4.16 mainly to display this phenomenon. Only the curves for collars that exhibited significant yielding are labelled in the figure.

The graphs of collar axial force, F, versus moment, M, interaction are normalized by the axial yield force, F_y, and yield moment, M_y, of the collar section. A yield surface (i.e., point of first yielding on the cross-section) and plastic surface (i.e., point of fully yielded cross-section) are also plotted with the interaction curves. Points along the interaction curve between the yield and plastic surfaces represent a partially yielded

cross-section. The yield surface and plastic surface are defined by Equations 4.2 and 4.3, respectively.

$$\frac{F}{F_y} + \frac{M}{M_y} = 1.0 \qquad [4.2]$$

$$\left(\frac{F}{F_y}\right)^2 + \frac{M}{1.5M_y} = 1.0 \qquad [4.3]$$

The axial force versus moment interaction curves in Figures 4.14 to 4.16 report the behaviour of the collar leg at the middle of the column face (where strain gauges were mounted). This location is likely the last position for a plastic hinge to form before the collar leg forms a mechanism; yielding of the collar ends (starting with the bolted end) occur much earlier than the middle of the collar. Considering this, it is important to realize that even if Figures 4.14 to 4.16 do not show yielding at the middle of the collar, yielding may have occurred at the ends of the collar.

Examination of Figures 4.14 to 4.16 reveals important differences between the collar behaviour of the columns with and without a strain gradient. Collars from concentrically loaded columns had a more developed yielded pattern by the time the peak load was reached, while in the case of eccentrically loaded columns, yielding of the collar occurred later in the load history. The exception is column CE03, where the widely spaced collars led to earlier failure and reduced the confinement demand. Furthermore, yielding was generally isolated to the North face (compression face) of the column, and the East and West faces of selected specimens with low initial eccentricity. This observation demonstrates that the collars of the columns with eccentric loading and an associated strain gradient are not engaged to the same degree as those in concentrically loaded columns. Moreover, since the benefits of the presence of collars accrue primarily to the compression region of the cross-section, collars on the columns with steeper strain gradients and less concrete area in compression tended to exhibit smaller deformations.

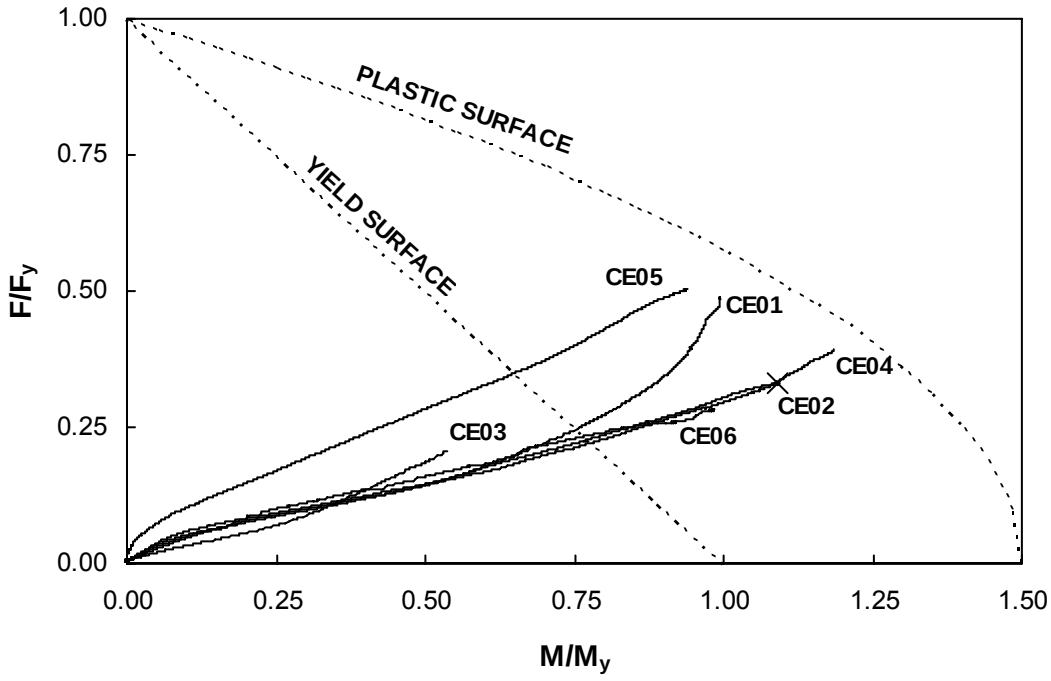

a) At Column Peak Load

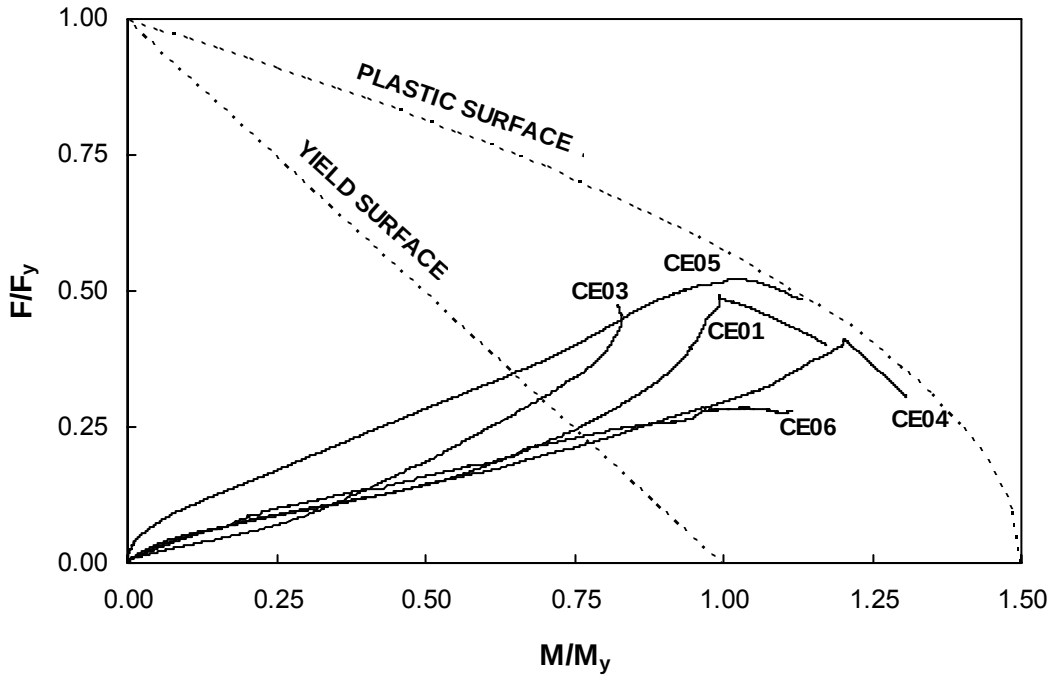

b) At Column Failure Load

Figure 4.14: Collar Axial Force versus Moment Interaction of Concentrically Loaded Columns

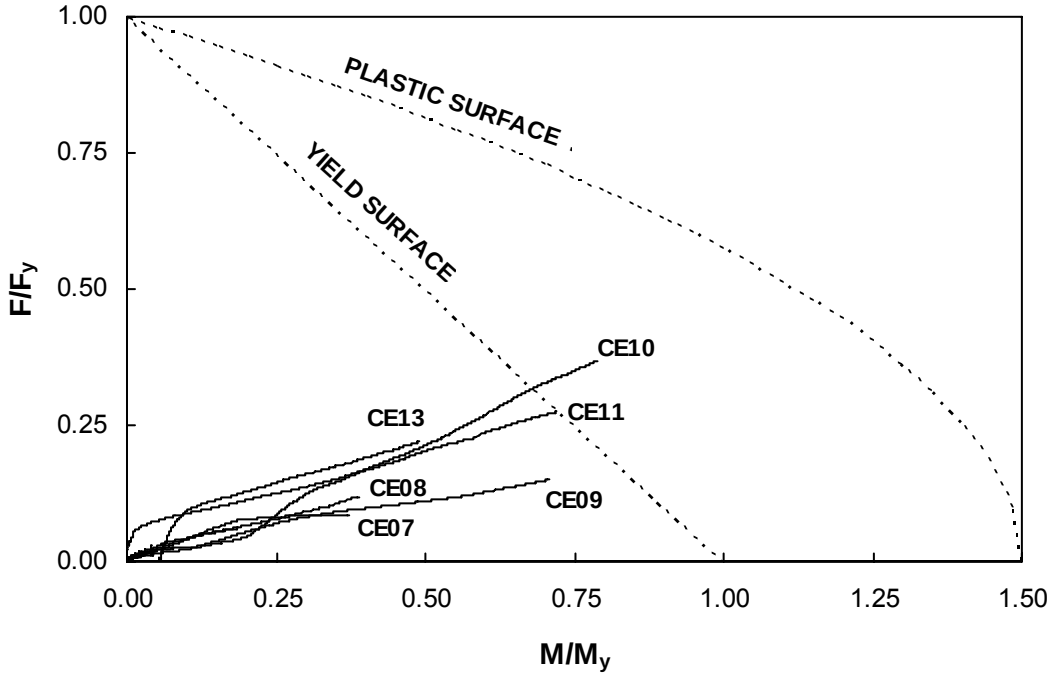

a) At Column Peak Load

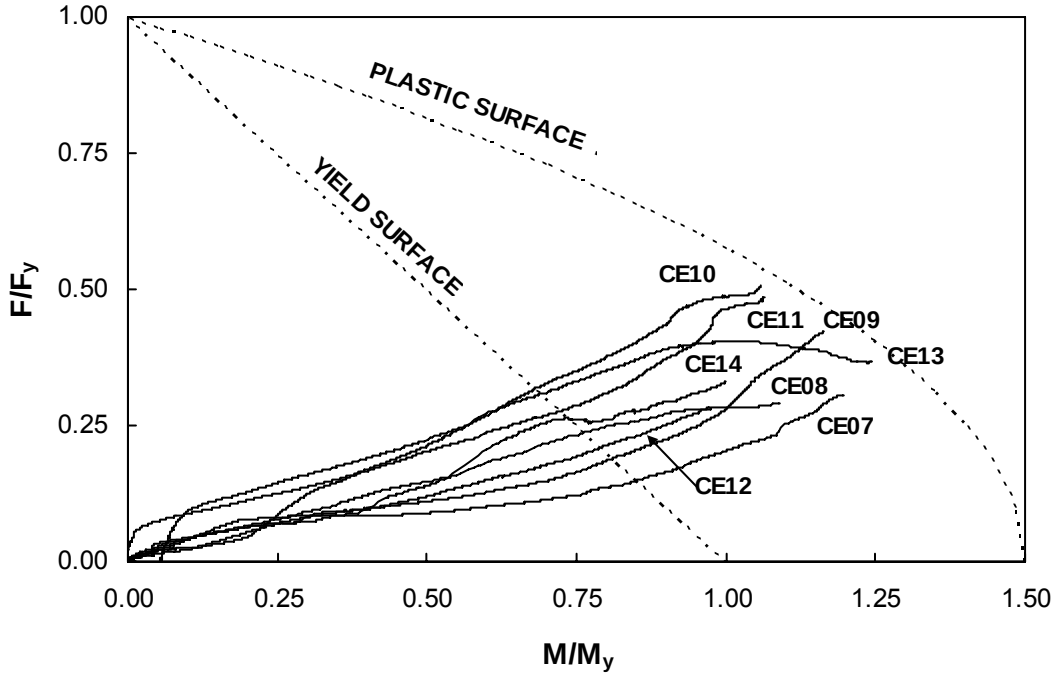

b) At Column Failure Load

Figure 4.15: Collar Axial Force versus Moment Interaction for North Face of Eccentrically Loaded Columns

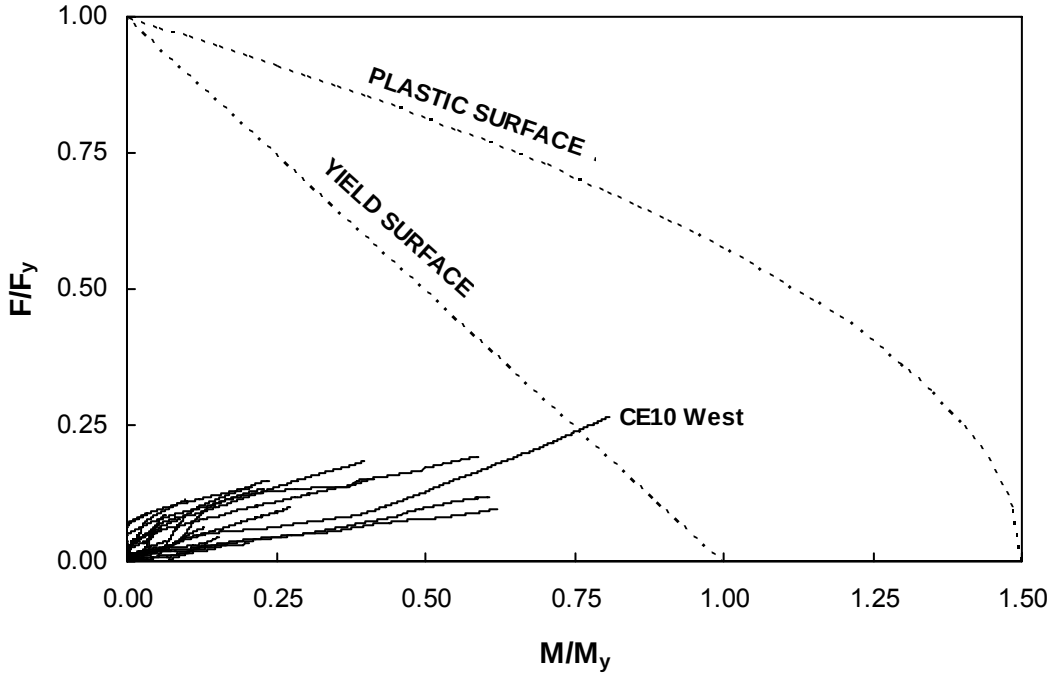

a) At Column Peak Load

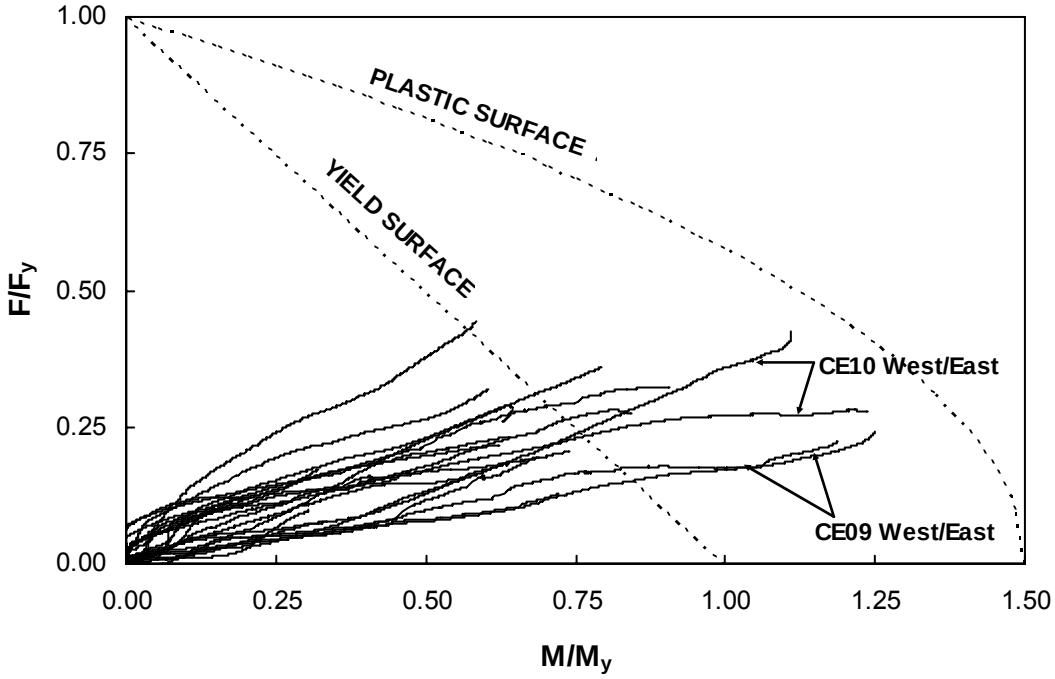

b) At Column Failure Load

Figure 4.16: Collar Axial Force versus Moment Interaction for South, West and East Faces of Eccentrically Loaded Columns

4.5 Discussion of Column Performance Enhancement

The performance of the tested columns is evaluated using ratios of experimental versus theoretical column axial load and moment capacities, as shown in Table 4.4. In order to isolate the benefit achieved from the external collars, the theoretical column capacity is taken as the nominal design capacity of an equivalent non-collared column with tie reinforcement, as described in Section 4.2.2.2. The CSA A23.3-04 design interaction envelope represents all combinations of axial load and moment that would cause failure of a non-collared column, otherwise equivalent to the tested columns. Accordingly, the theoretical capacity of the tested columns is taken as the point that the experimental interaction curve crosses the design envelope. Figure 4.17 shows a typical column interaction curve that crosses the design interaction envelope displaying the selected location of experimental and theoretical values used for comparisons made in this report.

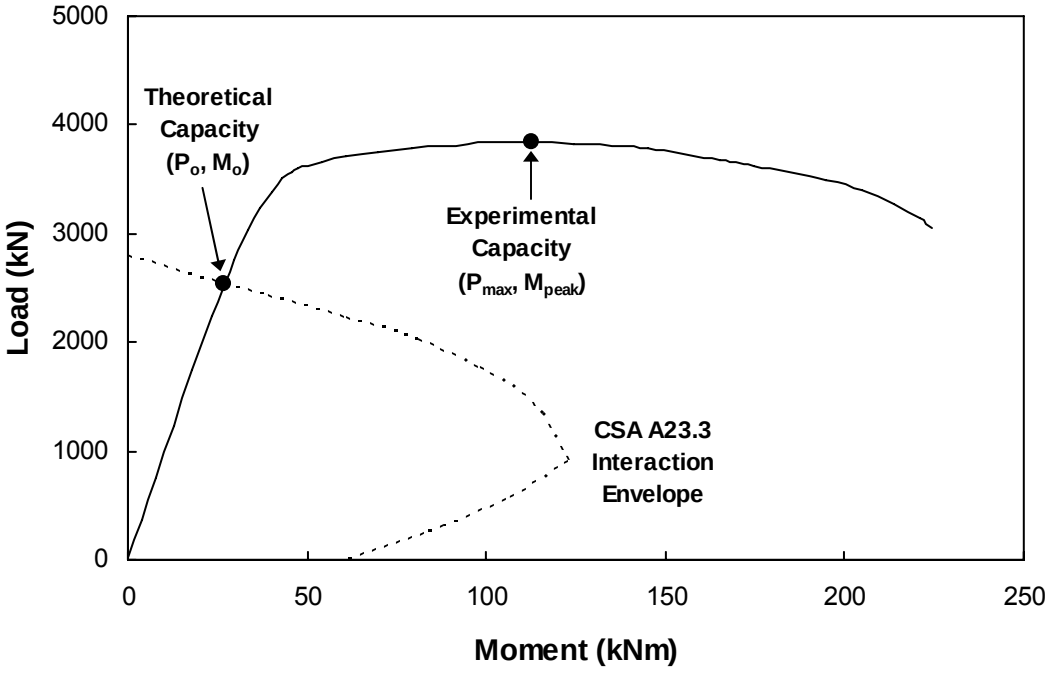

Figure 4.17: Generalized Axial Load versus Moment Interaction

Since the internal reinforcing steel in the column does not benefit from the confinement provided by external collars, two distinct capacity ratios are presented: the total column capacity (including steel reinforcing) and the column concrete-only capacity. For experimental values, the peak concrete-only column capacity, P_{cmax}, is calculated by subtracting the contribution from the internal steel reinforcing from the peak total column

capacity, P_{max}. Similarly, the experimental column concrete-only moment capacity, M_{cpeak}, is calculated by subtracting the steel contribution from the total moment capacity, M_{peak}. The forces in the steel reinforcing are evaluated from strain values recorded at the peak axial load during testing from electrical resistance strain gauges mounted on the reinforcing bars (reported in Table 4.3). The corresponding theoretical values for concrete-only capacity, P_{oc} and M_{oc}, are calculated based on total column capacity, P_o and M_o, by subtracting the contribution of steel reinforcing based on the linear strain distribution assumed in the calculation of the design interaction envelope.

The performance of the columns can be seen by studying the ratios of experimental to theoretical column capacities presented in Table 4.4. Ratios for collared columns are greater than 1.0 due to the benefit achieved from increased confinement levels. Ratios presented for columns C00A and C00B should equal 1.0 as these columns represent the same condition as the theoretical column. However, the P_{max}/P_o ratios for C00A and C00B are 1.12 and 1.06, respectively, with the value for C00B corresponding to the first peak attained. Hussain and Driver (2005a) attributed this discrepancy primarily to variability in the strength of concrete within the test column as compared to the concrete cylinder strengths measured.

The values for axial and flexural strength enhancement of collared columns presented in Table 4.4 are based on the ratio of experimental to theoretical column concrete-only capacity, P_{cmax}/P_{oc} and M_{cpeak}/M_{oc} (there are several exceptions as indicated by table footnotes and explained subsequently). Concrete-only capacities are used because these are believed to be the most indicative values for evaluating the influence of confinement directly. The highest level of axial strength enhancement achieved was 165% by specimen CE02, with concentric loading and the closest collar spacing tested, which is a lower bound value because the column could not be failed in the testing equipment used. The lowest level of strength enhancement achieved was 30% by specimen CE12, with eccentric loading and the widest collar spacing tested. In general, eccentrically loaded specimens had lower axial strength enhancement values than equivalent concentrically loaded specimens. Results varied widely with the variation of test parameters. The influence of specific test parameters on strength enhancement and ductility of columns are discussed in detail in the following sections of this chapter and are summarized in Table 4.5 at the end of the chapter.

Table 4.4: Column Strength Enhancement Summary

	Theoretical				Experimental				Ratios				Strength Enhancement (%)	
Column	P_o (kN)	P_{oc} (kN)	M_o (kNm)	M_{oc} (kNm)	P_{max} (kN)	P_{cmax} (kN)	M_{peak} (kNm)	M_{cpeak} (kNm)	$\frac{P_{max}}{P_o}$	$\frac{P_{cmax}}{P_{oc}}$	$\frac{M_{peak}}{M_o}$	$\frac{M_{cpeak}}{M_{oc}}$	Axial	Flexural
C00A	3114	2597	–	–	3475	2939	–	–	1.12	1.13	–	–	13	–
C00B	3159	2642	–	–	3342* 3419**	2850* 2747**	–	–	1.06*	1.08*	–	–	96 §	–
CE01	2786	2252	–	–	5200	4666	–	–	1.87	2.07	–	–	107	–
CE02	2786	2252	–	–	6500§§	5966§§	–	–	2.33§§	2.65§§	–	–	165§§	–
CE03	2786	2252	–	–	3905	3371	–	–	1.40	1.50	–	–	50	–
CE04	2786	2252	–	–	5607	5073	–	–	2.01	2.25	–	–	125	–
CE05	2786	2252	–	–	5950	5416	–	–	2.14	2.40	–	–	140	–
CE06	2786	2252	–	–	5516	4982	–	–	1.98	2.21	–	–	121	–
CE07	2150	1818	68.4	51.8	2997	2649	124	109	1.39	1.46	1.81	2.10	46	110
CE08	1570	1363	108	81.0	2276	2276	177	133	1.45	1.67	1.64	1.64	67	64
CE09	2535	2148	26.8	14.7	3861	3327	113	113	1.52	1.55	4.22	7.68	55	668
CE10	2780	2252	0.50	0	4490	3956	66	66	1.62	1.76	132	†	76	13 100††
CE11	2150	1818	68.4	51.8	3415	3258	193	162	1.59	1.79	2.82	3.13	79	213
CE12	2150	1818	68.4	51.8	2744	2361	94	82	1.28	1.30	1.37	1.58	30	58
CE13	2150	1818	68.4	51.8	3695	3308	166	154	1.72	1.82	2.43	2.97	82	197
CE14	2150	1818	68.4	51.8	3171	2805	127	113	1.47	1.54	1.86	2.18	54	118

* Value for first load peak
** Value for second load peak
§ Using P_{cmax}/P_{occ} ratio for second peak
§§ Lower bound value
† Denominator of ratio equals zero (M_{oc}=0)
†† Using M_{peak}/M_o ratio

Specimen C00B, with closely spaced ties, had two distinct peak loads and is consequently treated differently than other specimens while examining the performance of the column. The theoretical column capacities, P_o and P_{oc}, are computed using the overall column dimensions (including cover), which is appropriate for comparison with the first peak reached. However, by the second peak all of the cover concrete had spalled away leaving only the core concrete intact. A modified theoretical column capacity based on the column core area only, P_{occ}, is used for comparison with the second peak load. The resulting ratio P_{cmax}/P_{occ} for specimen C00B equals 1.96. Using this ratio, the axial strength enhancement value for specimen C00B reported in Table 4.4 is 96%, which is representative of the benefit from confinement of the remaining core concrete achieved using closely spaced internal reinforcing ties based on the seismic design criteria of standard A23.3-04. Clearly, most of this strength benefit is unusable due to the concomitant reduction in column area due to cover spalling.

Specimen CE10 is also treated differently than other specimens in Table 4.4. In order to provide a more tangible value for comparison, the flexural strength enhancement value reported for specimen CE10 (13 100%) is based on the total column capacity because the value based on the concrete-only capacity equals infinity. The reason for these high values is that the interaction curve of specimen CE10 crosses the A23.3-04 design interaction envelope before starting to accumulate second order moments. Consequently, the second order bending effects significantly increased the experimental value of moment but did not influence the theoretical moment value.

In the following sections, comparisons between specimens are made using the difference (i.e., one value subtracted from the other) in the strength enhancement values (shown in Table 4.4) of those specimens. This difference in strength enhancement, although reported as either an increase or decrease in percent, should not be confused with the mathematical operation for calculating the percentage difference between two numbers. The comparison is intended to show increased or decreased performance achieved as compared to the theoretical (unconfined) column capacity, rather than the percent benefit or disbenefit of one collar configuration compared to the other.

4.5.1 Effect of Collar Spacing

Collar spacing was found to be the most influential test parameter when comparing column strength enhancement and ductility values. Increased collar spacing caused decreases in both column strength and ductility. The region of unconfined concrete between collars, which spalled away during loading, is defined by the arching action of the concrete between the collars. As the collar spacing is increased, the depth of the unconfined concrete region becomes larger, decreasing the concrete area that benefits from the collar confinement.

By comparing specimens CE03 (4 collars), CE01 (6 collars) and CE02 (8 collars), the effect of collar spacing on column strength enhancement of concentrically loaded specimens can be seen. Specimens CE03, CE01, and CE02 had axial strength enhancements of 50%, 107% and 165%, respectively. A similar comparison can be made for eccentrically loaded columns by comparing specimens CE12 (4 collars), CE07 (6 collars), and CE11 (8 collars), all with an initial eccentricity 30 mm. Specimens CE12, CE07, and CE11 had axial strength enhancements of 30%, 46% and 79%, respectively, and flexural strength enhancements of 58%, 110% and 213%, respectively. Clearly, as collar spacing is decreased higher axial and flexural strength enhancements are achieved.

Hussain and Driver (2005b) found that for concentrically loaded columns, doubling the clear spacing between collars resulted in approximately a 60% decrease in axial strength gain for the range of collar spacings they tested. They developed a relationship using the ratio of the larger to the smaller clear collar spacing, s_1'/s_2', of two specimens to calculate the associated ratio in axial strength enhancement, N:

$$N = \left(\frac{s_1'}{s_2'} \right)^{-1.5} \qquad [4.4]$$

Based on Equation 4.4, comparisons among specimens with 4, 6 and 8 collars in the test region give values for the ratio s_1'/s_2' of 1.60, 1.67, and 2.67; the resulting ratios of axial strength enhancement, N, are 0.49, 0.46, and 0.23, respectively. Only one of the

three comparisons is available for concentrically loaded columns because the true capacity of specimen CE02 is unknown; for the ratio s_1'/s_2' of 1.67 (columns CE01 and CE03), the experimental value of N is 0.47, which is very close to the predicted value of 0.46. For the other two ratios, Equation 4.4 implies that Specimen CE02 would have achieved a capacity of 7690 kN, which appears from Figure 4.3 to be a reasonable estimate. The associated comparisons among the eccentrically loaded columns give values for N of 0.58, 0.65 and 0.38. Thus, Equation 4.4 has good accuracy when making comparisons of the concentrically loaded specimens but appears not to be appropriate for the eccentric specimens tested. In all eccentrically loaded cases, the reduction in strength enhancement caused by increasing the collar spacing is less than that predicted by Equation 4.4. This result suggests that eccentrically loaded specimens are less sensitive to collar spacing than concentrically loaded specimens.

Strain at peak stress (shown in Table 4.1 for concentrically loaded specimens and Table 4.3 for eccentrically loaded specimens) is used as an indicator of column axial ductility for comparison among specimens. By comparing the strain at peak stress of concentrically loaded specimens CE01 (6 collars) and CE03 (4 collars) it can be seen that an increase in collar spacing causes a decrease in column ductility. Specimen CE01 had a strain at peak stress of 0.0344, while specimen CE03 had a much lower strain at peak stress of 0.0104. Increased collar spacing had a similar effect on eccentrically loaded columns which can be seen by comparing specimens CE11 (8 collars), CE07 (6 collars), and CE12 (4 collars). Specimens CE11, CE07, and CE12 had average strains at peak stress of 0.0217, 0.0100, and 0.0048, respectively on the compression face of the column.

Besides the effects arising from reduced concrete confinement efficiency, the lower capacity and ductility of columns with larger collar spacings can also be attributed to the lack of support provided to the longitudinal steel reinforcing in the spaces between collars. The longitudinal reinforcing bars of specimen CE03 buckled in several locations along the column height (shown in Figure 4.16) causing accelerated failure of the column, although the behaviour is still markedly better than a conventionally tied column such as C00A. In a rehabilitation scenario, existing columns would have internal reinforcing ties that provide additional support to the longitudinal bars; if these tie locations can be determined, wider spacings of external collars could potentially be

used. Alternatively, the spacing of external collars could simply be designed to provide adequate lateral support for the specific diameter of longitudinal bars in the column to be rehabilitated, neglecting the presence of the ties.

Figure 4.16: Specimen CE03 - Buckling of Longitudinal Reinforcing

4.5.2 Effect of Collar Flexural Stiffness

The collars used in this experimental program have solid rectangular cross-sections; therefore, changing the flexural stiffness of the collar, while keeping the axial stiffness constant, also requires an adjustment of the collar width. Consequently, the flexural stiffness of collars could not be investigated without also affecting the collar clear spacing. In maintaining the centre-to-centre collar spacing, the specimens with the larger collar flexural stiffness have a 10 mm wider collar clear spacing. Based on Equation 4.4, this difference in collar spacing would result in a strength enhancement ratio, N, of 0.82 for the concentrically loaded case and it would likely be somewhat closer to 1.0 for the eccentric case, as discussed in the previous section. Therefore, the increase in collar

clear spacing would be expected to offset some of the benefit achieved from the increased collar flexural stiffness.

Two different geometries of external collars were investigated to evaluate the effect of their flexural stiffness on the behaviour of tested columns. The collar geometries were selected to maintain approximately the same cross-sectional area of steel, allowing an investigation of the most efficient material usage. Specimens CE06 and CE14 had external collars with a moment of inertia equal to 417×10^3 mm^4, while all other specimens had collars with a moment of inertia equal to 229×10^3 mm^4. Comparison of the results between concentrically loaded specimens CE01 and CE06 shows that an increase in collar flexural stiffness of 82% results in an increase in axial strength enhancement of 14% of the unconfined case. However, comparison of the results between eccentrically loaded specimens CE14 and CE07 shows that the same increase in collar flexural stiffness only provides an increase in axial strength enhancement of 8%. This result suggests that collar flexural stiffness is less influential when the collars are used on eccentrically loaded columns. However, these results quantify the differences in strength enhancement as compared to the theoretical unconfined case. Due to the generally higher degree of enhancement in the concentric cases considered here, the percentage benefit in enhancement is about the same for the concentric and eccentric cases when the two collared columns in each group are compared to each other.

Values of strength enhancement for specimens CE06 and CE14 are considered to be a lower bound when referring to the influence of the collar flexural stiffness due to the counteracting effect of the wider collar spacing discussed earlier. Nonetheless, it seems that there is a relatively small benefit achieved from a significant increase in collar flexural stiffness. This result suggests that there is an optimal collar flexural stiffness, beyond which there are diminishing returns, a conclusion consistent with observations of Hussain and Driver (2005a) for columns with HSS collars.

The influence of collar flexural stiffness on column ductility could not be fully isolated from the effect of differences in collar clear spacing. However, by examining the axial load versus strain curve of specimen CE06 (Figure 4.3), it is evident that the behaviour of the column can be divided into two distinct zones. The first zone shows the influence of the increased collar flexural stiffness, which improves the column strength over that of

CE01. The second zone shows the eventual dominance of the wider collar clear spacing, which decreases the column ductility causing accelerated degradation of the column after the peak load. Similar observations can be made for eccentrically loaded columns from Figure 4.8 by comparing the response of column CE14 with that of CE07.

4.5.3 Effect of Active Confining Pressure

Through bolt pretensioning, an active confining pressure was applied to specimens CE05 and CE13. The active confining pressure provided significant improvement in column strength enhancement in both cases. Specimens CE05 and CE13 had strength enhancements of 140% and 82% over their theoretical non-collared column capacities. These values are 33% and 36% higher for CE05 and CE13, respectively, compared with their column counterparts without active confining pressure (CE01 and CE07). The benefits in column capacity are clearly event in Figures 4.3 and 4.8. Specimen CE13 also had an increase in flexural strength enhancement of 197% over the theoretical non-collared column.

The effect of active confining pressure on the ductility of concentrically loaded specimens can be seen by comparing the strain at peak stress of specimens CE01 and CE05. Specimens CE01 and CE05 reached peak loads at axial strain values of 0.0344 and 0.0189, respectively. In addition, the capacity of specimen CE05 decreased more rapidly than CE01 in the post-peak region. Therefore, by applying an active confining pressure, the strength of the column was increased but the column ductility was decreased. Hussain and Driver (2005b) made similar observations about specimens with active confining pressure in their test program. The introduction of active confining pressure did not have a discernable influence on the ductility of eccentrically loaded specimens; strains at peak stress for specimens CE07 and CE13 were similar.

4.5.4 Effect of Column Preloading

In order to simulate the service condition of an existing building column needing rehabilitation, specimen CE04 was preloaded to 1400 kN before the external collars were installed. Preloading of specimen CE04 without collars did not result in any degradation in column performance. In fact, specimen CE04 had 18% higher strength

enhancement than CE01 and achieved the highest level of axial strain at failure in the test program. The discrepancy between the behaviour of specimen CE01 and CE04 may be attributed to the inclusion of internal reinforcing ties in specimen CE04, which were required to prevent premature buckling of the longitudinal reinforcing during preloading. Despite their strategic positioning at the same elevations as the external collars, the ties may have contributed to the delay of softening of the concrete in specimen CE04.

4.5.5 Effect of Load Eccentricity

Distinction is required between the effect of strain gradient and the effect of load eccentricity, even though these two test parameters are interrelated. In section 4.5.6, comparisons are made between specimens with and without a strain gradient. In this section, comparisons are made between specimens that both have strain gradient but also have varying levels of bending moment due to variation of the initial load eccentricity.

A decrease in initial load eccentricity resulted in lower values of bending moment at the peak column load and generally higher values of strength enhancement when eccentricity was the only variable. Specimens CE08 (e=60 mm), CE07 (e=30 mm), CE09 (e=10 mm), and CE10 (e=0 mm) had moment values at peak load of 177 kN·m, 124 kN·m, 113 kN·m, and 66 kN·m, respectively. The axial strength enhancement values for those specimens (CE08, CE07, CE09 and CE10) are 67%, 46%, 55% and 76% and values for flexural strength enhancement are 64%, 110%, 668% and 13 100%, respectively. As discussed previously, the flexural strength enhancement value reported for specimen CE10 (13 100%) is based on the total column capacity and is comparatively large because of the influence of second-order moments.

The different levels of initial load eccentricity used had a well-defined influence on the axial load versus moment interaction curves. Each load eccentricity (0 mm, 10 mm, 30 mm, or 60 mm) gave rise to a curve that had a distinct initial slope, as shown in Figure 4.19. This point is exemplified by the observation that all five specimens tested with 30 mm eccentricity followed the same initial slope and then began to diverge at a common point (shown in Figure 4.20).

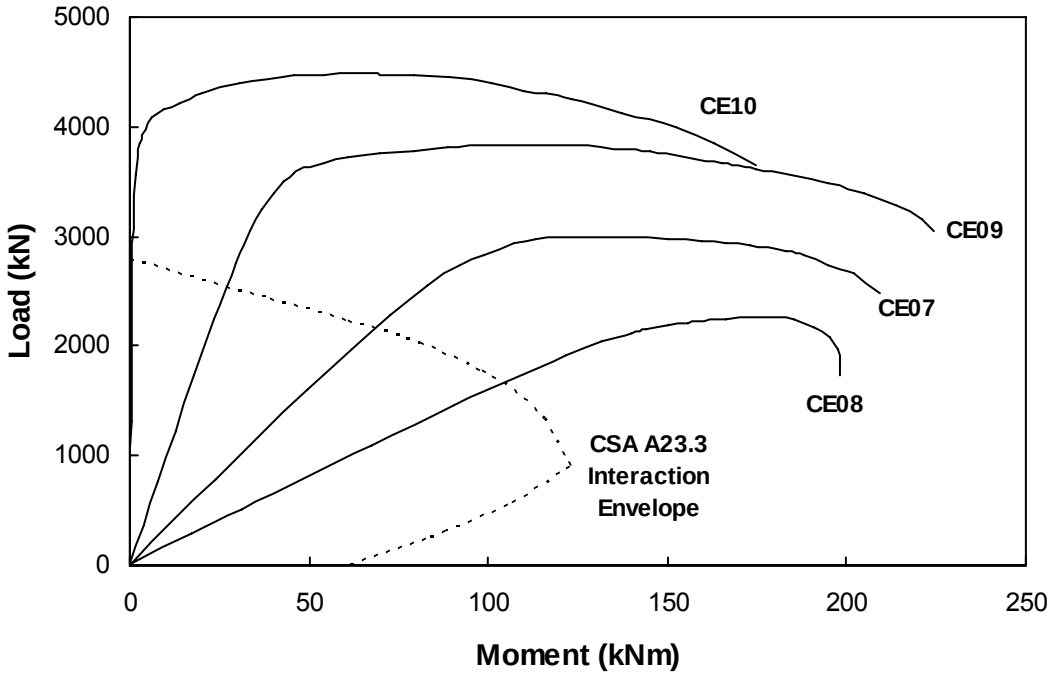

Figure 4.19: Axial Load versus Moment Interaction of Comparable Specimens with Different Initial Load Eccentricities

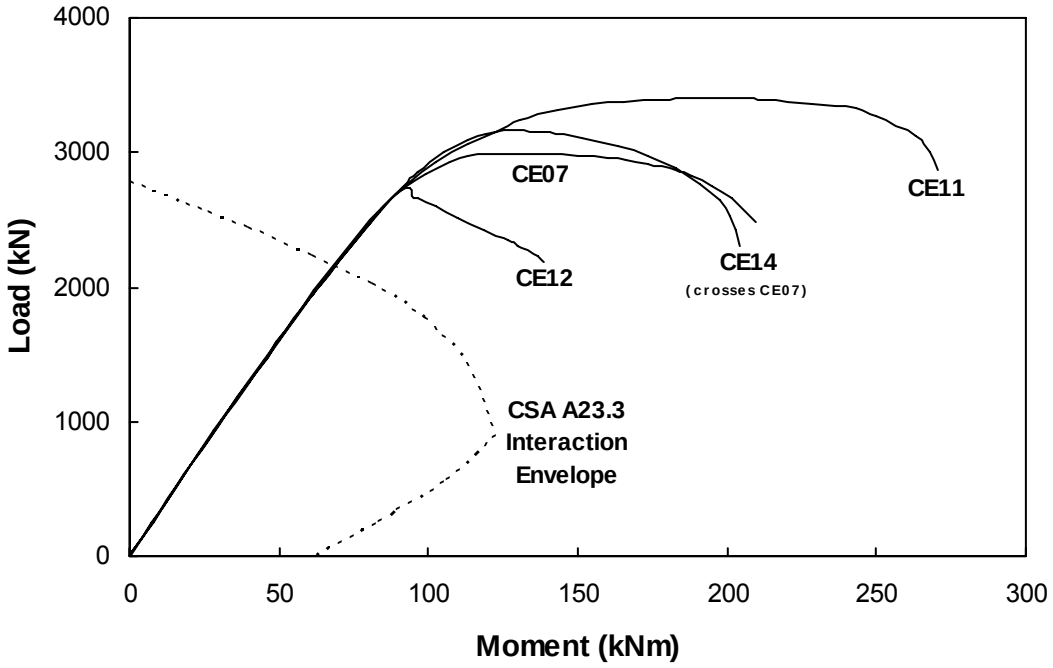

Figure 4.20: Axial Load versus Moment Interaction for Specimens with 30 mm Initial Load Eccentricity

4.5.6 Effect of Strain Gradient

Strain gradient was not a controlled parameter in this experimental program. However, the general influence of the presence of a strain gradient on the column cross-section is of interest and is examined in the following discussion.

All concentrically loaded specimens except CE04 had eccentrically loaded counterparts that differed only in the inclusion of strain gradient. To show the influence of strain gradient, comparisons can be made between the following pairs of specimens: CE01 and CE07, CE01 and CE08, CE01 and CE09, CE01 and CE10, CE02 and CE11, CE03 and CE12, CE05 and CE13, and CE06 and CE14. The variation of other test parameters (i.e., collar spacing, collar stiffness, bolt pretension, and initial load eccentricity) among the different pairs of specimens being compared does not allow a general trend to be developed using all pairs. Nevertheless, comparison within each pair allows the influence of strain gradient to be demonstrated. Specimens with a strain gradient had between 20% and 86% lower axial strength enhancement values compared with equivalent concentrically loaded specimens. The lower extreme (20%) pertains to the widest spaced collars and the upper extreme (86%, which would have been higher had specimen CE02 reached its ultimate capacity) pertains to the most narrowly spaced collars. All comparisons of columns with the middle collar spacing fell between these extremes. When comparing the four pin-ended columns with various eccentricities (CE07 through CE10) to the concentrically loaded column with fixed ends (CE01), the larger initial eccentricities did not necessarily result in the greatest reduction in strength enhancement, indicating the importance of the second order effects. In fact, in specimen CE10 the strain gradient existed only because of second order effects. Specific results can be found in Table 4.5.

The general trend of lower strength enhancement with columns that have a strain gradient can be explained using the behaviour of the collar confinement mechanism. In order for the column to benefit from the confining action of the external collars, it must dilate outward under the presence of compressive axial strain, engaging the collar. When a strain gradient is present, the level of concrete dilation varies across the column section, or in the case of tensile strain the concrete will not dilate at all. Therefore, both the amplitude and distribution of strain have an influence on the effectiveness of the

confinement mechanism. Only regions of the column cross-section with an axial compressive strain adequately high to cause significant dilation will benefit from the confining pressure that develops as the dilation is restrained by the collar. This phenomenon is reflected in Figures 4.12 through 4.14, which show that yielding of the collar occurs mainly on faces of columns that are in compression.

4.5.7 Effect of Column End Restraint

By examining the difference in performance between specimens CE01 and CE10, the effect of the different column end restraints can be seen. Specimen CE01 was loaded concentrically with a fixed end condition. Specimen CE10 was also loaded concentrically but had end fixtures that allowed free rotation, creating a pinned end condition. The failure mode of these specimens was very different due to the second order moments that developed in specimen CE10. However, specimen CE10 behaved similar to CE01 until very close to the peak load when second order moments began to accumulate, as shown in Figure 4.8. The peak load of specimen CE01 was 5200 kN, while CE10 only reached 4490 kN; from Table 4.4 the associated values of strength enhancement are 107% and 76%, respectively. Therefore, the reduction in axial strength enhancement due to the pinned end restraint is 31%, showing the large effect on capacity of the second order effects. This reduction in strength enhancement is relatively low compared with nominally identical columns tested using larger initial eccentricities. The cross-section of specimen CE10 remained fully in compression with little strain gradient until very close to the peak load, allowing the concrete to receive more benefit from collar confinement than other specimens with less favourable strain distributions.

Table 4.5: Column Strength Enhancement Comparison Summary

Parameter Changed	Specimens Compared	Parameter Change Description		Strength Enhancement Difference (%)	
				P	M
Collar Clear Spacing	CE01 – CE02	72 to 45 mm (6 vs 8 collars)		+ 58 *	–
	CE01 – CE03	72 to 120 mm (6 vs 4 collars)		- 57	–
	CE07 – CE11	72 to 45 mm (6 vs 8 collars)		+ 33	+ 103
	CE07 – CE12	72 to 120 mm (6 vs 4 collars)		- 16	- 52
Collar Stiffness	CE01 – CE06	229×10^3 to 417×10^3 mm^4		+ 14	–
	CE07 – CE14	229×10^3 to 417×10^3 mm^4		+ 8	+ 8
Active Confinement (Bolt P/T)	CE01 – CE05	25 to 144 kN		+ 33	–
	CE07 – CE13	25 to 135 kN		+ 36	+ 87
Column Preload	CE01 – CE04	0 to 1400 kN		+ 18	–
Initial Load Eccentricity (pinned ends)	CE10 – CE09	0 to 10 mm		- 21	–
	CE10 – CE07	0 to 30 mm		- 30	–
	CE10 – CE08	0 to 60 mm		-9	–
Strain Gradient	CE01 – CE07	constant strain (e = 0 mm with fixed ends) to strain gradient (pinned ends)	e=30 mm	- 61	–
	CE02 – CE11			- 86 *	–
	CE03 – CE12			- 20	–
	CE05 – CE13			- 58	–
	CE06 – CE14			- 67	–
	CE01 – CE10		e=0 mm	- 31	–
	CE01 – CE09		e=10 mm	- 52	–
	CE01 – CE08		e=60 mm	- 40	–

* Lower bound value

4.6 Summary and Conclusions

Fourteen columns were tested to evaluate the performance of a rehabilitation technique for reinforced concrete columns using a system of discrete external steel collars. Columns were tested under both concentric and eccentric monotonic loading. Parameters investigated include: collar spacing, collar flexural stiffness, active confining pressure, and load eccentricity. The following main conclusions were identified:

- Through the development of passive confining pressure, columns with external collars show significant improvements in both strength and ductility compared with conventionally reinforced columns. The maximum level of column axial strength enhancement achieved during testing was 165%. At peak load, concentrically loaded collared columns reached axial strain levels 5 to 17 times higher than would be expected for unconfined normal strength concrete (taken here as 0.002).

- Collar spacing was found to be the most influential parameter on the performance of specimens tested; increasing collar spacing resulted in decreased strength and decreased ductility enhancement.

- Only a marginal benefit in strength enhancement was achieved from a significant increase in the collar flexural stiffness, suggesting that there is an optimal collar flexural stiffness beyond which there are diminishing returns. Increasing the collar flexural stiffness appeared to decrease the ductility of the column, although a slightly larger clear spacing for the higher stiffness collars may have influenced this result somewhat.

- The application of an active confining pressure through pretensioning of the collar connection bolts provided up to a 36% increase in column axial strength enhancement over equivalent columns without active confining pressure. However, reductions in ductility were observed for concentrically loaded columns.

- Eccentrically loaded specimens generally had lower strength enhancement than equivalent concentrically loaded specimens. The reduced effectiveness of the collar system in columns with bending is attributed to the decrease in lateral dilation of the

column due to the presence of a strain gradient on the cross-section, which lowers the applied confining pressure.

- Installing the external collars after a column is under significant preload was found not to decrease the eventual strength or ductility of the column as compared to the case of installing the collars prior to the application of any axial load. Therefore, all test results are considered to be directly applicable to rehabilitations conditions.

5. ANALYTICAL MODEL

5.1 Introduction

The analytical model presented in this chapter provides a means of predicting the behaviour of axially loaded concrete columns that have been rehabilitated using steel collars. It is based on the work presented by Hussain and Driver (2005b), except that it eliminates the need for finite element modelling to determine the confining pressures induced by the collars. As an alternative, the proposed model uses a simplified plastic analysis to predict confinement pressures. The primary objective of this part of the research program was to provide a means of predicting the column capacity under concentrically applied load. The secondary objective was to trace the column behaviour throughout the loading history up to the peak load. The predicted load history is partially extended into the descending branch of column response to display the potential for the model to trace the full load history, and also to highlight specific requirements for future development of the model.

5.2 Prediction by Current Models

The success of an analytical model is largely rooted in its ability to describe the material behaviour of all elements in the system accurately. Confined concrete columns have two main elements: concrete and confining devices. Accurate models for confined concrete behaviour have already been established (e.g., Kent and Park (1971); Sheikh and Uzumeri (1982); and Mander et al. (1988a)) that have been substantiated by the work of many researchers. Consequently, the current challenge in modelling confined column behaviour is the ability to describe the behaviour of the confining elements themselves, as well as their interaction with the column response.

Typically, confinement for concrete columns is provided internally using transverse steel reinforcing bars (ties), but recent research has focused on external confinement using thin steel jackets or composite materials, primarily as a means of strengthening existing columns. Those confining devices are significantly different from the steel collars used in the present study. Thus, established models are unable to predict confinement levels

developed using steel collars. The failure of the existing models, as reported by Hussain and Driver (2005b), is a result of one or more of the following reasons:

a) Existing confinement models lack an explicit flexural stiffness parameter. The significance of the flexural stiffness of steel collar confining elements has been demonstrated through finite element analysis by Hussain and Driver (2001).

b) Many conventional models for confinement using internal transverse steel reinforcement assume for simplicity that a constant confining pressure is applied throughout the loading history. This assumption is justified in cases where the reinforcement yields prior to reaching the column capacity. However, because of the substantial strength of steel collars they may only experience partial yielding. Thus, the variation of the confining pressure under the collars throughout the loading history must be accounted for.

c) Most existing models are unable to accommodate the combination of active and passive confining pressures that can be achieved through pretensioning of bolted collar connections.

In order to demonstrate that the existing confinement models are unable to predict the behaviour of concrete confined by collars with high axial and flexural stiffness, Hussain and Driver (2005b) analyzed a typical collared column using the following models: modified Kent and Park model (Park et al., 1982); Sheikh and Uzumeri (1982); Mander et al. (1988a); Saatcioglu and Razvi (1992); and Légeron and Paultre (2003). None of these confinement models was able to provide a good prediction of the behaviour of the collared column.

With the aforementioned deficiencies in mind, Hussain and Driver (2005b) presented two analytical models to predict the behaviour of collared columns. The first model required the use of finite element modelling software to generate the confining pressure versus lateral expansion response of the collars. The second model used an empirical approach with non-dimensional parameters to describe the confinement pressure. The latter model was specific to cases with hollow structural section (HSS) or solid collars, rectangular in cross-section, having rigid corner connections. Both models gave excellent predictions

of the column behaviour observed in tests. The collars in the present research program utilize a combination of continuous and bolted corner connections, a condition that violates the boundary conditions imposed by the empirical model of Hussain and Driver. Furthermore, the dependence on finite element modelling is seen as a being impractical for use in a design scenario. A simplified design approach that covers a wide range of collar configurations is presented in the following sections.

5.3 Model for Prediction of Collared Column Behaviour

This section describes the development of independent behavioural representations for the steel collar and the confined concrete based on a simple rational approach. Once these independent relationships have been established, an equilibrium confining pressure can be calculated based on displacement compatibility, which expresses the interaction between the two elements (see Section 5.3.3).

5.3.1 Collar Behaviour

The following sections describe the development of an idealized relationship between collar lateral deflection and confining pressure that is independent of the concrete behaviour. The collar behaviour is ultimately expressed by a single term, the collar secant modulus, E_{collar}, which is the ratio of collar pressure to lateral strain.

5.3.1.1 Collar Beam Element Idealization

Confinement collars can be fabricated in many different configurations using standard structural shapes (HSS, channels, etc.) or solid sections (bar stock, flat plate, etc.). There are also many different methods with which the collars can be secured to the column exterior (clamping using bolted collar corners, welding the collar corners and then grouting, etc.). As such, a generalized approach to modelling is required. The proposed collar model uses the following idealizations (also shown in Figure 5.1):

a) Collars are modelled as elastic beam elements between the corners of the column with a length equal to the width of the column, h. The beam elements have flexural and axial stiffnesses equal to those of the collar section used.

b) Collar corner connections and the element mid-span are modelled as rigid–plastic hinges (for rotation only). The connection is considered to undergo plastic rotation once the following condition is met:

$$\left(\frac{F}{F_y}\right)^2 + \frac{M}{M_p} = 1.0 \qquad [5.1]$$

where F and F_y are the axial force present in the element and the force that would cause yielding of the element in the absence of bending moment, respectively, and M and M_p are the bending moment present at the hinge location and the plastic moment capacity of the element in the absence of axial force, respectively. Although Equation 5.1 is a closed form solution that applies to rectangular cross-sections, for simplicity it is used for all cross-sections in the current analysis (the implications of this assumption are discussed in Section 5.3.1.4). Other equations could be derived for more complex shapes. Moreover, the cross-sectional capacity could be limited to account for local buckling, if applicable.

c) The pressure developed under the collar, σ_{collar}, is idealized as an equivalent uniform pressure applied to the beam element.

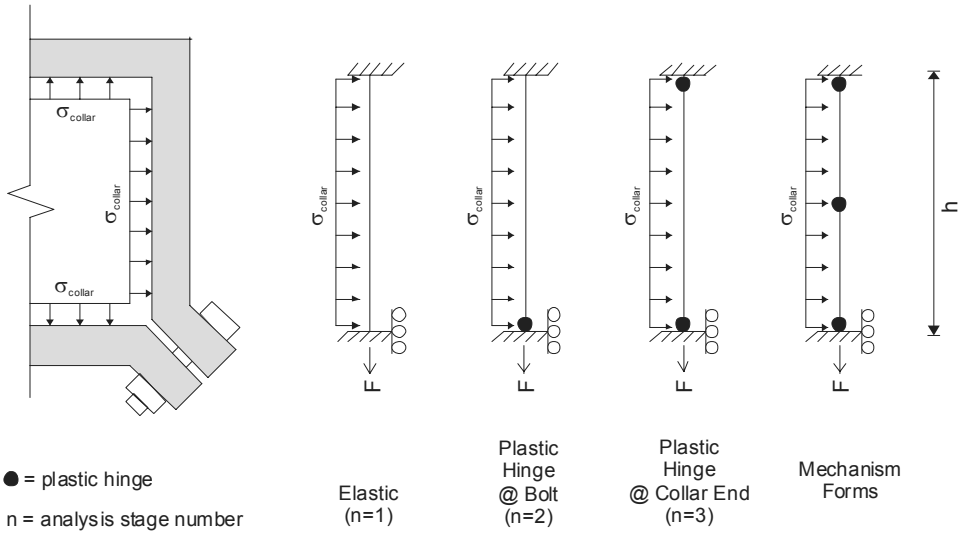

Figure 5.1: Collar Beam Element Idealization

5.3.1.2 Plastic Analysis of Collars

An incremental plastic analysis of the beam element is performed to determine the uniform pressure that will cause plastic hinging at each end of the collar (bolted or continuous), in turn, and finally between the two ends (at which time a mechanism forms). The beam element behaves elastically within each stage of the plastic analysis, with the appropriate boundary being updated to a plastic hinge after each stage. The behaviour of the collar beam element and the location of plastic hinging along the element change throughout the analysis; variables are thus given an index notation to indicate which analysis stage, n, they represent. The stages depicted in Figure 5.1 are particular to the type of collars tested during the present research. In the cases of continuity at all collar corners or bolts at all corners, the two ends of the beam element would hinge under the same pressure, followed by the mid-point, resulting in the ends of stages 1 and 2 occurring simultaneously.

Equation 5.2 governs the development of a plastic hinge in a given analysis stage, n, due to some combination of axial tension, $F_{n\,total}$, and bending moment, $M_{n\,total}$. The axial tension force is introduced into the collar beam element from the pressure on the collar legs of the adjacent column faces and pretensioning of the bolts at the corners of the collar.

$$\left(\frac{F_{n\,total}}{F_y}\right)^2 + \frac{M_{n\,total}}{M_p} = 1.0 \qquad [5.2]$$

The values F_y and M_p refer to the axial yield force and plastic bending moment of the collar element at the location where the next hinge will form during a specific analysis stage. For collar arrangements using bolted corner connections, the values of F_y and M_p refer to the capacity of the bolt itself when hinging is occurring at the bolted end of the beam element.

The collar axial force, F_n, and bending moment, M_n, induced during a particular analysis stage, n, are defined by Equations 5.3 and 5.4, respectively, and are functions of the incrementally applied pressure, σ_n. The total collar axial force, $F_{n\,total}$, and total bending

moment, $M_{n\,total}$ are defined by Equations 5.5 and 5.6, respectively, and include a summation of the axial force and bending moment from the current and previous analysis stages.

$$F_n = \frac{\sigma_n th}{2} \qquad [5.3]$$

$$M_n = \frac{\sigma_n th^2}{C} \qquad [5.4]$$

$$F_{n\,total} = \sum_{i=1}^{n-1} F_i + F_n \qquad [5.5]$$

$$M_{n\,total} = \sum_{i=1}^{n-1} M_i + M_n \qquad [5.6]$$

The value σ_n is defined as the additional (incremental) collar pressure required to cause the next plastic hinge to occur. The contact surface between the collar and concrete is defined by the beam element thickness, t, and length, h. The coefficient C is related to the bending moment of the elastic curve and is equal to a value of 12 initially (stage n = 1), and eight after the first plastic hinge has formed (stage n = 2 or n = 3).

Equation 5.2 can be solved for the incremental collar pressure, $\sigma_{n,}$ during each stage of the plastic analysis. The equation can be solved using the general solution for a quadratic equation; the final form of which is:

$$\sigma_n = \frac{-\left(\frac{\sum F_i th}{F_y^2} + \frac{th^2}{CM_p}\right) + \sqrt{\left(\frac{\sum F_i th}{F_y^2} + \frac{th^2}{CM_p}\right)^2 - \left(\frac{th}{F_y}\right)^2 \left[\left(\frac{\sum F_i}{F_y}\right)^2 + \frac{\sum M_i}{M_p} - 1.0\right]}}{0.5\left(\frac{th}{F_y}\right)^2} \qquad [5.7]$$

Although the indices have been removed from above and below the summation signs (Σ) in Equation 5.7, in all cases the summation is performed over all analysis stages preceding the current stage, as indicated in Equations 5.5 and 5.6.

Ultimately, as the collar pressure, σ_{collar}, is increased, the beam element will form a mechanism. The mechanism load determined from the plastic analysis is considered the maximum collar pressure, σ_{max}, that can be developed by that collar:

$$\sigma_{max} = \sum_{n=1}^{3} \sigma_n \qquad [5.8]$$

The collar pressure then remains constant at this maximum value as the beam element continues to deflect outward due to the dilation of the concrete beyond the point required to form the mechanism in the collar.

5.3.1.3 Collar Pressure versus Lateral Strain Relationship

The lateral deformation of the collar beam element, Δ_n, during a particular analysis stage includes components from bending, Δ_{bend}, and axial elongation of the adjacent sides, Δ_{axial}, that are both functions of the collar pressure, σ_n, applied during that stage. In order to generate an average value of lateral strain across the width of the column, the collar bending deflection is averaged over the length of the beam element by integrating the area under the elastic deflection curve and dividing by h. This idealization also helps to offset the assumption of a uniformly distributed collar confinement pressure, which is known to vary along its length, increasing near the corners of the column due to the additional restraint offered by the collar legs on the adjacent sides. As a result of the incremental approach, both components of the lateral deflection are calculated using elastic equations (presented in Table 5.1). Aside from localized rotation at plastic hinges (modelled as true hinges in stages subsequent to the hinge formation), all deformation is assumed to be elastically distributed over the length of the beam. The total collar deflection at the end of each analysis stage, $\Delta_{n\,total}$, is calculated by adding deflections from previous analysis stages, Δ_i, to the deflection during the current stage, Δ_n:

$$\Delta_{n\,total} = \sum_{i=1}^{n-1} \Delta_i + \Delta_n \qquad [5.9]$$

$$\Delta_n = \Delta_{bend} + \Delta_{axial} \qquad [5.10]$$

The average lateral strain at the end of each analysis stage, $\varepsilon_{lat\,n}$, is described by Equation 5.11.

$$\varepsilon_{lat\,n} = \frac{2\Delta_{n\,total}}{h} \qquad [5.11]$$

Table 5.1: Equations for Collar Beam Element Deflection

Analysis Stage * n	**Beam End Condition**	**Elastic Deflection Curve $\Delta(x)$ ****	**Bending Deflection Δ_{bend}**	**Axial Deflection Δ_{axial}**
1	fixed / fixed	$\frac{\sigma_n t x^2 (h-x)^2}{24 E_s I_{collar}}$	$\frac{\sigma_n t h^4}{720 E_s I_{collar}}$	$\frac{\sigma_n t h^2}{4 A_{collar} E_s}$
2	fixed / pinned	$\frac{\sigma_n t x (h^3 - 3hx^2 + 2x^3)}{48 E_s I_{collar}}$	$\frac{\sigma_n t h^4}{320 E_s I_{collar}}$	$\frac{\sigma_n t h^2}{4 A_{collar} E_s}$
3	pinned / pinned	$\frac{\sigma_n t x (h^3 - 2hx^2 + x^3)}{24 E_s I_{collar}}$	$\frac{\sigma_n t h^4}{120 E_s I_{collar}}$	$\frac{\sigma_n t h^2}{4 A_{collar} E_s}$

* These stages correspond to a collar with a mixed bolted/continuous end condition

** The quantity x represents the distance from the beam end (pinned end for stage 2)

The resulting relationship between collar pressure and lateral strain is a multi-linear curve that represents the behaviour of the collar throughout the loading of the column. A generalized curve is shown in Figure 5.2. The common points along the curve between linear sections represent the formation of plastic hinges, after which the behaviour of the collar changes (becomes less stiff). A distinct curve exists for each combination of collar section properties, corner connections, bolt pretension, and column size.

The collar pressure versus lateral strain relationship cannot be described by a single continuous function without making additional assumptions because the behaviour of the

collar changes during each stage of the plastic analysis. Instead, the behaviour of the collar is described using the collar secant modulus, E_{collar}, which is defined as the current collar pressure divided by the corresponding lateral strain from the multi-linear curve generated during the plastic analysis, as shown in Figure 5.2.

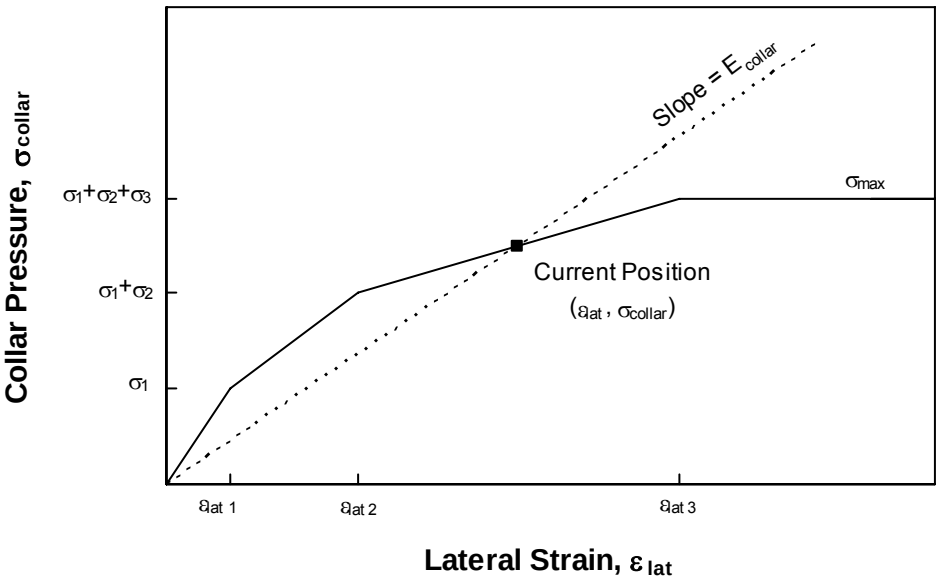

Figure 5.2: Generalized Collar Pressure versus Lateral Strain

The collar pressure versus lateral strain curves for the present experimental program are shown in Figure 5.3 and comparable curves for the tests by Hussain and Driver (2005a) are shown in Figure 5.4. The orientation of the collars represented in Figures 5.3 and 5.4 in all cases is the same as that of the collars used in testing, with the longer length perpendicular to the column face except for the 50x38 solid collar which has the 50 mm side parallel to the column face. Plastic hinging at bolted corner connections occurs relatively early in the load history due to the small cross-section of the bolt as compared to the collar itself. Consequently, the first segment of the curve is truncated close to the origin in those cases. Where bolt pre-tensioning has been implemented, plastic hinging at the bolts is further expedited. Because of this, the idealization of considering the bolted connections to be fixed until the bolt plastifies is not particularly influential in the overall behaviour. The bolt cross-section assumed in the development of the curves in Figure 5.3 neglects the threads because the threaded length in the bolts used was relatively short and the plastic deformation of the bolts was observed to occur mainly in the unthreaded shank.

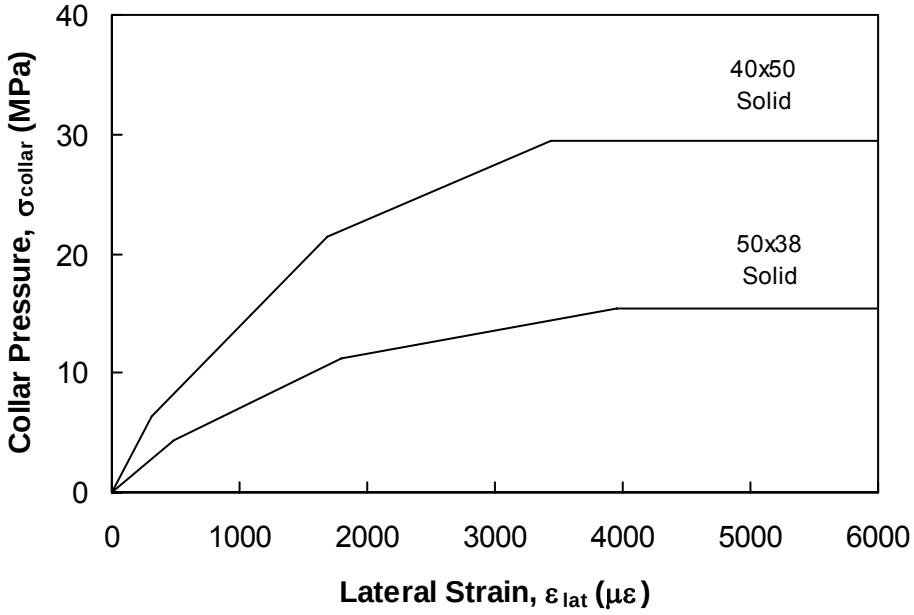

Figure 5.3: Collar Pressure versus Lateral Strain (current research)

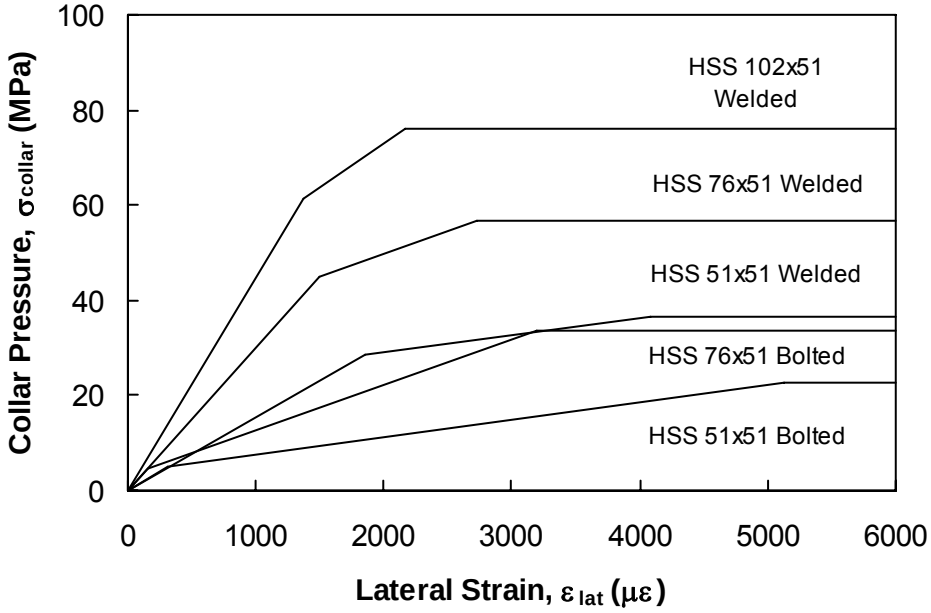

Figure 5.4: Collar Pressure versus Lateral Strain (Hussain and Driver (2005a) research)

The general lateral deflection of the collar, Δ_{collar}, due to any applied uniform pressure can be determined using the procedures described above based on the plastic analysis. If the secant modulus, E_{collar}, is known for a particular pressure, σ_{collar}, the lateral displacement of the collar under that pressure can be conveniently expressed as follows:

$$\Delta_{collar} = \frac{h\sigma_{collar}}{2E_{collar}} \qquad [5.12]$$

The total confining pressure developed by the collar system has two components: an active component from the clamping action of the collar when bolted connections are pretensioned, and a passive component that develops due the restraint of dilation of the concrete under axial compression. The collar pressure versus lateral strain curves shown in Figures 5.3 and 5.4 do not explicitly distinguish between these two components since, as mentioned previously, they are generic lateral pressure terms. However, in considering the compatibility condition between the steel collar and the concrete column (Section 5.3.3), Equation 5.12 is considered to represent only the passive pressure component. The active portion of the confining pressure is a constant value that is added to the passive pressure derived from the compatibility condition in order to determine the total confining pressure. However, there is an indirect influence from the active confining pressure on establishing compatibility under the passive pressure; the pretensioning of bolted connections introduces an axial force into the collar and bolts, which accelerates the collar plastic hinging.

5.3.1.4 Discussion of Collar Modelling Assumptions

The approach presented above is distinct from other models because of the simple behavioural modelling of the confinement collars based on a generalized plastic analysis. Several simplifying assumptions regarding the inelastic behaviour of the beam element have been made:

a) By assuming rigid-plastic behaviour at plastic hinge locations and elastic beam behaviour between the hinges, the effects of partial plasticity are neglected.

b) Plastic hinges are modelled using true hinge behaviour, thus inelastic rotation is assumed to occur at a point (i.e., the length of the plastic hinge is neglected).

c) Due to the modelling of the hinge as purely rotational, axial force is permitted to accumulate in the hinge after the rotational hinge is triggered. Furthermore, the inelastic elongation of the beam element at the plastic hinge is not captured by the model. However, axial deformation is accounted for by assuming an elastic distribution along the length of the beam element throughout the analysis.

d) The equation used to describe the plastic hinging condition (Equation 5.2) applies to solid rectangular cross-sections, but for simplicity it has been utilized for all cross-sections in the current model. The implication of this assumption is that the plastic hinging of bolts (circular cross-section) is not modelled correctly. However, the plastic hinging of the bolts occurs early in the load history and has a relatively small influence on the overall behaviour of the collar. Thus, the use of a single equation for the plastic hinging condition was felt to be warranted.

e) The location of the final collar hinge (at formation of a mechanism) is assumed, for simplicity, to occur at the midpoint of the collar beam element. Due to asymmetric support conditions, the true location of the final hinge will be slightly offset from the midpoint in collars with mixed connection types (e.g., bolted and continuous corners).

f) The effect of the active confining pressure on the beam element is assumed to be purely axial. It is believed that differences in the mode of application of the active pressure (through bolt pretensioning) compared with the passive pressure result in different collar behaviour.

These assumptions simplify the analysis procedure significantly and improved inelastic modelling would likely require the use of a computer software package, which is seen as being contrary to the intended practicality of the model.

As the column dilates laterally, collar elements are subjected to a combination of tension and bending. There is a second order effect from the tensile force, neglected in the

analysis, which reduces the total collar lateral deflection and tends to increase the confining pressure produced by the collar. Using a computer model of the collar beam element generated using the commercial software SAP2000 (Computers and Structures 2004), the second order influence of the tensile force was found to be acceptably small justifying its exclusion from the simplified model.

Further justification of the assumptions made is demonstrated by the effectiveness of the approach (as discussed in Section 5.3.7.2) over a range of collar sizes and configurations, including both solid and HSS members, and corner connections, including bolted, welded, and combined bolted/continuous.

5.3.2 Concrete Behaviour

The following procedure for modelling concrete behaviour was developed by Hussain and Driver (2005b) and is repeated here for convenience. The net concrete lateral displacement can be described using the superposition of two loading conditions. First, the concrete is loaded axially and allowed to dilate laterally without restriction. The free lateral expansion of the concrete outward, Δ_{co}, is governed by the Poisson effect:

$$\Delta_{co} = \frac{\nu_c h \varepsilon_{cc}}{2} \qquad [5.13]$$

where ν_c is the secant Poisson's ratio of concrete at the applied axial strain, ε_{cc} is the axial strain, and h is the column width. Second, a uniform confining pressure, σ_h, is imposed on the concrete surfaces in the two directions orthogonal to the original uniaxial strain. The inward lateral contraction of the concrete, Δ_{ci}, is described by the following plane stress constitutive relationship:

$$\Delta_{ci} = \frac{(1-\nu_c) h \sigma_h}{2E_c} \qquad [5.14]$$

where E_c is the secant modulus of the concrete, defined as the ratio of concrete stress to its associated axial strain. By utilizing secant values of the material properties, ν_c and E_c,

and a constant value of confining pressure, σ_h, an incremental approach is required to trace the full response of the concrete, but as long as the increments are relatively small the behaviour within each increment can be considered linear. Therefore, the net lateral displacement of the concrete, Δ_c, due to a column axial load and uniform lateral confining pressure is found by the summation of the previous two equations:

$$\Delta_c = \Delta_{co} - \Delta_{ci} \qquad [5.15]$$

Analogous to the discussion in Section 5.3.1 relating to the collar behaviour, in considering the compatibility condition between the steel collar and the concrete column (Section 5.3.3), Equation 5.15 is considered to represent only the passive pressure component.

The secant Poisson's ratio, ν_c, required for the determination of Δ_c in Equation 5.15, varies throughout the column load history and also varies with the magnitude of the confining pressure. Gardner (1969) tested concrete cylinders and reported average lateral strain versus axial strain curves at different levels of confining pressure, σ_h. Using those results, Fam and Rizkalla (2001) developed the following empirical relationship for the secant Poisson's ratio, which is used in the present model:

$$\nu_c = \nu_{co}\left[C_1\left(\frac{\varepsilon_{cc}}{\varepsilon_{cc}'}\right)+1\right] \le 0.5 \qquad [5.16]$$

$$C_1 = 1.914\left(\frac{\sigma_h}{f_{co}'}\right) + 0.719 \qquad [5.17]$$

where ν_{co} and ε_{cc}' are the initial Poisson's ratio and strain at peak stress of confined concrete, respectively, the latter of which varies with the confining pressure. The parameter f_{co}' is the unconfined concrete material strength. General agreement on a suitable upper limit for the effective (i.e., including dilation due to cracking) Poisson's ratio of concrete at high levels of axial strain could not be found in the literature reviewed. However, an upper limit of 0.5 is imposed on the secant Poisson's ratio in the present investigation as suggested by Madas and Elnashai (1992).

5.3.3 Confining Pressure

Independent models have been established in the previous two sections for the behaviour of the collar and concrete when subjected to generic confining pressures, σ_{collar} and σ_h, respectively. The formulation of an equilibrium passive confining pressure is achieve by simultaneously satisfying both static equilibrium and lateral displacement compatibility at the interface between the collar and the concrete. The compatibility condition states that the concrete surface and collar surface remain in contact throughout the column load history, during which the passive pressure is mobilized. This condition is supported by experimental observation, as there was no separation of the collar and concrete observed during testing.

The lateral displacement compatibility condition over the column load history (i.e., for all levels of passive confining pressure) between the collar and the concrete surface is:

$$\Delta_{collar} = \Delta_c \qquad [5.18]$$

where Δ_{collar} is determined from Equation 5.12 and Δ_c from Equation 5.15. By equating the collar pressure, σ_{collar}, and the column pressure, σ_h, to the equilibrium passive confining pressure, $\sigma_{passive}$, Equation 5.18 can be solved for the equilibrium passive confining pressure:

$$\sigma_{passive} = \frac{\nu_c \varepsilon_{cc}}{\frac{1}{E_{collar}} + \frac{(1-\nu_c)}{E_c}} \qquad [5.19]$$

If an active confining pressure, σ_{active}, exists due to bolt pretensioning, it is calculated separately and then added to the equilibrium passive confining pressure to calculate the total confining pressure, σ_{total}:

$$\sigma_{total} = \sigma_{passive} + \sigma_{active} \qquad [5.20]$$

The addition of the active confining pressure results in an upward shift of the total confining pressure curve. A generalized total confining pressure curve, showing active and passive pressure components, is shown in Figure 5.5.

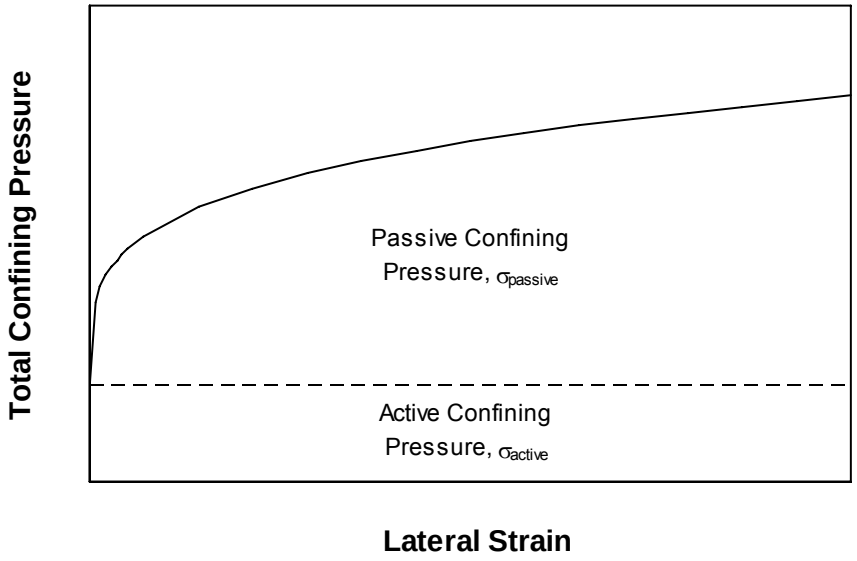

Figure 5.5: Generalized Total Confining Pressure Curve

5.3.4 Confinement Efficiency

Although the confining pressure derivation in the previous sections implies a uniform pressure along the column height, the proposed collar system actually provides confinement in discrete strips under the collars themselves and the remaining concrete is confined only by bridging action. Consequently, due to the spacing of the collars there are regions that are confined less effectively than at the collar level.

No concrete spalling was observed at the collar level during testing of columns in this research program. Based on this observation, it is assumed that due to the high flexural and axial stiffnesses of the collars, there are no ineffectively confined regions at the collar level. (Note that the stiffnesses have already been taken into account in the derivation of the confinement pressure itself.) However, there are ineffectively confined regions between the collars that spall during loading of the column. The spalled regions were observed to be approximately parabolic in shape. Previous researchers have also

reported parabolic-shaped spalled concrete regions (Hussain and Driver (2005a), Sheikh and Uzumeri (1982), Saadatmanesh et al. (1994), Cusson and Paultre (1995), Mander et al. (1988b)). An average maximum spalling depth of 0.25s', measured close to the peak column load, was observed during the testing of concentrically loaded columns of the present experimental program. Hussain and Driver reported a slightly larger average maximum spalling depth of 0.29s'. However, they based the clear spacing of their collars on the full width of the HSS collars, as opposed to the contact width of the HSS, which is smaller due to the section corner radius and tends to offset the difference in reported spalling depth.

The proposed model uses a two part efficiency factor to represent the effects of collar spacing and confinement effectiveness. The confinement efficiency factor, K, is defined as:

$$K = K_{dist}\, K_{eff} \qquad [5.21]$$

The factor K_{dist} is a semi-empirical distribution factor that spreads the confinement stress at the collar level over the height of the column. A ratio of the concrete area (in elevation) with direct confinement pressure to concrete area without direct confinement pressure is used:

$$K_{dist} = \frac{t}{s'} \quad \leq 1.0 \qquad [5.22]$$

With very closely spaced collars where the clear spacing is less than the collar depth the factor K_{dist} becomes greater than 1.0, and is therefore given an upper bound. This implies that when collars are spaced within a clear distance of t, the pressure is sufficiently well distributed to approximate the case of a uniformly distributed confining pressure. Nevertheless, specifying such closely spaced collars is considered an impractical application of the system.

The factor K_{eff} provides a penalty to the confining pressure for areas of the column cross-section that are ineffectively confined. The minimum effectively confined area is taken as the smallest net cross-sectional area using a 45 degree parabola to define the

ineffectively confined concrete region where spalling ultimately takes place, as shown in Figure 5.6. The depth of the selected parabola equals the average measured depth of spalling, 0.25s'. This component of the efficiency factor is calculated as:

$$K_{eff} = \frac{(h - 0.5s')^2}{h^2} \qquad [5.23]$$

As a future research consideration, the prediction of eccentrically loaded column capacity would require a revised efficiency factor, K_{eff}, that accounts for a reduced effectively confined area due to the strain gradient on the column cross-section.

The confinement efficiency factor, K, is applied to the total confining pressure, σ_{total}, to generate an equivalent confining pressure, σ_{total}', that is applied uniformly over the height of the column:

$$\sigma_{total}' = K\sigma_{total} \qquad [5.24]$$

The efficiency factors presented above are based on physical phenomena observed during testing. When the spacing of the collars is very close, maximum confinement efficiency is achieved and K approaches a value of one. When the spacing of collars is wide there is little or no benefit achieved and K approaches a value of zero.

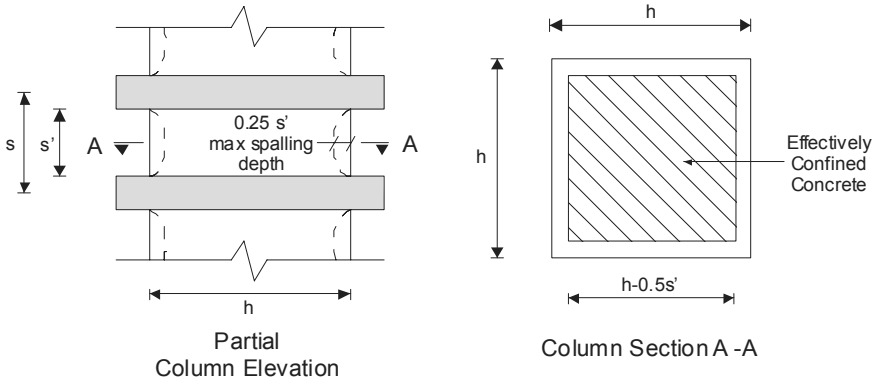

Figure 5.6: Area of Effectively Confined Concrete used for Efficiency Factors

5.3.5 Confined Concrete Strength and Strain at Peak Stress

Once the equivalent uniform confining pressure, σ_{total}', has been established, there are various equations available for calculating the peak stress of confined concrete, f_{cc}'. The present model makes use of the following equation which was established by Willam and Warnke (1975):

$$f_{cc}' = f_{co}' \left[2.254 \sqrt{1 + \frac{7.94\sigma_{total}'}{f_{co}'}} - 2\frac{\sigma_{total}'}{f_{co}'} - 1.254 \right] \qquad [5.25]$$

Equation 5.25 is used in many established confined concrete models such as those reported by: Mander et al. (1988a), Saadatmanesh et al. (1994), Ghobarah et al. (1997), Fam and Rizkalla (2001), Tsai and Lin (2002), and Hussain and Driver (2005b) Equation 5.25 was derived based on tests with a constant hydrostatic confining pressure. However, for most types of confining elements confining pressure develops gradually throughout the load history, changing in response to the material behaviour. The equation remains valid, however, if an incremental approach is used where confining pressure can reasonably be assumed constant over a small range; this approach is used in the current model to account for variable confining pressure.

The present model also makes use of an established equation (Equation 5.26) for the confined concrete strain at peak stress, ε_{cc}', proposed by Richart et al. (1928). It is assumed that the strain at peak stress of confined concrete is equal to five times the concrete strength gain due to confinement.

$$\varepsilon_{cc}' = \varepsilon_{co}' \left[1 + 5 \left(\frac{f_{cc}'}{f_{co}'} - 1 \right) \right] \qquad [5.26]$$

where ε_{co}' is the unconfined concrete strain at peak stress. It will be shown in the following section that the use of Equation 5.26 is not consistently effective for the calculation of strain at peak stress. Hussain and Driver (2005b) derived an empirical model for strain at peak stress, the use of which does not apply to the current investigation because of different collar boundary conditions. The formulation of a more

suitable equation for concrete confined by collars is considered a required future research development that is beyond the scope of the current program.

5.3.6 Concrete Stress versus Strain Relationship

The proposed model utilizes an established relationship for unconfined concrete stress versus strain developed by Popovics (1973), modified to apply to confined concrete (i.e., f_{cc} versus ε_{cc}):

$$f_{cc} = \frac{f_{cc}' \, x \, r}{r - 1 + x^r} \qquad [5.27a]$$

$$r = \frac{E_{co}}{E_{co} - E_c'} \qquad [5.27b]$$

$$E_c' = \frac{f_{cc}'}{\varepsilon_{cc}'} \qquad [5.27c]$$

$$x = \frac{\varepsilon_{cc}}{\varepsilon_{cc}'} \qquad [5.27d]$$

where f_{cc} and ε_{cc} are general values for confined concrete stress and strain, respectively, and f_{cc}' and ε_{cc}' are the values for peak confined concrete stress and strain at peak stress, respectively. The constant value E_{co} is the initial concrete tangent modulus. A value of $3900\sqrt{f_{co}'}$ is used in the current model based on observations from the tested concrete cylinders.

5.3.7 Application of Proposed Model

5.3.7.1 Solution Strategy

The proposed model makes use of an equation (Equation 5.25) for confined concrete strength that was originally developed for concrete under constant confining pressure. Mander et al. (1988b) showed that the equation could be used for columns confined with conventional transverse steel reinforcement because the steel ties yield relatively early in the load history and essentially exert a constant confining pressure thereafter. However, unlike conventional tie reinforcement, the confining pressure developed by steel collars varies significantly throughout the load history. In order to make use of Equation 5.25, an incremental–iterative approach is used that assumes a constant confining pressure within each small increment.

The procedure requires the axial strain in the column, ε_{cc}, as an input value. As the axial strain is incremented upward, points along the confined concrete stress versus strain curve are formulated. Within each increment, initial values for unknown parameters are assumed and iteration is performed until convergence is reached.

A solution strategy is presented below that outlines the steps required to generate the axial load versus strain history of concrete columns confined with external steel collars:

A) Plastic analysis of the external steel collars themselves produces intermediate values of confining pressure, σ_n, (using Equation 5.7) and lateral strain, $\varepsilon_{lat\ n}$, (using Equation 5.11 and Table 5.1) corresponding to the formation of plastic hinges. A maximum value of collar pressure, σ_{max}, is also calculated that limits the level of passive confining pressure, $\sigma_{passive,}$ that can be generated by the collar system.

B) The equilibrium passive confining pressure, $\sigma_{passive}$, can be calculated from Equation 5.19 which has four variables (ε_{cc}, ν_c, E_c, E_{collar}):

1. The concrete axial strain, ε_{cc}, is an input variable that is incremented upward to generate the load history.

2. The secant Poisson's ratio, ν_c, is calculated from Equation 5.16. The value of σ_h in Equation 5.17 is taken as the total equivalent confining pressure, σ_{total}'.

3. The concrete secant modulus, E_c, is the ratio between concrete stress and strain, f_{cc}/ε_{cc}.

4. The collar secant modulus, E_{collar}, is the ratio between collar pressure and lateral strain, $\sigma_{collar}/\varepsilon_{lat}$, and is calculated from the curve generated in step (A) once the value of column lateral strain is known (as shown in Figure 5.2).

An iterative process is used because the variables ν_c, E_c and E_{collar} are functions of confining pressure. Initially, values for the unconfined concrete properties (ν_{co} and E_{co}) and the starting value of E_{collar} (before first plastic hinge forms) are used for the unknowns. Next, the values for equilibrium passive confining pressure, $\sigma_{passive}$, and peak confined concrete strength, f_{cc}', are calculated, then the values for ν_c, E_c, and E_{collar} are updated. Iterations (steps B to D) are performed until convergence is achieved. This process is readily executed using a spreadsheet.

C) The equivalent uniform confining pressure, σ_{total}', based on the total confining pressure ($\sigma_{active} + \sigma_{passive}$) can be calculated from Equation 5.24, using values for the confinement efficiency factor, K, from Equations 5.22 and 5.23.

D) The peak confined concrete strength, f_{cc}', and strain at peak stress, ε_{cc}', are calculated from Equations 5.25 and 5.26, respectively.

E) The confined concrete stress, f_{cc}, at each increment of axial strain, ε_{cc}, is calculated using Equation 5.27.

F) The column axial load, P, is calculated using a modified version of the code-based equation for column axial strength, with concrete strength, f_{co}', replaced by confined concrete strength, f_{cc}, and without material resistance factors:

$$P = \alpha_1 f_{cc}(A_g - A_s) + A_s f_s \qquad [5.28]$$

where A_g and A_s are the gross concrete area and area of longitudinal steel reinforcement, respectively, and f_s is the stress in the longitudinal steel reinforcement. The contribution of the longitudinal steel reinforcement is calculated using strain compatibility between the concrete and steel assuming elastic-plastic behaviour. The value α_1 in Equation 5.28 is defined by CSA Standard A23.3-04 (Canadian Standards Association 2004) as follows:

$$\alpha_1 = 0.85 - 0.0015 f_{co}' \quad \geq 0.67 \qquad [5.29]$$

G) The process (steps B to F) is repeated with increasing levels of axial strain, ε_{cc}.

5.3.7.2 Model Results and Validation

The model proposed above was applied to the six concentrically loaded columns with solid steel collars (CE01 to CE06) from the current research program and validated using nine concentrically loaded columns with HSS collars (C01 to C09) from the experimental program by Hussain and Driver (2005a). Predicted column axial load histories are compared with the associated experimental curves in Figures 5.7 through 5.21. The experimental curves are truncated at the designated failure load (85% of peak load in the descending branch). In most cases, the predicted curves are truncated at a strain level equal to that at failure of the experimental column. For specimens CE02 and C05, which could not be failed in the testing equipment used, the predicted curve is extended until it reaches a peak.

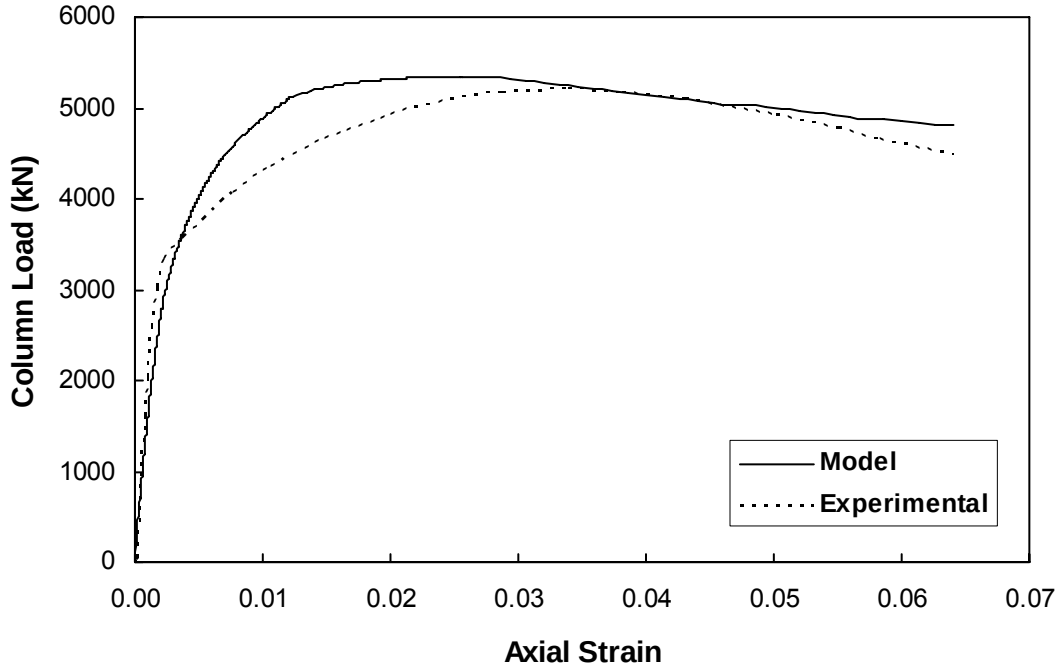

Figure 5.7: Specimen CE01 Column Load versus Axial Strain

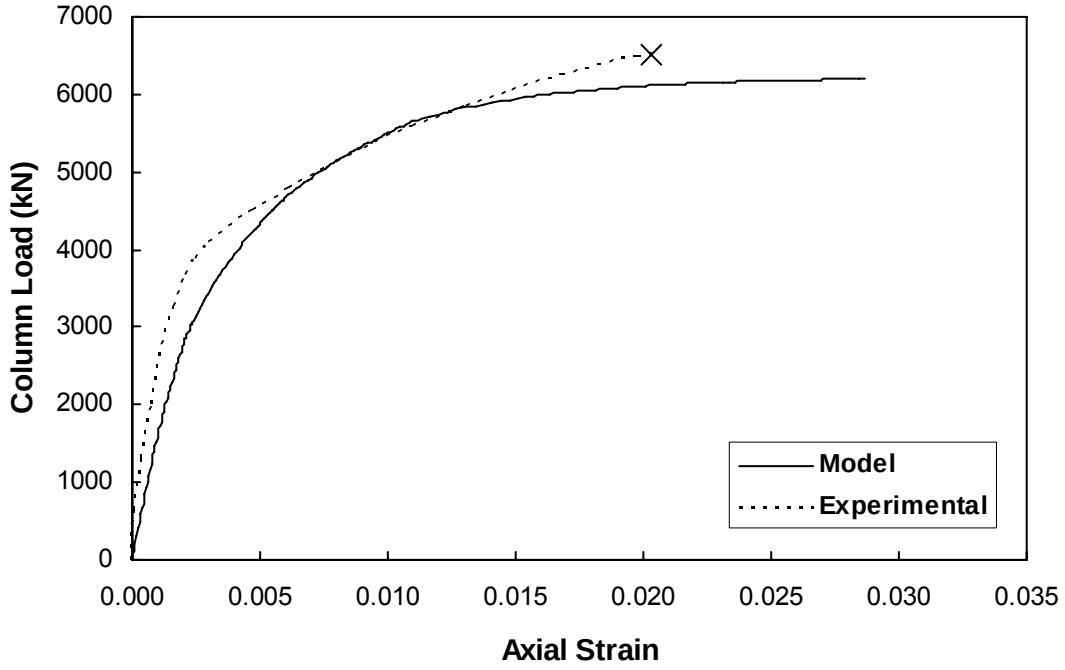

Figure 5.8: Specimen CE02 Column Load versus Axial Strain

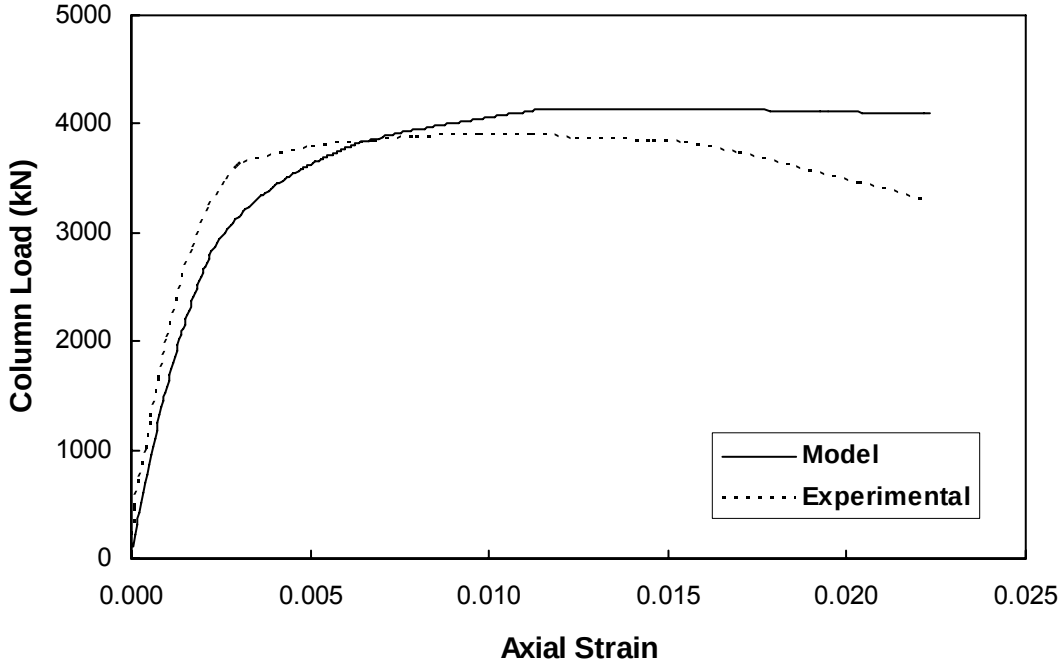

Figure 5.9: Specimen CE03 Column Load versus Axial Strain

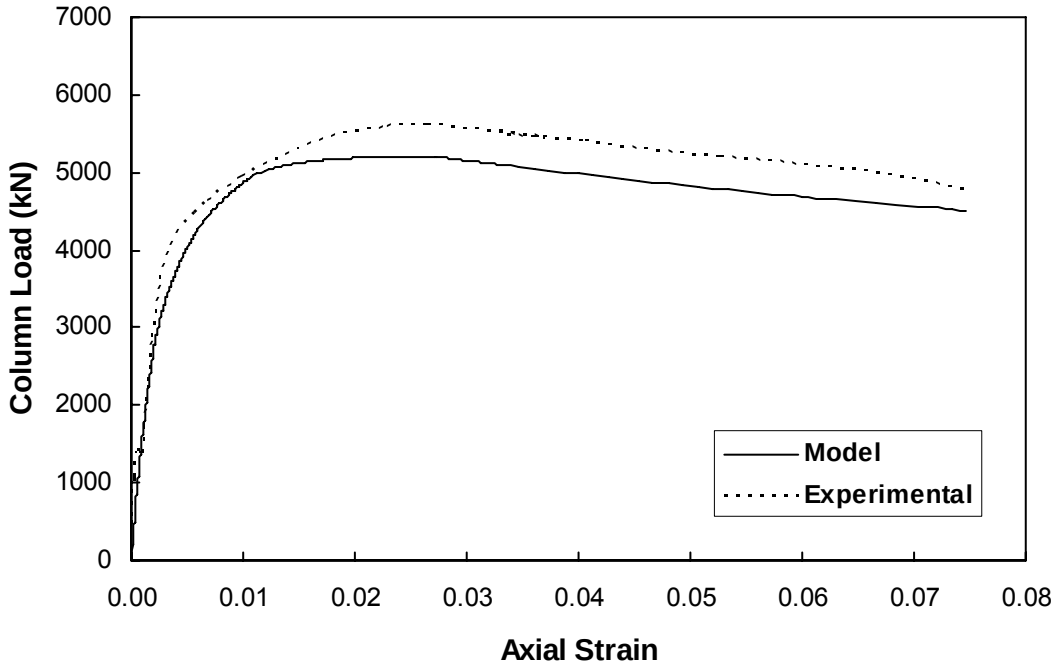

Figure 5.10: Specimen CE04 Column Load versus Axial Strain

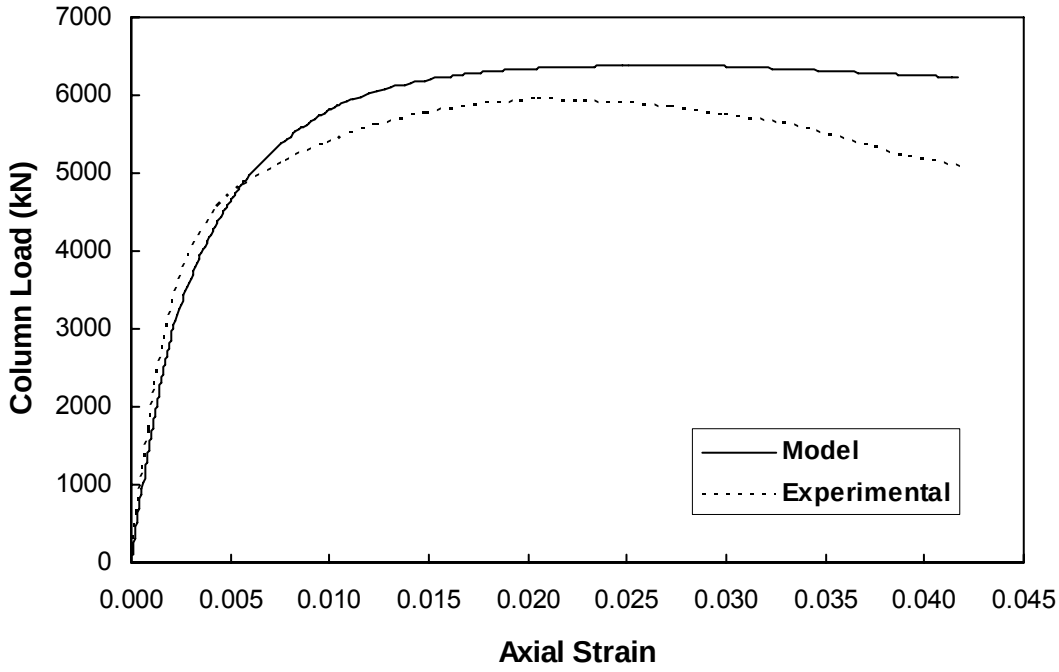

Figure 5.11: Specimen CE05 Column Load versus Axial Strain

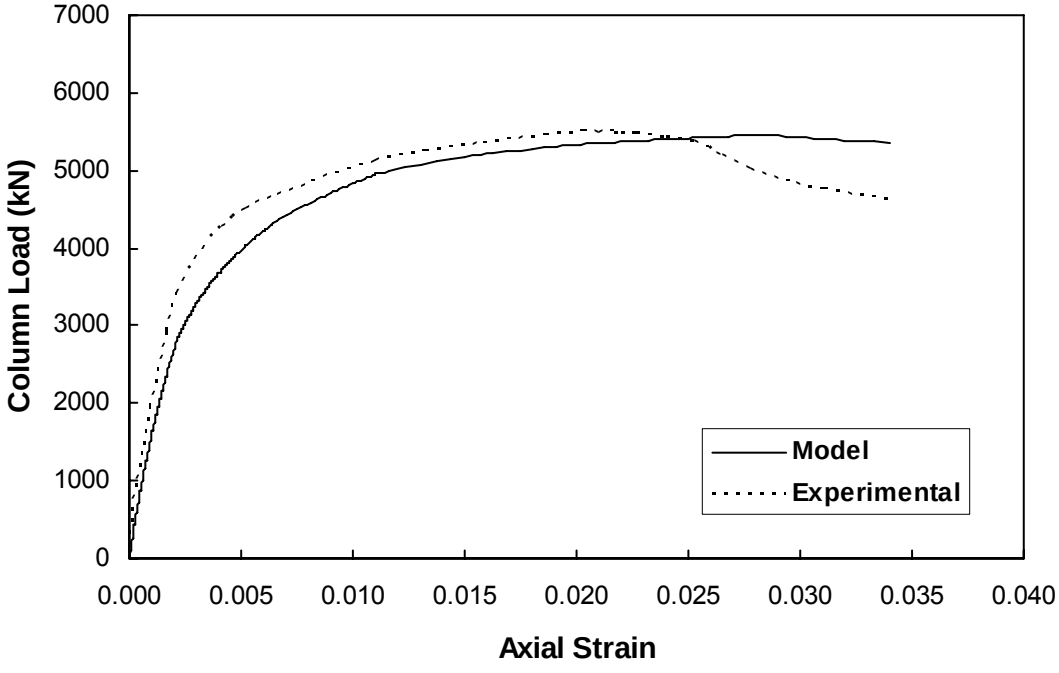

Figure 5.12: Specimen CE06 Column Load versus Axial Strain

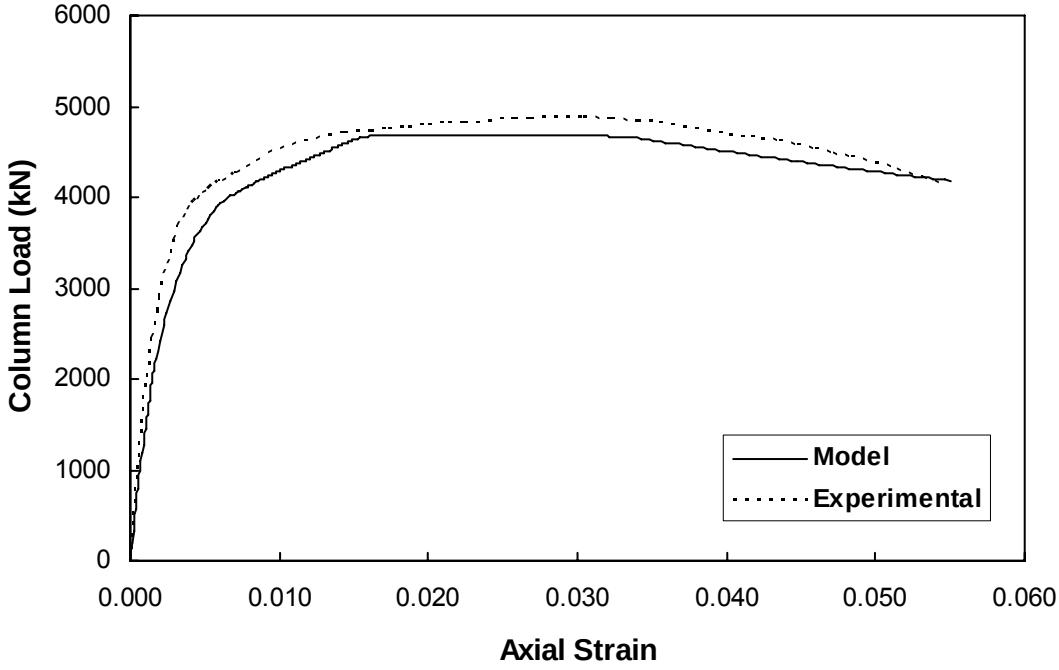

Figure 5.13: Specimen C01 Column Load versus Axial Strain

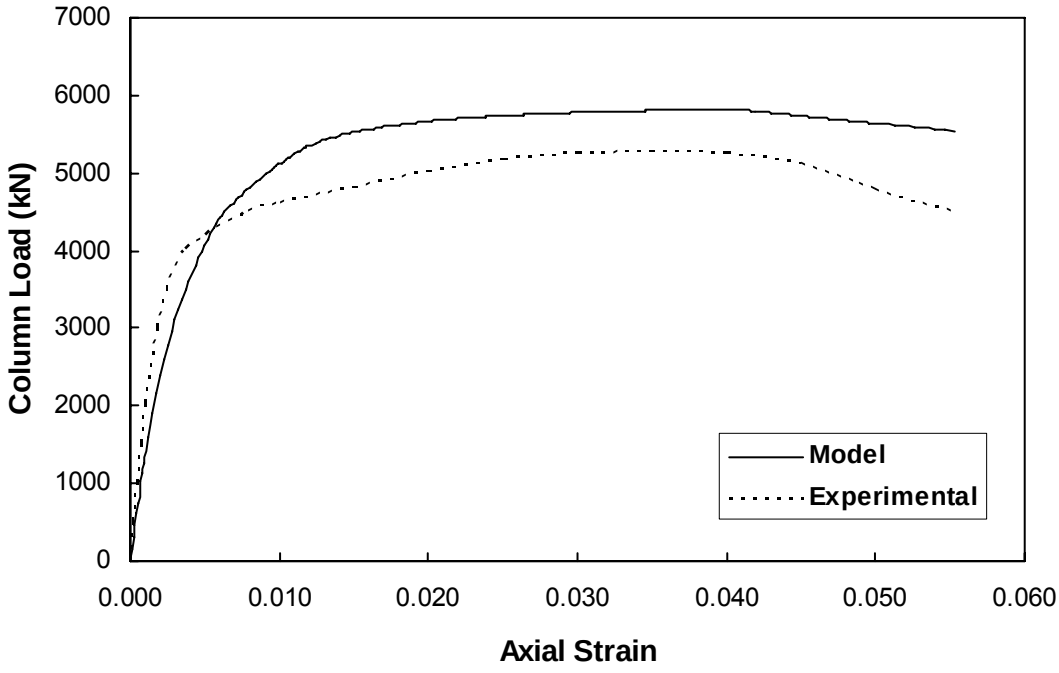

Figure 5.14: Specimen C02 Column Load versus Axial Strain

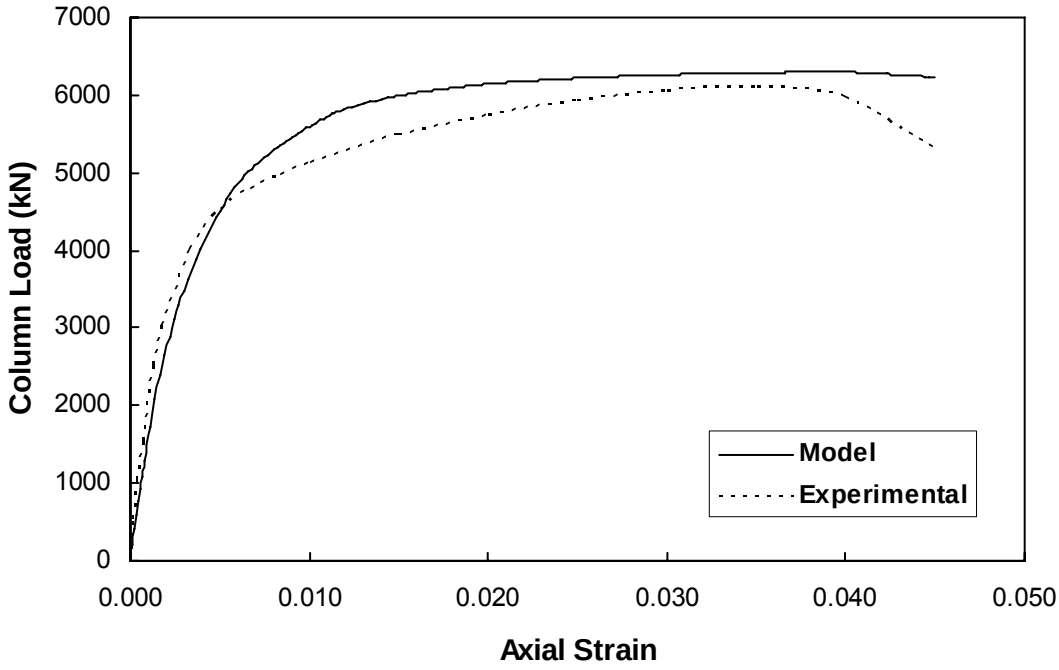

Figure 5.15: Specimen C03 Column Load versus Axial Strain

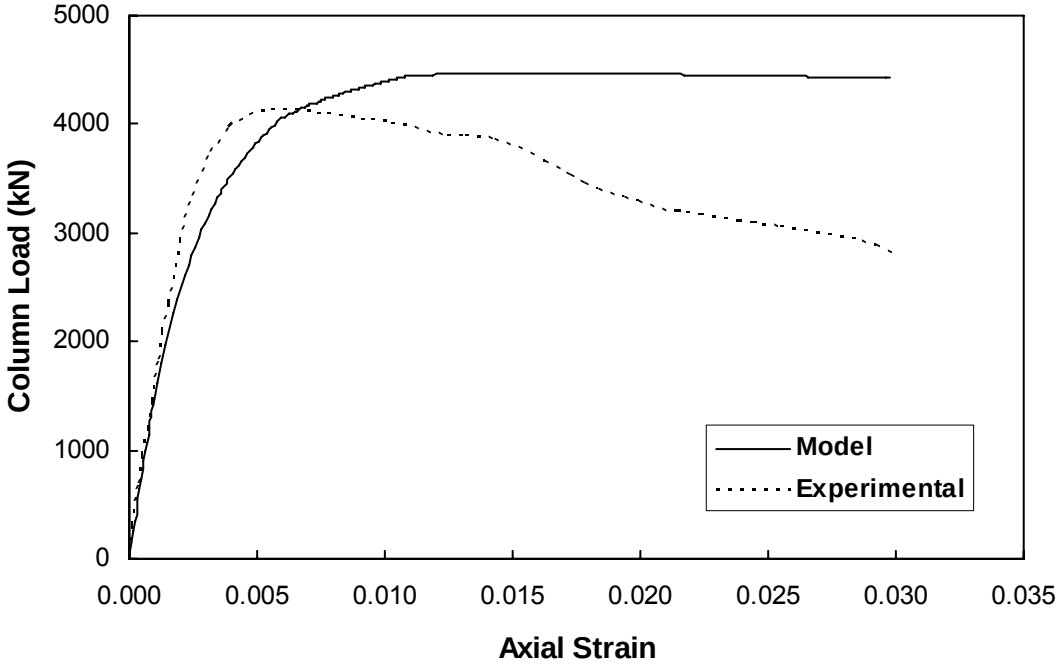

Figure 5.16: Specimen C04 Column Load versus Axial Strain

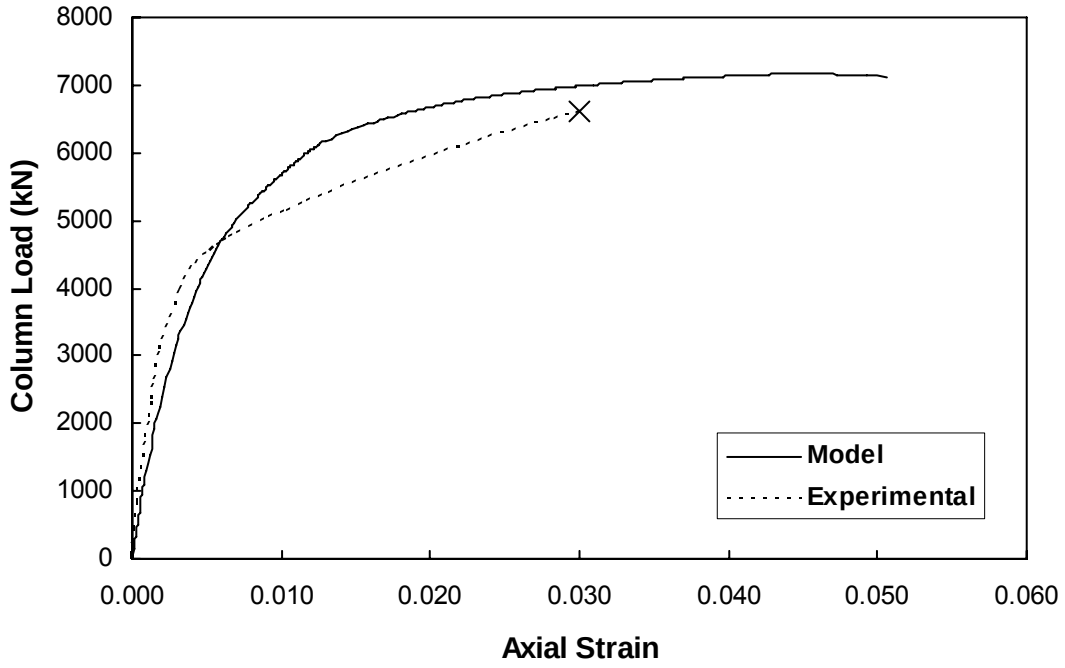

Figure 5.17: Specimen C05 Column Load versus Axial Strain

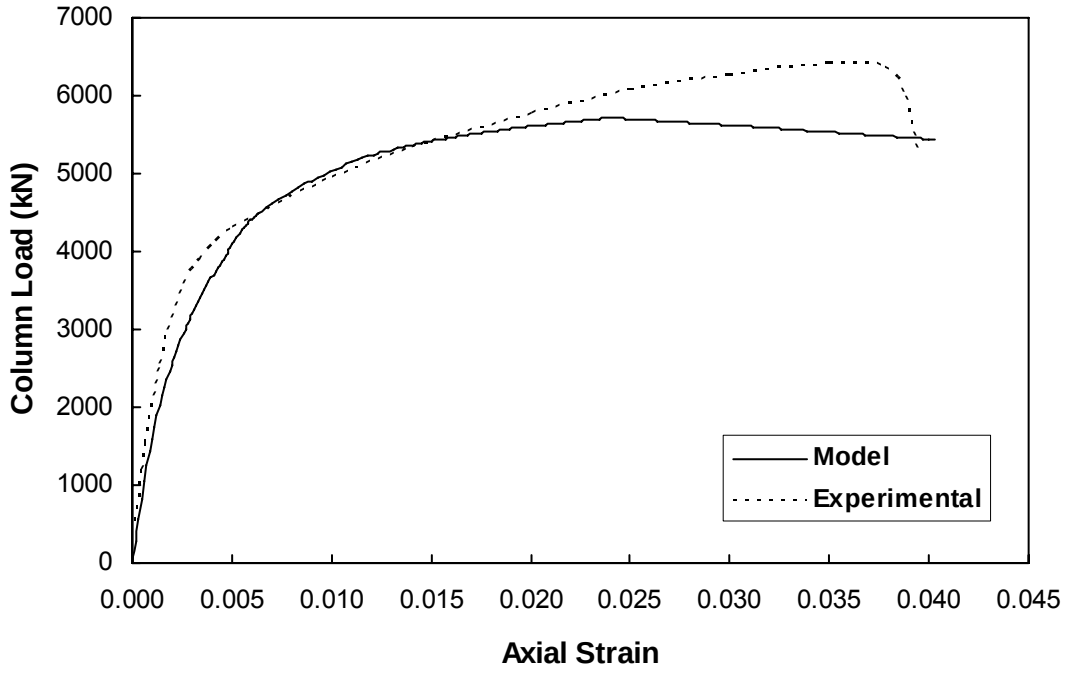

Figure 5.18: Specimen C06 Column Load versus Axial Strain

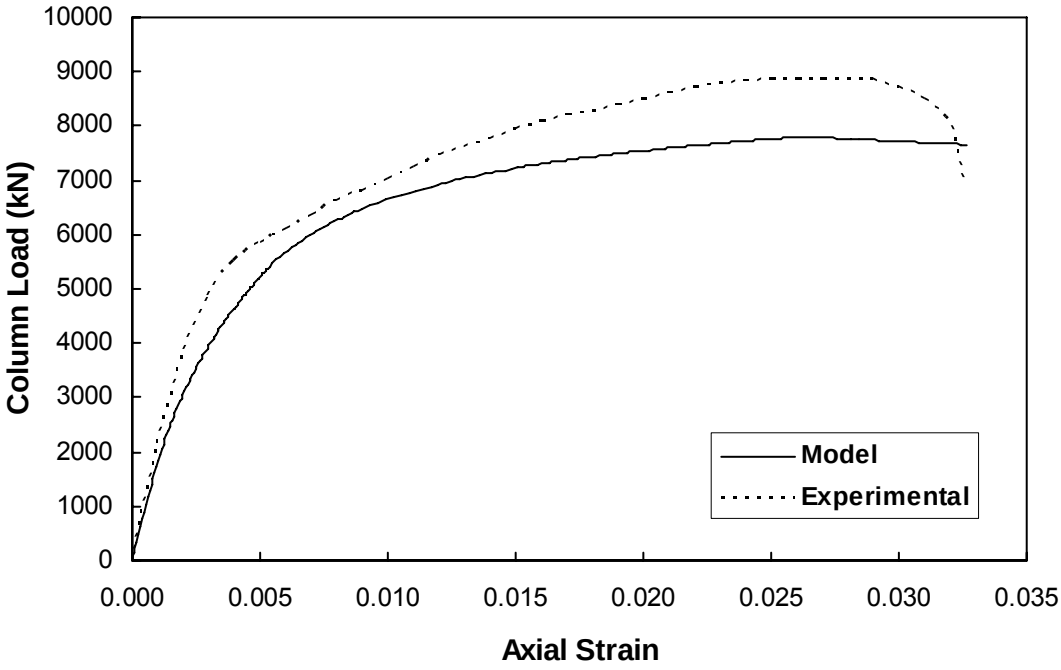

Figure 5.19: Specimen C07 Column Load versus Axial Strain

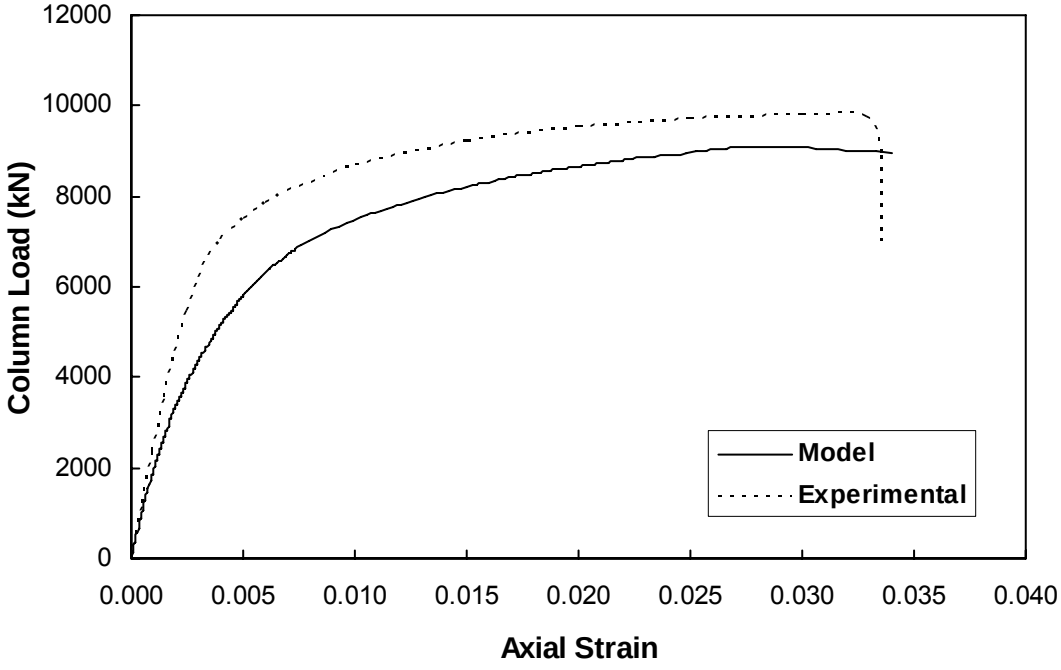

Figure 5.20: Specimen C08 Column Load versus Axial Strain

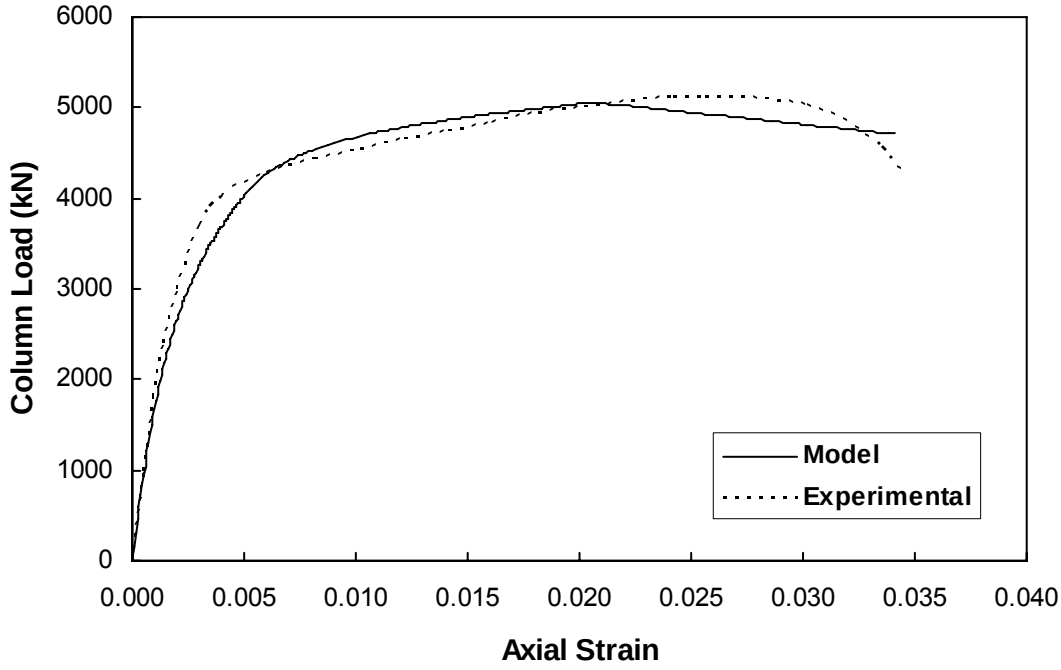

Figure 5.21: Specimen C09 Column Load versus Axial Strain

Good agreement was achieved between experimental and predicted axial load histories of specimens featuring a wide range of parameters, displaying the flexibility of the proposed model. The most significant success of the model was its ability to predict the general trend of both increased strength and ductility of concrete columns with external steel collars. The initial column stiffness and initiation of column softening were also predicted well.

In the proposed model, the stress versus strain behaviour in both the ascending and descending portion of the load history curve is described by a single equation (Equation 5.27). Despite the lack of an explicit formulation for the descending branch, the model does a good job in capturing the slow decay of the column capacity exhibited during testing. However, the model was unable to predict the accelerated localized failure in specimens with wide collar spacings due to crushing of the concrete and buckling of longitudinal steel bars between collars (specimens CE03 and C04) or the fracture of collar corner welds (specimens C06 to C09). Improvement of the model for predicting the descending branch is recommended for future consideration.

The main objective of this analytical model was to predict the capacity of collared columns accurately. Therefore, as an indicator of the success of the model, predicted values of column capacity, P_{max}, are compared with experimental values in Table 5.2 and compared graphically in Figure 5.22. The predicted and experimental values of strain at peak load, ε_{pmax}, are also compared in Table 5.2.

Table 5.2: Performance of Analytical Model

Specimen	P_{max} Experiment (kN)	P_{max} Model (kN)	P_{max} Ratio: Exp. / Model	ε_{pmax} Experiment	ε_{pmax} Model	ε_{pmax} Ratio: Exp. / Model
Current Research						
CE01	5200	5350	0.97	0.0344	0.0271	1.27
CE02	6500*	6198	1.05*	n/a	0.0291	n/a
CE03	3905	4140	0.94	0.0104	0.0136	0.76
CE04	5607	5200	1.08	0.0275	0.0253	1.09
CE05	5950	6380	0.93	0.0189	0.0268	0.70
CE06	5516	5456	1.01	0.0219	0.0280	0.78
Hussain and Driver (2005a)						
C01	4874	4688	1.04	0.0300	0.0221	1.36
C02	5283	5822	0.91	0.0356	0.0406	0.88
C03	6093	6300	0.97	0.0350	0.0397	0.88
C04	4135	4475	0.92	0.0064	0.0150	0.43
C05	6600*	7177	0.92*	n/a	0.0453	n/a
C06	6409	5713	1.12	0.0359	0.0240	1.50
C07	8882	7801	1.14	0.0283	0.0263	1.08
C08	9802	9106	1.08	0.0318	0.0280	1.14
C09	5123	5055	1.01	0.0267	0.0206	1.30

* Lower bound value

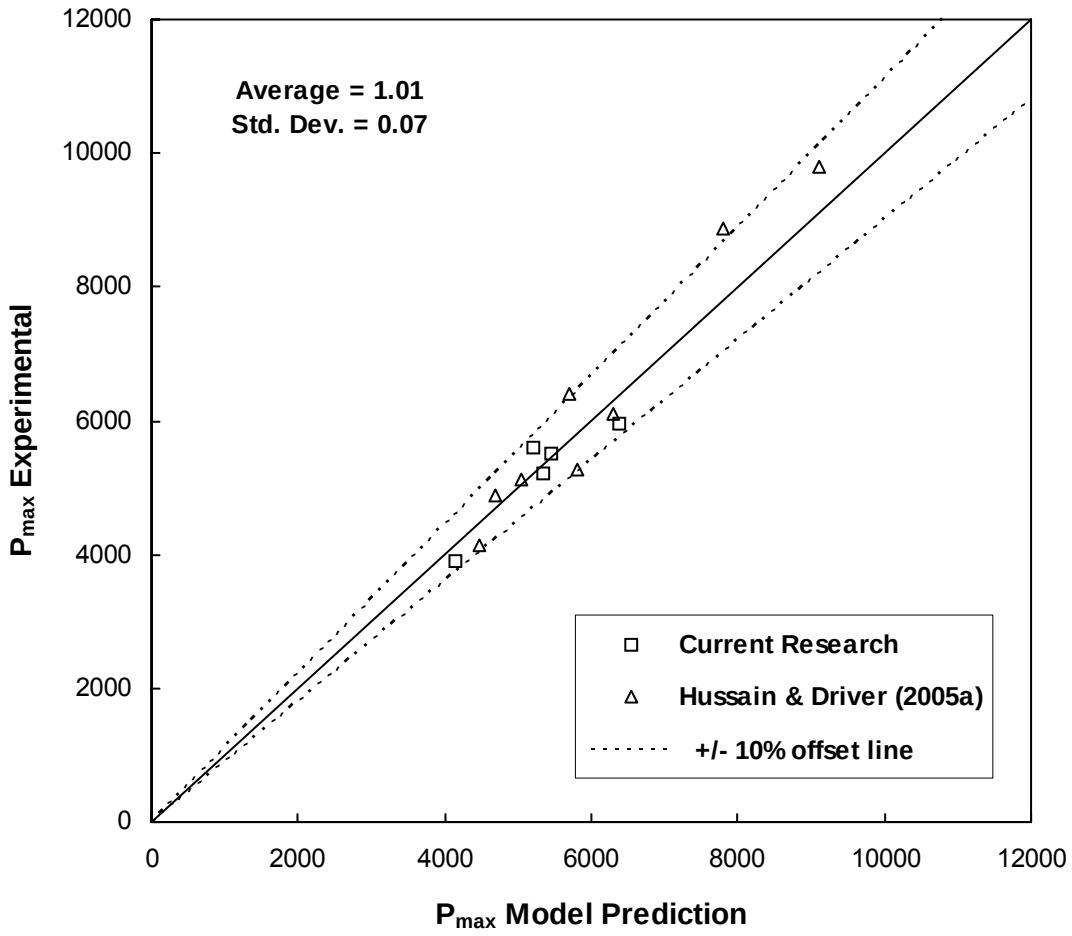

Figure 5.22: Performance of Analytical Model for Predicting Collared Column Capacity

Good accuracy was achieved with the model in all cases for predicting the capacity of columns with external steel collars. The average value for the ratio between experimental and predicted column capacity is 1.01 with a standard deviation of 0.07 (including specimens from Hussain and Driver 2005a). The results from specimens CE02 and C05 are lower bound values and are excluded from Figure 5.22 and statistical calculations.

The average value of the ratio between experimental and predicted strain at peak load is 1.01 with a standard deviation of 0.28 (including specimens from Hussain and Driver 2005a). The model could not consistently predict the strain at peak load, as indicated by the large standard deviation. The equation used for strain at peak stress (Equation 5.26) simply assumes an increase in strain equal to five times the gain in strength due to

confinement. The performance of the model in this aspect may improve when a more suitable equation for strain at peak stress is developed specifically for collared columns.

The model tended to under-predict slightly the capacities of columns with HSS collars having welded corner connections (C06 to C09), as seen in Figures 5.18 to 5.21 and the values listed in Table 5.2. This may be attributed to the exclusion of the epoxy used to bond the welded collars to the column exterior. The contribution of the epoxy layer was assumed to be negligible in the development of the model, but may have had a beneficial effect on the collar system. One such benefit may be increased confinement efficiency due to the direct transfer of confining pressure to the concrete surface; the epoxy fills any irregularities between the collar and concrete contact surfaces. Conversely, with collars secured by bolts, the confining pressure is only fully transferred once the concrete dilates outward and perhaps crushes slightly locally, filling any surface irregularities between the steel and concrete. This deficiency in the model is not seen as significant because the high cost of using fully welded collars will likely negate the use of that connection scheme during most practical applications of the system.

5.4 Summary and Conclusions

Through experimental testing it has been demonstrated that the application of external steel collars can significantly improve both the strength and ductility of concrete columns. The work of Hussain and Driver (2005b) showed that existing confinement models are unable to predict the stress versus strain behaviour of concrete columns confined by steel collars. Existing confinement models are deficient because of the following: (1) lack of an explicit flexural stiffness parameter for the confining elements; (2) inability to account for variability of the confining pressure through the column axial load history; (3) inability to accommodate a combination of active and passive confining pressures.

An analytical model was developed and presented that can be used to predict the axial load versus strain history of concrete columns confined with external steel collars. The approach is distinct from other models because of the simple, yet effective, behavioural modelling of the collars based on a generalized plastic analysis. The plastic analysis allows the axial and flexural stiffnesses of the collars to be incorporated into the

confinement model. The use of a generalized plastic analysis also ensures that the proposed model is versatile enough to handle a wide range of collar cross-sections and corner connection configurations. The proposed model also makes use of existing concrete behavioural models originally presented by Willam and Warnke (1975) for peak confined concrete stress, Richart et al. (1928) for confined concrete strain at peak stress, Fam and Rizkalla (2001) for secant Poisson's ratio, and Popovics (1973) for the confined concrete stress-strain relationship.

The model was applied to eight concentrically loaded columns from the present experimental program and validated using nine concentrically loaded columns from an experimental program conducted by Hussain and Driver (2005a). Good agreement was achieved between experimental and predicted column axial load versus strain histories. The magnitude of the peak load was predicted with a high level of accuracy in most cases; the average ratio of experimental-to-predicted peak load values was 1.01 with a standard deviation of 0.07. Further development of the model is required to improve the prediction of the strain at peak stress and the descending branch of the load history. More testing is also required to calibrate the model for a larger range of column and collar properties. With some refinement, the proposed model will be useful as a design tool for rehabilitation projects using external steel collars.

6. CONCLUSION

6.1 Research Summary

Fourteen full-scale columns were tested to evaluate the performance of a rehabilitation technique for square or rectangular reinforced concrete columns using a system of discrete external steel collars. Unlike other external confinement methods such as steel jacketing or FRP wrapping, the proposed collar system exploits the benefits of confining elements with high flexural stiffness. Specimens were tested under both concentric and eccentric quasi-static, monotonically applied, axial loading. Through a combination of active and passive confining pressure, columns with external collars showed significant improvements in both strength and ductility compared with conventionally reinforced columns. By preventing spalling beneath the collars and inhibiting spalling between them, the effectively confined concrete core area was significantly increased compared with that contained within conventional reinforcing ties. Parameters investigated in the experimental program include: collar spacing, collar flexural stiffness, active confining pressure, and load eccentricity.

The column axial strength enhancement (over the theoretical unconfined column capacity) achieved during testing was between 50% and 165% for concentrically loaded specimens. Doubling the column strength (i.e., 100% strength enhancement) is considered to be readily achievable under concentric loading conditions using the proposed external collar system. Eccentrically loaded specimens had comparatively lower axial strength enhancements of between 30% and 82%. The reduced effectiveness of the collar system in columns with bending is attributed to the decrease in lateral dilation of the column due to the presence of a strain gradient on the cross-section, which lowers the applied confining pressure.

Columns typically exhibited a ductile response with a long strain plateau before reaching a peak load, followed by a gradual post-peak load decline. At peak load, collared columns reached axial strain levels 5 to 17 times higher than would be expected for unconfined normal strength concrete.

Of the parameters investigated, collar spacing was found to be the most influential on the performance of the specimens tested; increasing collar spacing resulted in significantly decreased strength and ductility enhancements. Specimens with the widest collar spacing used (s/h = 0.57) had comparatively lower strength enhancement versus other specimens. However, collar spacing as wide as the internal tie spacing limit should provide acceptable performance, but may not result in any appreciable strength increase over the use of internal ties.

Although the collar flexural stiffness is seen as an important benefit of the collar system, only a marginal increase in strength enhancement was achieved from a significant increase in the collar flexural stiffness, suggesting that there is an optimal collar flexural stiffness beyond which there are diminishing returns. Increasing the collar flexural stiffness appeared to decrease the ductility of the column, although a slightly larger clear spacing for the higher stiffness collars may have influenced this result somewhat.

The application of an active confining pressure through pretensioning of the collar connection bolts provided up to a 36% increase in column axial strength enhancement over equivalent columns without active confining pressure. However, reductions in ductility were observed for concentrically loaded columns with pretensioned bolts.

Installing the external collars after a column is under significant preload (equal to the factored design capacity of the column) was found not to decrease the eventual strength or ductility of the column as compared to the case of installing the collars prior to the application of any axial load. Therefore, all test results are considered to be directly applicable to rehabilitations conditions.

The previous work of Hussain and Driver (2005b) showed that existing confinement models are unable to predict the stress versus strain behaviour of concrete columns confined by steel collars. Existing confinement models are deficient because of one or more of the following: (1) lack of an explicit flexural stiffness parameter for the confining elements; (2) inability to account for variability of the confining pressure through the column axial load history; (3) inability to accommodate a combination of active and passive confining pressures.

An analytical model was presented that can be used to predict the axial load versus strain response of concentrically loaded concrete columns with external steel collars. The approach is distinct from other models because of the simple, yet effective, behavioural modelling of the collars based on a generalized plastic analysis. The plastic analysis allows both the axial and flexural stiffnesses of the collars to be incorporated into the confinement model and provides representative confining pressures that increase as the column is loaded. Moreover, the model can be used with or without active confinement. The use of a generalized plastic analysis also ensures that the proposed model is versatile enough to be used with any collar cross-section and corner connection configurations. The model was applied to eight concentrically loaded columns from the present experimental program and validated using nine concentrically loaded columns from another (Hussain and Driver 2005a). Good agreement was achieved between experimental and predicted column axial load versus strain histories. The magnitude of the peak load was predicted with a high level of accuracy in most cases; the average ratio of experimental to predicted peak load values was 1.01, with a standard deviation of 0.07.

6.2 Recommendations for Future Research

6.2.1 Experimental Research

Additional testing is required to determine the applicability and performance of the external collar system for column geometries and material properties other than those reported. Columns with larger square or rectangular cross-sections will likely require collar sizes larger than those reported, in order to achieve comparable results; the flexural stiffness of collars is a function of both the collar cross-sectional geometry and the span between the corners of the column. In addition to geometric sensitivity, the collar system may yield differing results for concrete with material properties other than those reported. For example, high strength concrete typically exhibits a lower lateral dilation than regular strength concrete around the peak load. Consequently, high strength concrete columns may not mobilize the confining action of the external collars to the same degree as normal strength concrete columns.

The column specimens tested in all previous and current research programs have included continuous longitudinal reinforcing bars. Lap splicing of longitudinal reinforcing just above the floor level of a building, in a potential plastic hinging region, was common practice in the construction of older structures, even in zones of moderate and high seismicity. The existence of such lap splices combined with other reinforcement detailing deficiencies such as inadequate confinement from ties make these locations susceptible to premature failure during major loading events. The use of external steel collars is expected to improve the performance of columns at lap splice locations. An experimental investigation is required to confirm the expected behaviour and quantify the benefit attained through use of the external collar system.

Strain gradients are common in building columns due to imbalanced floor loading and construction tolerances causing out-of-straightness, and can become severe during a seismic event. Through testing under eccentric load, the influence of strain gradient on the column cross-section was shown in the current research program to decrease the degree of axial strength enhancement significantly compared with concentrically loaded specimens. However, direct comparisons among specimens with different strain gradients were not possible due to the concurrent variation of other test parameters (i.e., collar spacing, collar flexural stiffness, and bolt pretensioning). More research on columns with a strain gradient is required to quantify the specific effect of strain gradients on the confinement mechanism and efficiency of the collar system.

Previous research programs utilized standard HSS sections in a four-piece collar configuration. The evolution of the system into a two-piece configuration allowed the collar to be secured using the clamping action of the bolted corners, while benefiting from the increased stiffness of the continuous collar at opposite corners. Significant improvement in fabrication time and cost was achieved using the new collar configuration and providing that relatively tight tolerances could be met, installation on the existing column remained simple. However, the two-piece configuration caused difficulty during the installation of collars on some columns; a gap between the steel and concrete surfaces required shimming in some cases. The source of the problem was an error in the fabrication of the collars; the angle between collar legs was not cut as specified (90 degrees). As a result, two practical issues regarding the use of a two-piece collar system were highlighted. First, careful attention must be paid to the level of collar

fabrication tolerance required during fabrication. Second, variation of the column cross-section is expected due to construction tolerances (e.g., corners of the existing column may not be 90 degrees). Therefore, the desired contact between the collar and concrete will likely require column-specific fabrication or the use of a filler (e.g., steel shims, epoxy grout, etc.), both of which result in a loss of fabrication and installation efficiency. The use of a four-piece collar system would alleviate some sensitivity to fabrication tolerance.

A potential modified four-piece collar system, shown in Figure 6.1, utilizes solid collar sections, similar to the collars in the current research program, with four bolted corner connections. The collar sections can be fabricated from square or rectangular bar stock requiring only a single cut (to length) for each side of the collar, which will improve fabrication efficiency. For larger collar cross-sections that are unavailable as standard bar stock, the collars may be cut from thick steel plate using a process similar to the one used in the current research program. The corner connection requires a bolt hole in one end of the collar section and a threaded recess in the opposite end; for a square column, all four collar pieces would be identical. The bolt hole can be oversized to avoid problems with alignment of the adjacent collar legs. Each collar side is truncated short of the adjacent collar leg leaving a small gap, which allows a clamping force (and associated active confining pressure) to be applied to the column during collar installation through pretensioning of the bolts.

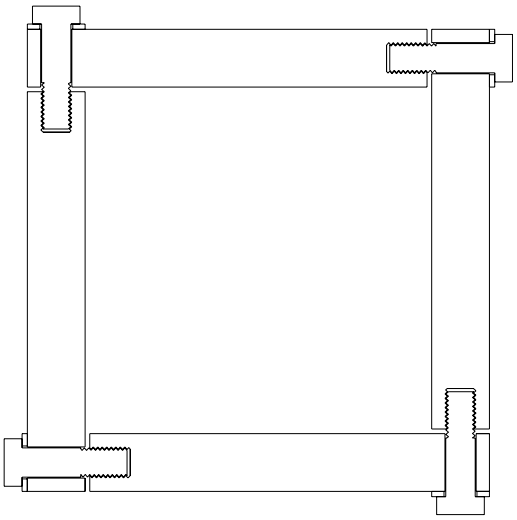

Figure 6.1: Cross-section of Proposed Four-piece Collar Configuration

6.2.2 Analytical Research

The equations used for the strain at peak stress and the descending branch in the analytical model presented in Chapter 5 are based on confinement models for conventional tie reinforcing. The behaviour of collared columns was not consistently predicted in those aspects using the proposed model. The formulation of more appropriate equations for strain at peak stress and the descending branch is recommended to improve the performance of the analytical model over the entire load history.

A substantial amount of data has been collected on the behaviour of collared columns through experimental testing and analytical modelling. The external confinement system using steel collars has proven its potential for rehabilitation of reinforced concrete columns. However, the global response of a building structure with columns rehabilitated using external collars has not yet been addressed. An analytical investigation into the implementation of the proposed system that incorporates the work of previous research is needed. The investigation should include a detailed analysis of the post-rehabilitation structural response achieved using the collar system. Different building configurations should be analyzed to determine the practical limitations of the system. An analysis of the redistribution of structural damage should be performed to identify critical components that may also need rehabilitation, in addition to the buildings columns.

REFERENCES

Aycardi, L.E.; Mander, J.B.; and Reinhorn, A.M. (1994). "Seismic Resistance of Reinforced Concrete Frame Structures Designed Only for Gravity Loads: Experimental Performance of Subassemblages." ACI Structural Journal, 91(5), pp.552-563.

Bracci, J.M.; Reinhorn, A.M.; and Mander, J.B. (1995a). "Seismic Resistance of Reinforced Concrete Frame Structures Designed for Gravity Loads: Performance of Structural System." ACI Structural Journal, 92(5), pp.597-609.

Bracci, J.M.; Reinhorn, A.M.; and Mander, J.B. (1995b). "Seismic Retrofit of Reinforced Concrete Buildings Designed for Gravity Loads: Performance of Structural Model." ACI Structural Journal, 92(6), pp.711-723.

Computers and Structures. (2004) SAP2000 version 9.0.1.

Canadian Standards Association. (2004) Standard A23.3-04 - Design of Concrete Structures.

Cusson, D., and Paultre, P. (1994). "High-Strength Concrete Columns Confined By Rectangular Ties." Journal of Structural Engineering, ASCE, 120(3), pp.783-804.

Fam, A.Z., and Rizkalla, S.H. (2001). "Confinement Model for Axially Loaded Concrete Confined by Circular Fibre-Reinforced Polymer Tubes." ACI Structural Journal, 98(4), pp.451-461.

Gardner, N.J. (1969). "Triaxial Behaviour of Concrete." ACI Journal, 114(8), pp.136-146.

Ghobarah, A.; Aziz, T.S.; and Biddah, A. (1997). "Rehabilitation of Reinforced Concrete Frame Connections Using Corrugated Steel Jacketing." ACI Structural Journal, 94(3), pp.283-294.

Hussain, M.A., and Driver, R.G. (2001). "Finite Element Study on the Strength and Ductility of Externally Confined Rectangular and Square Concrete Columns." Proceedings, 29th Annual conference of the Canadian Society for Civil Engineering, Victoria, BC, Canada, May 30-June 2.

Hussain, M.A., and Driver, R.G. (2003). "Behaviour of Externally Confined Reinforced Concrete Columns Under Extreme Lateral Cyclic Loading." Proceedings, 1st Conference on Response of Structures to Extreme Loading, Toronto, ON, Canada, August 3-6.

Hussain, M.A., and Driver, R.G. (2005a). "Experimental Investigation of External Confinement of Reinforced Concrete Columns by HSS Collars." ACI Structural Journal, 102(2), pp.242-251.

Hussain, M.A., and Driver, R.G. (2005b). "Seismic Rehabilitation of Reinforced Concrete Columns Through Confinement by Steel Collars." Structural Engineering Report No. 259, Department of Civil and Environmental Engineering, The University of Alberta, Edmonton, AB, Canada.

Hussain, M. A., and Driver, R. G. (2005c). Discussion of “Retrofit of Reinforced Concrete Columns Using Partially Stiffened Steel Jackets” by Xiao, Y., and Wu, H. Journal of Structural Engineering, ASCE, 131(2), pp.364-366.

Kent, D.C., and Park, R. (1971). “Flexural Members with Confined Concrete.” Journal of the Structural Division, ASCE, 97(ST7), pp.1969-1990.

Khaloo, A.R., and Bozorgzadeh, A. (2001). “Influence of Confining Hoop Flexural Stiffness on Behaviour of High Strength Lightweight Concrete Columns.” ACI Structural Journal, 98(5), pp.657-664.

Khaloo, A.R.; El-Dash, K.M.; and Ahmad, S.H. (1999). “Model for Lightweight Concrete Columns Confined by Either Single Hoops or Interlocking Double Spirals.” ACI Structural Journal, 96(6), pp.883-890.

Légeron, F. and Paultre, P. (2003). “Uniaxial Confinement Model for Normal and High-Strength Concrete Columns.” Journal of Structural Engineering, 129(2), pp.241-252.

Madas, P. and Elnashai, A.S. (1992). “A New Passive Confinement Model for the Analysis of Concrete Structures Subjected to Cyclic and Transient Dynamic Loading.” Earthquake Engineering and Structural Dynamics, 21, pp.409-431.

Mander, J.B.; Priestly, M.J.N.; and Park, R. (1988a). “Theoretical Stress-Strain Model for Confined Concrete.” Journal of Structural Engineering, ASCE, 114(8), pp.1804-1826.

Mander, J.B.; Priestly, M.J.N.; and Park, R. (1988b). “Observed Stress-Strain Behavior of Confined Concrete.” Journal of Structural Engineering, ASCE, 114(8), pp.1827-1849.

Mirmiran, A.; Shahawy, M.; Samaan, M.; Echary, H.E.; Mastrapa, J.C.; and Pico, O. (1998). “Effect of Column Parameters on FRP-Confined Concrete.” Journal of Composites for Construction, 2(4), pp.175-185.

Parvin, A., and Wang, W. (2001). “Behavior of FRP Jacketed Concrete Columns Under Eccentric Loading.” Journal of Composites for Construction, 5(3), pp.146-152.

Park, R.; Priestly, M.J.N.; and Gill, W.D. (1982). “Ductility of Square-Confined Concrete Columns.” Journal of the Structural Division, ASCE, 108(ST4), pp.929-950.

Popovics, S.A. (1973). “A Numerical Approach to the Complete Stress-Strain Curve of Concrete.” Cement and Concrete Research, Pergamon Press Inc., No. 3, pp.583-599.

Willam, K.J., and Warnke, E.P. (1975). “Constitutive Model for the Triaxial Behaviour of Concrete.” Proceeding, International Association of Bridge Structural Engineers, 19, pp.1-30.

Richart, F.E.; Brandtzaeg, A.; and Brown, R.L. (1928). “A Study of the Failure of Concrete Under Combined Compressive Stresses.” University of Illinois Engineering Experimental Station, Bulletin No. 185.

Rodriguez, M., and Park, R. (1994). “Seismic Load Tests on Reinforced Concrete Columns Strengthened by Jacketing.” ACI Structural Journal, 91(2), pp.150-159.

Saadatmanesh, H.; Ehsani, M.R.; and Li, M.W. (1994). “Strength and Ductility of Concrete Columns Externally Reinforced with Fiber Composite Straps.” ACI Structural Journal, 91(4), pp.434-447.

Saatciouglu, M., and Razvi, S.R. (1992). “Strength and Ductility of Confined Concrete.” Journal of Structural Engineering, ASCE, 118(6), pp.1590-1607.

Saatciouglu, M.; Salamat, A.H.; and Razvi, S.R. (1995). “Confined Columns Under Eccentric Loading.” Journal of Structural Engineering, ASCE, 121(11), pp.1547-1556.

Schickert, G., and Winkler, H. (1979). “Results of Tests Concerning Strength and Strain of Concrete Subjected to Multiaxial Compressive Stresses.” Deutscher Ausschuss fur Stahlbeton, Heft 277, Berlin, West Germany.

Sheikh, S.A., and Uzumeri, S.M. (1982). “Analytical Model for Concrete Confinement in Tied Columns.” Journal of the Structural Division, ASCE, 108(ST12), pp.2703-2722.

Terro, M.J., and Hamoush, S.A. (1996). “Inelastic Analysis of Sections Subjected to Axial Force and Bending Moment.” Computers and Structures, 59(1), pp.13-19.

Tsai, K.C., and Lin, M.L. (2002). “Seismic Jacketing of RC Columns for Enhanced Axial Load Carrying Performance.” Journal of the Chinese Institute of Engineers, 25(4), pp.389-402.

Valluvan, R; Kreger, M. E.; and Jirsa, J.O. (1993). “Strengthening of Column Splices for Seismic Retrofit of Nonductile Reinforced Concrete Frames.” ACI Structural Journal, 90(4), pp.432-440.

Xiao, Y., and Wu, H. (2003). “Retrofit of Reinforced Concrete Columns Using Partially Stiffened Steel Jackets.” Journal of Structural Engineering, ASCE, 129(6), pp.725-732.